Prediction of maximum thermal crack width in RC abutments and investigation on influential factors using artificial neural networks

（人工ニューラルネットワークを用いた RC 橋台の温度ひび割れの最大ひび割れ幅の予測と影響要因の分析）

By

Mehboob Rasul

A thesis presented to the

Graduate School of Urban Innovation

Yokohama National University

Yokohama, Japan

In partial fulfilment of the Requirements for the Degree of

Doctor of Philosophy in Engineering

Supervised by

Prof. Akira Hosoda

September 2019

Yokohama National University, Japan

Graduate School of Urban Innovation

This thesis, written by Mehboob Rasul has been accepted by his advisor and thesis committee members. And, it is presented to Graduate School of Urban Innovation, Yokohama National University, Japan in partial fulfilment of the requirement for the degree of Doctor of Philosophy in Engineering.

Advisor	**Committee members**
Prof. Akira Hosoda	Prof. Koichi Maekawa
	Prof. Hitoshi Yamada
	Prof. Hiroshi Katsuchi
	Dr. Chikako Fujiyama

Acknowledgment

All praises and thanks are due to ALLAH Subhanaho wa taala for blessing me with the countless blessings, health, knowledge and patience to complete this thesis. May the peace and blessings of ALLAH be upon the Prophet Muhammad (Peace be upon him), his family, and his companions.

I would like to acknowledge Yokohama National University, Japan and Graduate School of Urban Innovation for granting me opportunity to pursue my doctoral studies with MEXT scholarship in state of the art academic and research facilities. I want to thank Ministry of Education, Culture, Sports, Science and Technology (Japan) for proving me scholarship to support my studies and stay in Japan.

I want to express my heartiest gratitude to my respected advisors Prof. Akira Hosoda, and Prof. Koichi Maekawa for their sincere continuous guidance and kind support. It is a vital life time experience for me to work under the umbrella of such great experts of my field. They not only technically supported me during my research but also helped me to boost up my morale and confidence. I am also grateful to Prof. Akito Sakurai (Yokohama National University) for his guidance.

I also acknowledge the sincere support of Dr. Satoshi Komatsu, Dr. Arifa Iffat Zerin, Dr. Chamila Kumara Rankoth, Mr. Keitai Iwama during my research and stay in Japan. I also want to thank all other faculty, staff members and secretaries for their support throughout my studies and stay in Japan.

I am really grateful to all of friends especially, Mr. Muhammad Ali Hafeez and Mr. Sohail Hasan for their technical and moral support throughout my research work and stay in japan.

Last but not the least, I want to acknowledge my parents and brothers for their unconditional love, support, prayers and encouragement throughout my life.

Table of Content

List of Tables

List of Figures

ABSTRACT

In the present study, an attempt is made to predict the occurrence of externally retrained thermal cracking and maximum width of externally restrained thermal cracks in massive RC abutments using artificial neural network (ANN) and actual construction data. Feed forward multilayer perceptron artificial neural networks were developed by considering basic geometric and material properties, and ambient environmental conditions. After obtaining the most efficient ANNs by performing enormous trials, parametric studies were performed to study the influence of various parameters i.e., width, thickness, height, reinforcement ratio, lift interval, initial concrete temperature and concrete strength on maximum crack width. All parametric studies were performed in three environmental conditions i.e., cold weather, normal weather and hot weather.

In this study, dataset was chosen from Yamaguchi prefecture database in Japan, which contains data of all high-quality RC abutments constructed in the prefecture since 2005. A sophisticated dataset for developing ANNs was considered by removing all apparently wrong entries and cross verification was performed for all individual entries of dataset. 362 reliable lifts of RC abutments were selected, in which, 248 lifts were categorised as vertical walls and remaining 114 lifts as parapets. For data analysis and neural networks, IBM SPSS Statistics with neural network package and MATLAB with machine learning and deep learning toolboxes were employed.

The results from the ANNs have shown an appreciable potential in predicting occurrence of thermal cracking and maximum width of thermal cracks. In predicting the occurrence of thermal cracking, the accuracy level of 81.5% and 87.6% was achieved for vertical walls and parapets, respectively. In predicting the maximum width of thermal cracking for vertical walls, the accuracy level of 90.95 % with ±0.1 mm allowable error and 69 % with ±0.05 mm allowable error in residual crack width was achieved. In predicting the maximum width of thermal cracking for parapets, the accuracy level of 94.7 % with ±0.1 mm allowable error and 90.8 % with ±0.05 mm allowable error in residual crack width was achieved.

The results of parametric studies have shown strong influence of seasonal variations, cement content, width, thickness, height, reinforcement ratio, lift interval and initial concrete temperature on maximum crack width for vertical walls. These results will be helpful in mitigating the harmful thermal cracks by providing the understanding of the influence of various input parameters which are relatively easy to control in practice and valuable inputs for the establishment of the guidelines to mitigate thermal cracks.

1 Introduction

1.1 Thermal cracks

Thermal stresses are generated in the concrete resulting from restraint in volume change due to heat of hydration of cement and autogenous shrinkage. Sometimes, the thermal stress can exceed the sum of the stresses caused by other external loads. In a massive concrete structure, the thermal stress can not only cause cracking but also have an impact on the stress state of the structure. If thermal stresses exceed from the tensile strength of the concrete, then cracks may generate as shown in figure 1-1.

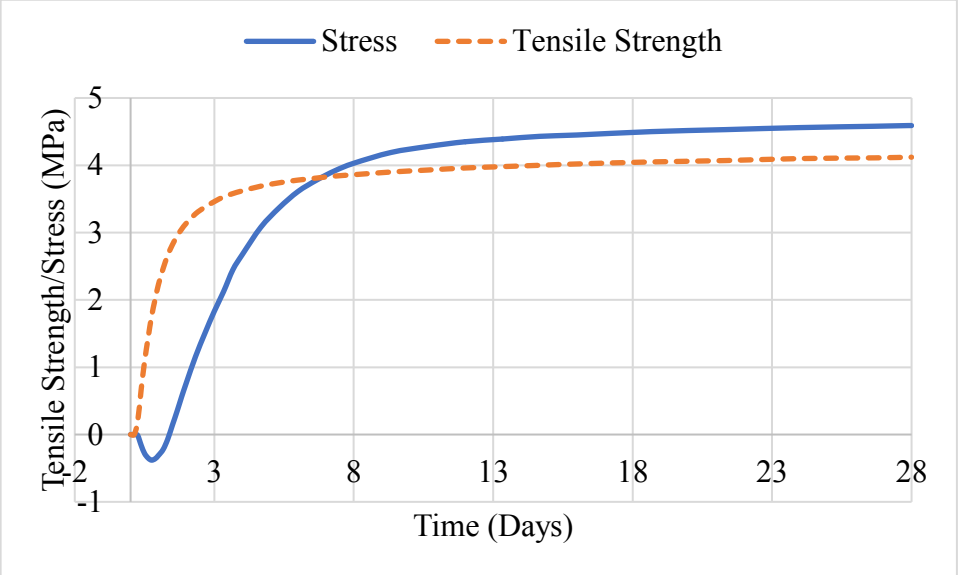

Figure 1-1 Typical development of stress and tensile strength in externally restrained wall

The restraint may be external, internal or combined. Internal restraint is caused by the temperature gradient between inner and outer part of the concrete mass, and/or reinforcement. Whereas external restraint is caused by the foundation or the previous lift. This study is focused on the externally restraint thermal cracks. A typical example of externally restraint thermal cracks is shown in figure 1-2. There are several factors which affect the thermal cracking, i.e., type of structures, boundary conditions, materials, mixture proportions, construction methods, weather conditions, etc. Cracks are serious concerns towards construction management, durability, water tightness, and aesthetics. If the crack width exceeds a certain limit, then it may initial several durability issues, i.e.,

reinforcement corrosion etc. [1]–[4]. Due to influence of several factors, it is not easy to predict the thermal cracking. Presently, JCI has a system to predict the cracking probability and crack width using thermal and stress analysis[1]. But there is a considerable variation in prediction and actual cracking conditions as shown in the Figure 1-3 [3]. So, there is a need of an alternative approach to counter this issue and predict the cracking condition.

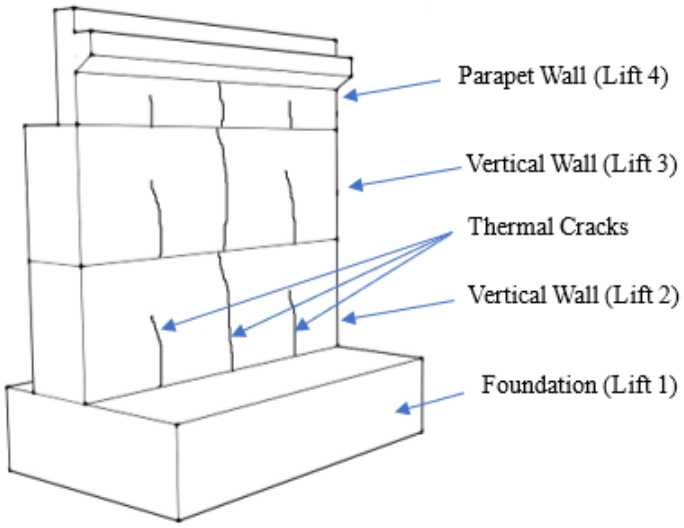

Figure 1-2 Typical example of RC abutment with multiple lifts and externally restrained cracks

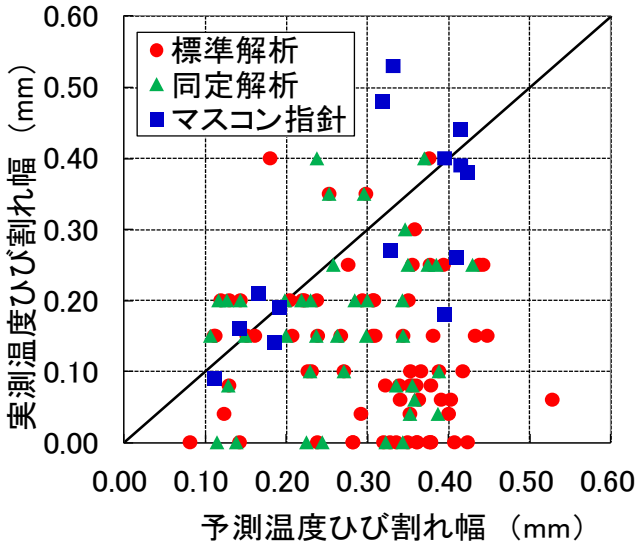

Figure 1-3 Relationship between actual and predicted crack width by JCI system

1.2 Yamaguchi prefecture database

Yamaguchi prefecture is among 47 prefectures of Japan which has established a crack control system for massive concrete structures by engaging all key stakeholders, i.e., local government, private companies, and academic institutions. PDCA cycle of Crack control system in Yamaguchi prefecture is shown in Figure 1-4.

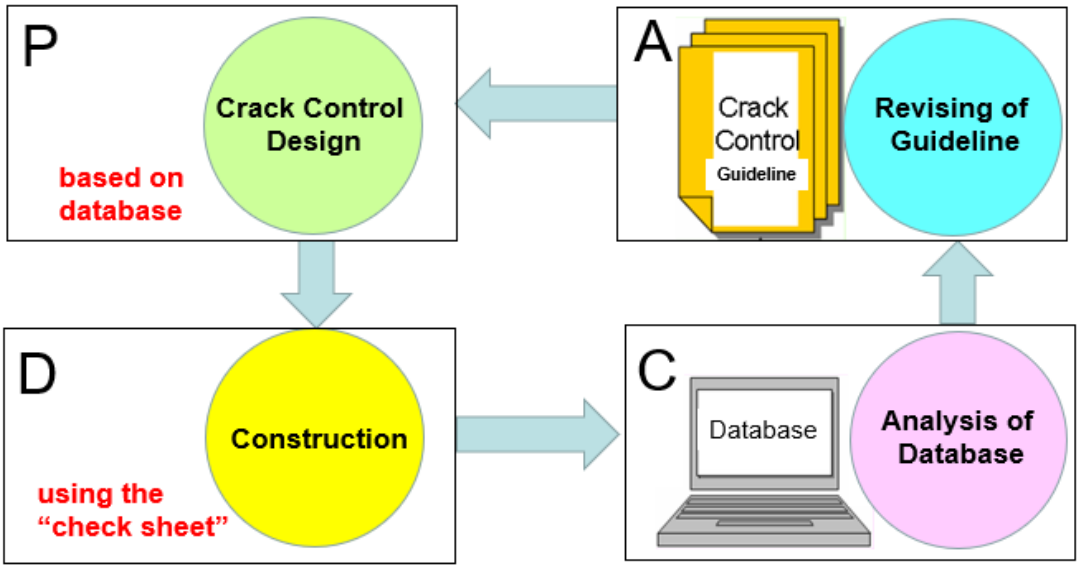

Figure 1-4 PDCA cycle of Crack control system in Yamaguchi prefecture

One vital component of this system is the database of structures established in 2005, in which all important geometric and material properties of structures are enlisted. Thermal properties measured in the structures are also included for some structures. This crack control system has shown an appreciable effectiveness in controlling thermal cracks with the passage of time. One of the reasons for the success of this system is that good concreting work has been achieved in their system. In this system, cracks with 0.15mm width (or more) have to be repaired. Data of each lift of structures with good concreting work has been accumulated in Yamaguchi prefecture database [3]. The performance of the Yamaguchi system for attaining the quality is demonstrated in Figures 1-5 and 1-6 for vertical walls considered in this study. It can be observed that with the passage of time, maximum crack width and percentage of harmful crack width reduced significantly.

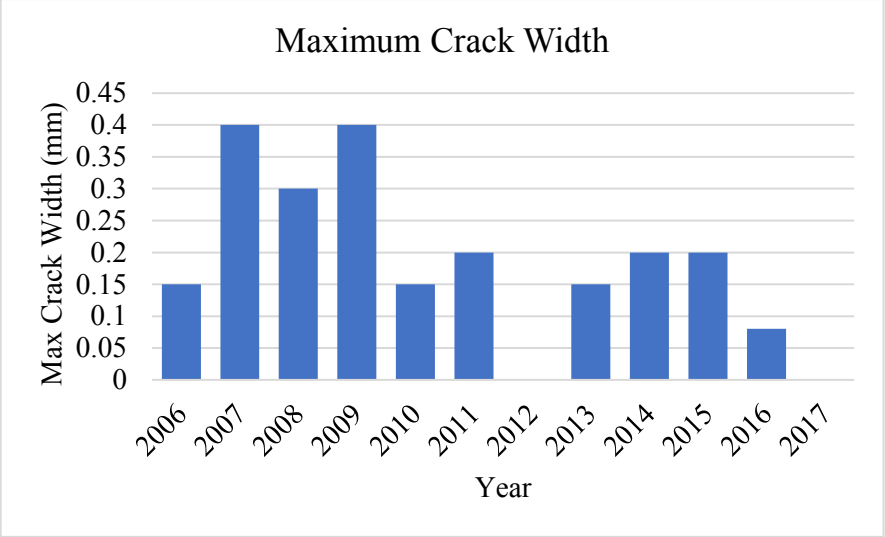

Figure 1-5 Year wise maximum crack width observed in vertical walls

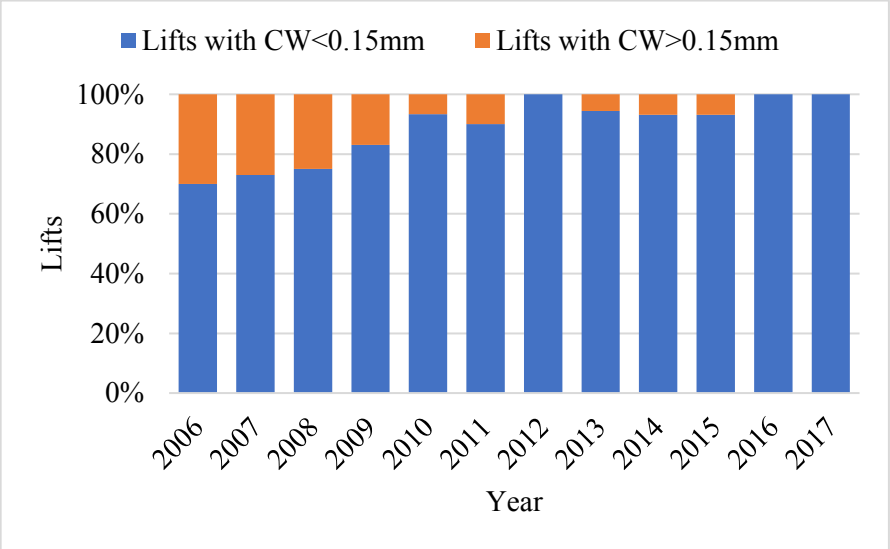

Figure 1-6 Year wise percentage of lifts of vertical walls with harmful cracking

1.3 Machine learning

Machine learning comes under the big umbrella of artificial intelligence (AI). It has been used to develop predictive models using empirical data without the necessity of having deep knowledge of the actual hidden physical mechanism [5], [6]. There are several types of machine leaning algorithms, for example, supervised learning, unsupervised learning, semi-supervised learning, reinforcement learning, transduction and learning to learn [7]. In supervised learning, the generated algorithms map the given outputs based on given inputs. Whereas, in unsupervised learning, models are generated without labelled responses. In semi-supervised learning, both labelled and unlabelled responses are

combined. In reinforced learning, algorithms learn according to a particular environment and environment provides the feedback to guide the learning environment. Transduction is like supervised learning, but instead of constructing a complicit function, it predicts new outputs by taking account the training inputs, training inputs and new outputs. Whereas, in learning to learn algorithms, algorithm learns its own bias based on its past experience [7].

1.3.1 Types of machine learning algorithms

The commonly used types of supervised learning algorithms are given as follows [8];

- Regression
    - Neural Networks
    - Decision Trees
    - Ensemble Methods
    - Nonlinear Regression
- Classification
    - Support Vector Machines
    - Naive Bayes
    - Discriminate Analysis
    - Nearest Neighbour
    - Neural Networks
    - Decision Trees
    - Ensemble Methods
    - Nonlinear Regression

The types of unsupervised learning algorithms are given as follows [8];

- Clustering
    - k-Means
    - Neural Networks
    - Gaussian Mixture
    - Hidden Markov Model
    - Hierarchical

1.4 Artificial neural networks

Artificial neural networks (ANNs) are based on the concept of biological neural networks in order to develop intelligent machines. ANNs consist of numerous numbers of parallel computing systems having a large number of interconnected simple processors. ANNs are powerful tools for classification, categorization, approximation, recognition and prediction [9]. They work as black-box and model-free with strong capability of learning and capturing essence of training data. Complex problems which are difficult to model and solve by conventional mathematical procedures can be good target problems for ANNs [10].

In the literature, ample applications of neural networks are reported in different fields. ANNs have been used in the field of structural engineering for structural analysis and design, design automation and optimization, damage diagnosis, fracture mechanics problems, structural system identification, structural condition assessment and monitoring, structural control, finite element mesh generation, structural material characterization and modelling, etc. [10].

Previously, using Yamaguchi prefecture database, Inadsu et al. made an attempt to predict the occurrence of thermal cracking and maximum accuracy was reported as 82.6 % for RC abutments [11].

1.5 Objectives

The key objectives of this research are as follows;

- Prediction of occurrence of thermal cracks in massive RC abutments using ANNs.
- Prediction of maximum thermal crack width of RC abutments using ANNs.
- Study on the influential parameters for maximum crack width using ANNs.

And the ultimate goal is to contribute in the guidelines to counter harmful thermal cracking for actual structures.

1.6 Methodology

In this study, an attempt is made to predict the occurrence of externally restrained thermal cracking and maximum crack width for RC abutments by using actual construction data from Yamaguchi prefecture database and Artificial neural networks (ANNs). One of the

key aspects is the choice of dataset. To obtain a reliable dataset to train, test and validate ANNs, dataset is sophisticated by removing suspicious entries and cross verification is performed for all entries of dataset. Dataset is divided into three portions, i.e., training, testing and holdouts for validation. 5-folds cross validation is also performed for performance evaluation of ANNs as shown in Table 1-1. T shows training and testing data and H shows holdouts for cross validation.

Table 1-1 Division of dataset in training and holdouts samples

K-Fold Cross Validation					
Dataset	**1**	**2**	**3**	**4**	**5**
Fold1	T	T	T	T	H
Fold2	T	T	T	H	T
Fold3	T	T	H	T	T
Fold4	T	H	T	T	T
Fold5	H	T	T	T	T

In this study, a feedforward type artificial network named as multilayer perception (MLP) was adopted. In MLP, supervised learning is carried out by backpropagation. It has three or more layers of nodes; input layer, hidden layer/layers and output layer. There can be one or more hidden layers. Each node in a layer is connected to all nodes of succeeding layer by a certain synaptic weight. Bias in input and hidden layers help the weighted sum of other nodes to obtain output. Values of biases are always 1 or some other constant that's why they are not connected to previous layers. When ANNs run, they use random number generation for subsamples selection and initialization of synaptic weights, which results into unidentical output after every run. So, it is important to optimize the results by ample number of trials. The details of ANNs used are categorically explained as follows;

1.6.1 Architecture of neural networks for prediction of occurrence of thermal cracking

In this study, the basic architecture of the ANN used to predict occurrence of thermal cracking is shown in Figure 1-7.

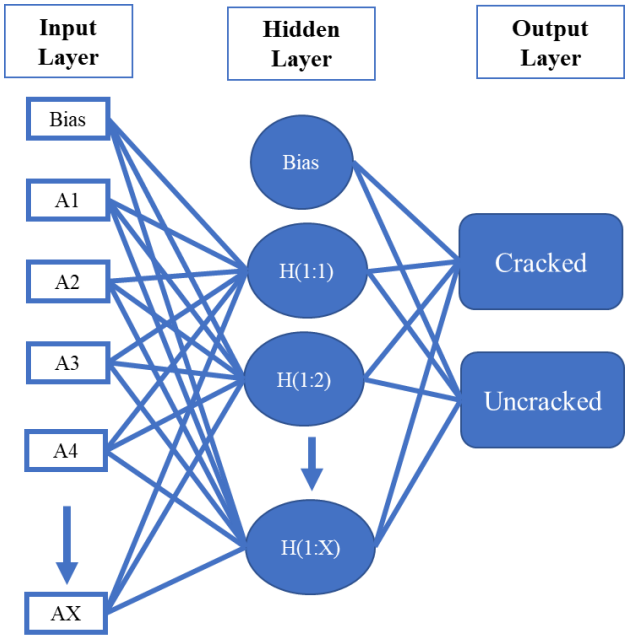

Figure 1-7 Architecture of ANN for prediction of cracks occurrence

To link the weighted sums of the nodes to the nodes of succeeding layer, activation function is needed [12], [13]. For hidden layer, hyperbolic tangent was used as an activation function. Equation for hyperbolic tangent function is given below in eq. 1. By this function, real-valued inputs (c) are transformed to the range from -1 to 1 [12].

$$Y(c) = \tanh(c) = \frac{e^{c} - e^{-c}}{e^{c} + e^{-c}} \qquad (1)$$

Softmax function was used as an activation function for output layer. The equation for softmax function is given below in eq. 2. This function transforms the vector of real-valued arguments (c) to a vector with the elements in the range from 0 to 1 and sum of 1 [12].

$$Y(c_k) = \frac{\exp(C_k)}{\sum_{i=1}^{k} \exp(C_k)} \qquad (2)$$

Scaled conjugate gradient was used as training function for estimation of synaptic weights. Output results are highly influenced by the input parameters, number of hidden layers and number of nodes in each hidden layer which depend on several factors i.e. quality and quantity of dataset, type of dataset, etc. So, it is important to select appropriate size of the network to avoid underfitting and overfitting. In this study, hit and trial method was employed to select appropriate number of nodes in the hidden layer. The trials were made by changing nodes in the hidden layer and those number were selected for which

prediction accuracy for holdout samples was higher to avoid overfitting. One hidden layer was used in all cases.

1.6.2 Architecture of neural networks for prediction of maximum thermal crack width

In this study, the basic architecture of the ANN used to predict maximum width of thermal cracking is shown in Figure 1-8.

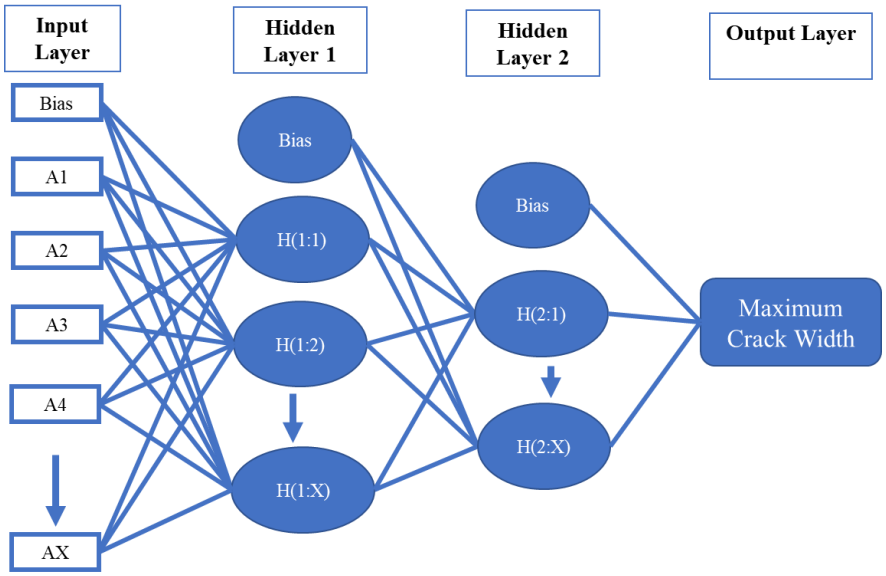

Figure 1-8 Architecture of ANN for prediction of maximum crack width

MATLAB with Machine Learning and Deep Learning Package was used for neural networks. For hidden layers, hyperbolic tangent was used as an activation function. Linear function was used as an activation function for output layer. Levenberg-Marquardt was used as training function for estimation of synaptic weights.

After development of appropriate machines, parametric studies were performed to give for proposals for design and construction practice.

1.6.3 Parametric studies on influential factors for maximum crack width

To study about the influential factors on maximum crack width, parametric studies are performed under different seasonal variations i.e., cold season, normal season and hot season. The effect of cement content, width, thickness, height, reinforcement ratio, lift interval and concrete strength are categorically studied.

2 Literature review

2.1 Prediction of early-age thermal-shrinkage cracking

In literature, some numerical methods are reported to predict thermal-shrinkage cracks. Some of those are summarized as follows;

JCI has a thermal and stress analysis-based system to predict probability of thermal cracking and maximum crack width. JCI also have an empirical equation to predict maximum crack width[1]. But, a considerable variation in the prediction and actual condition of cracking is reported. Yuan and Wan (2002) combined synthetic physical–mechanical processes, three-dimensional finite element and finite difference method to predict potential thermal-shrinkage cracks by considering effects of hydration, moisture transport and creep. Environmental influencing parameters, such as form removal time, curing conditions and ambient temperature and relative humidity. The study was performed on laboratory size specimen to obtain shrinkage strain and stress development with age. A good agreement was achieved between analytical and experimental results [14].

2.2 Applications of machine learning in civil engineering

In literatures, several applications of machine learning have been reported in the field of civil engineering. Many researchers used machine learning to predict compressive strength of concrete which is a vital characteristic of concrete. Young et al. (2019) predicted compressive strength of concrete mix proportions using a large dataset (<10,000 observations) by adopting machine learning approach. The developed models were used to design mixture proportions to satisfy strength requirement by minimizing cost and CO_2 emission. The root mean square error in prediction was reported as <10% [6]. Yu et al. (2018) used artificial neural networks to predict compressive strength of high-performance concrete using 1761 observation and reported a high accuracy with R^2 0.96. They also proposed a novel optimised self-learning method which resulted into least mean square error [15]. Deng et al. (2018) used deep learning to predict compressive strength of recycled concrete by using 74 sets of observations and reported that convolution neural network outperformed the conventional backpropagation neural network and support vector machine [16]. Naderpour et al. (2018) used artificial neural

networks to predict compressive strength of environmentally friendly concrete using 139 test samples and correlation coefficient was reported as 0.89 [17]. Chopra et al. (2018) predicted compressive strength of concrete using machine learning techniques to predict the compressive strength of concrete and reported that neural networks with R^2 0.91 outperformed the random forest and decision trees [18]. Nguyen et al. (2018) used high-order neural network to predict the strength of foamed concrete and a high correlation coefficient (0.9921) was reported [19]. Behnood et al. (2017) used M5P model tree algorithm to predict the compressive strength of normal and high-performance concrete using 1912 observations which showed R^2 0.9 [20]. Yaseen et al. (2017) proposed a machine learning algorithm named as extreme learning machine to predict compressive strength of foamed concrete and reported its superiority over multivariate adaptive regression spline (MARS), M5 Tree models and support vector regression (SVR) [21]. Chithra et al. (2016) used artificial neural networks in predicting compressive strength of high performance concrete containing Nano silica and copper slag using 264 observations and maximum reported R^2 was 0995 with root mean square error 1.0361 [22]. Abd and Abd (2016) used support vector machine to predict strength of lightweight foamed concrete and reported correlation was 0.99 with mean square error 3.267 [23]. Chou et al. (2014) reported the use of machine learning in predicting compressive strength of high strength concrete and reported that ensemble learning techniques (multiple classifiers, the voting, bagging, and stacking combination methods) were superior in performance than individual learning techniques (multilayer perceptron neural network, support vector machine, classification and regression tree, and linear regression [24]. Chou and Tsai (2012) also used machine learning to predict compressive strength of high strength concrete. Thy used hierarchical classification and regression approach which was reported as superior than the other conventional machine learning algorithms [25]. Dantas et al. (2012) used artificial neural networks in predicting compressive strength of concrete at 3, 7, 28, 91 days and achieved R^2 was 0.928 and 0.971 for training and testing phase, respectively [26]. Slonski (2010) used feed-forward layered neural networks to predict compressive strength of high strength concrete and reported Bayesian neural network as the most efficient among others with Pearson correlation coefficient R as high as 0.955 for testing phase [27].

Ding and An (2018) predicted workability of self-compacting concrete using deep learning approach and appreciable performance was reported for convolutional neural network and long short-term memory [28].

Mangalathu and Jeon (2018) used machine learning techniques to classify failure mode and predicted shear strength for RC beam-column joints using 536 experimental tests. Various machine learning techniques such as logistic, lasso logistic, discriminant analysis, k nearest neighbours, Naïve Bayes classification, support vector machines, decision trees, and random forest were used to establish a model to predict the failure mode and lasso regression model was suggested to predict failure modes [29]. Taffese and Sistonen (2017) reported the potential use of machine learning in structural health monitoring [8]. Reuter et al. (2017) predicted failure surfaces for concrete using machine learning approach using 88 experimental tests. Artificial neural networks, support vector machines and support vector regression were used to simulate the failure surface. Support vector regression outperformed the other methods as the total error was 1.94% which was lower than that given by the other machine learning methods and results were compared with the conventional methods, i.e. Drucker–Prager and Bresler–Pister surfaces [30]. Cheng and Shen (2017) used supervised learning to detect concrete abnormality [31]. Ye et al. (2018) used online machine learning for computerized hammer sound interpretation to assess the quality of concrete and reported its high efficiency [32].

Mangalathu and Jeon performed fragility analysis using support vector machine and reported its potential use in generating or updating the fragility curves for concrete bridges [33].

Cha et al. (2017) used convolution neural networks to detect crack damage using images. Activation function for hidden layer and output layer were ReLU and Softmax, respectively. The reported accuracy was 97.95% for training and validation [34]. Chatterjee et al. proposed a particle swarm optimization-based approach to train the neural networks to predict structural failure damage. The reported accuracy level was more than 90% which was claimed to be superior than common neural networks [35]. Pandey and Barai (1995) used MLP with two hidden layers and sigmoid function as an activation function for hidden layers were used to detect damage in steel bridges [36].

Aguilar et al. (2016) used artificial neural networks to predict the in-plane shear strength of reinforced masonry walls by utilising large experimental dataset (285 results). One

hidden layer was used with sigmoid activation function. The Lavenberg–Marquardt algorithm for training was used and training was performed by back propagation. Maximum achieved R^2 was greater than 0.9 [37]. Gupta et al. (2015) proposed the use of neural networks for predicting deflection in multi-span continuous steel-concrete composite bridges by taking input from numerical simulation technique. The Lavenberg–Marquardt algorithm for training was used and training was performed by back propagation using one hidden layer. A high level of accuracy (>95%) was achieved [38]. Lee and Lee (2014) used artificial neural networks to predict the shear strength of FRP-reinforced concrete flexural members using 106 tests set. Network was trained by back propagation and two hidden layers were used. A high level accuracy (>95%) was reported [39]. Plevris and Asteris (2014) used ANNs to predict masonry failure surface. Hyperbolic tangent activation function was used for hidden layers [40]. Mansouri and Kisb (2015) used neuro fuzzy and neural networks to predict debonding strength of masonry elements retrofitted with FRP composites and reported that combination of neuro fuzzy interface and ANN outperformed the other methods, i.e. multiple nonlinear regression, multiple linear regression and existing bond strength models [41]. Sanad and Saka (2001) used ANNs to predict the ultimate shear strength of RC deep beams using 111 samples. The results from ANNs were compared with other conventional methods, i.e. ACI, strut-and-tie, and Mau-Hsu methods. Performance of ANNs was reported as superior than the other methods [42].

Gopalakrishnan et al. (2017) used pre-trained deep convolution neural networks to detect pavement distress using transfer learning and big data of images (1056 samples). ReLU activation function was used in all hidden layers. The accuracy level in case of deep neural network was more than 0.9 and it outperformed other classifiers i.e. random forest, extremely random trees classifier, support vector machine and logistic regression [43]. Ling et al. (2017) predicted top-down cracking for asphalt pavement using numerical modelling and artificial networks. Using FEM, 194,400 cases were generated to give input for ANNs. Training was performed by back propagation. The Levenberg-Marquardt algorithm was employed for training. Reported R^2 was 0.99 which showed the potential of using ANNs [44]. Mirabdolazimi and Shafabakhsh (2017) used genetic programming and ANNs to predict rutting depth. The Levenberg-Marquardt algorithm was employed for training and high level of accuracy was achieved [45]. Gajewski and Sadowski (2014) used a hybrid artificial neural networks and finite element method to

perform sensitivity analysis of crack propagation in pavement bituminous layered structures. Some inputs for neural networks were obtained by preforming finite element analysis. The purpose of using ANNs was analogues to non-destructive testing to evaluate the material behaviours and crack propagation. Multilayer perceptron neural network reportedly performed better than Radial basis function neural network. Accuracy level of MLP NN was more than 90% [46]. Wu et al. (2014) used an ANN approach based on semi analytical FEA to predict stress intensity factor in pavement cracking. The activation functions for hidden layers and output layers were sigmoid and linear function, respectively. A high level of accuracy with 0.99 R^2 was reported [47]. Zhang et al. (2016) predicted road cracks using deep convolution neural network using images using ReLU as an activation function. The performance of CNN was reportedly superior than SVM and Boosting [48].

Ghafari et al. (2015) predicted fresh and hardened state properties of Ultra-high-performance-concrete using 53 mixtures. Binary sigmoid function was used as an activation function. A high level of accuracy (>95%) was reported [49]. Suleiman and Nehdi (2017) used hybrid genetic algorithm artificial neural network to model self-healing of concrete. Self-healing shows the way of modelling the width. Feed forward ANN with one hidden layer was used and tan-sigmoid function was used as an activation function for hidden layer and linear function for output layer. A high accuracy level (R^2>0.95) was reported [50]. Park et al. used ANNs to predict the properties of cement paste and sigmoid function was used as an activation function for hidden layers. ANNs showed good agreement with experimental results [51].

Jiang et al. (2016) used artificial neural networks to predict corrosion of concrete sewers using 4.5 years long corrosion data. Performance of ANNs was reportedly superior than multiple regression and a high accuracy level (>90%) was achieved for ANNs [52].

3 Characteristics of dataset

3.1 General

In Yamaguchi prefecture database, around 1555 lifts of concrete structures are enlisted since 2005 to date. For this research, 386 lifts of abutments were chosen. Among the reliable dataset, 24 lifts were ignored in which some other types of reinforcing materials than steel were used. Remaining 362 lifts of RC abutments were further categorized into 248 lifts of vertical walls and 114 lifts of parapet walls.

Table 3-1 Number of valid samples, missing data points and range of properties for vertical walls and parapets

Property	Lifts of Vertical Walls			Lifts of Parapet Walls		
	Valid	Missing	Range of Data	Valid	Missing	Range of Data
Maximum Crack Width (mm)	248	0	0~0.4	113	0	0.04~0.3
Thickness (m)	248	0	0.7~3.0	113	0	0.4~1.5
Width (m)	248	0	3.1~25	113	0	4.2~28.5
Lift Hight (m)	248	0	0.6~5.4	113	0	0.5~4.3
Reinforcement Ratio (%)	247	1	0.03~ 0.64	101	12	0.08~1.13
W/C (%)	242	6	49~55	110	3	49~55
Cement Content (kg/m^3)	233	15	282~333	106	7	277~331
Expansive Additive (kg/m^3)	248	0	0 or 20	113	0	0 or 20
Slump (mm)	228	20	6~10.5	103	10	6.5~10
Air Content (%)	228	20	3.6~5.8	103	10	3.7~5.6
Initial Concrete Temperature (^{o}C)	247	1	6~32	102	11	6~32
Initial Ambient Temperature (^{o}C)	247	1	-1.3~31	104	9	1~31
Concrete Strength (MPa)	235	13	28.1~ 40.9	99	14	28.9~40.8
Lift Interval (day)	235	13	3~139	106	7	1~94
Maximum Temperature (^{o}C)	200	48	16~75.5	77	36	13.6~69.1
Maximum Temperature Time (hr)	198	50	15~119	80	33	5.8~106
Form Removal Time (day)	238	10	2~74	96	17	2~35
Curing Period (day)	232	16	1~42	92	21	1~28

Among 248 lifts of vertical walls, 96 lifts were cracked, and 152 lifts were uncracked. And, maximum crack width was ranging from 0.04 mm to 0.4 mm. Among 114 lifts of parapet walls, 23 lifts were cracked, and 91 lifts were uncracked. And, maximum crack width was ranging from 0.04 mm to 0.3 mm.

Number of valid samples, missing data points and range of the data for both vertical and parapet walls are summarized in Table 3-1. Missing data points are partially those which were not measured in actual structures and remaining due to removal of ambiguous and apparently wrong entries to get reliable dataset.

Other properties which were not used in the study but represent the range of the properties in the dataset are summarised in Table 3-2.

Table 3-2 Number of valid samples, missing data points and range of other properties for vertical walls and parapets

Property	Lifts of Vertical Walls			Lifts of Parapet Walls		
	Valid	Missing	Range of Data	Valid	Missing	Range of Data
Chloride Content (%)	228	20	0.01~0.1	113	0	0.04~0.3
7-days Concrete Strength	222	26	16~29.7	113	0	0.4~1.5
Casting Month	248	0	Jan ~ Dec	113	0	4.2~28.5
Seasons	248	0	All	113	0	0.5~4.3
Maximum Temperature Rise (^{o}C)	198	50	6~57.4	113	41	2.7~38.1

In this study, several geometric and material properties of RC abutments were used, for example, thickness (m), width (m), lift height (m), reinforcement ratio in horizontal direction (%), water to cement ratio, unit cement content (kg/m3), unit content of expansive additive (kg/m^3), slump (mm), air content (%), initial concrete temperature (^{o}C), initial ambient temperature (^{o}C), 28-days concrete strength (MPa), lift interval (day), maximum temperature (^{o}C), maximum temperature time (hour), form removal time (day) and curing period (day).

Lift interval is the time gap between previous lift and the lift under consideration. Maximum temperature and maximum temperature rise were measured in the middle thickness of the lift. Curing period is the time for which the finished surface of a lift is

cured. Several diverse types of curing methods are included, for example, water sprinkling, blue sheets, blue sheet + sprinkling, curing mat, ponding etc., however the difference of curing methods were not investigated in this research. Characteristics of vertical and parapet walls are categorically explained in the following section.

3.2 Characteristics of vertical walls

3.2.1 Geometric properties

In the dataset, the lifts of vertical walls were 0.7 to 3.0 m thick with mean thickness 1.72 m and standard deviation was 0.439. The width was in the range of 3.1 to 25 m with mean width 10.92 m and standard deviation was 4.655. The range of the height of the lifts was 0.6 to 5.4 m with mean height 2.6 m and standard deviation was 0.92. The histograms for thickness, width and the height of the lifts of vertical walls are shown in Figures 3-1 and 3-2.

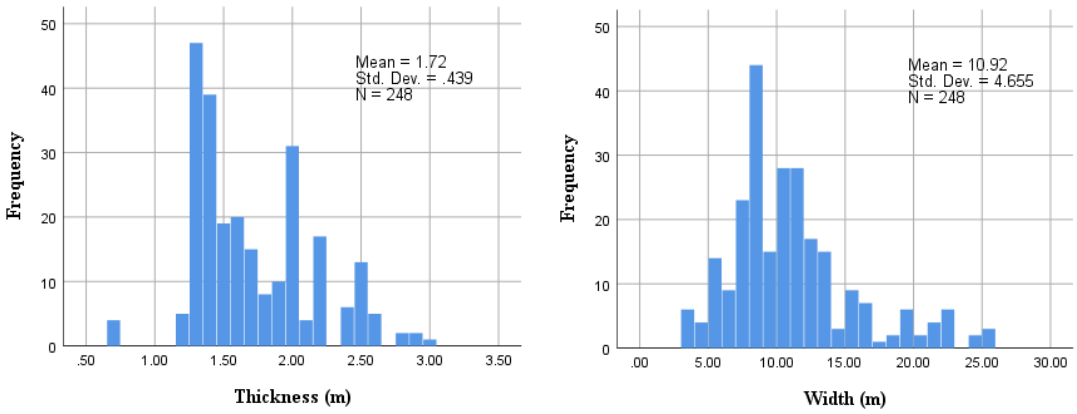

Figure 3-1 Histograms of thickness and width of the lifts of vertical walls

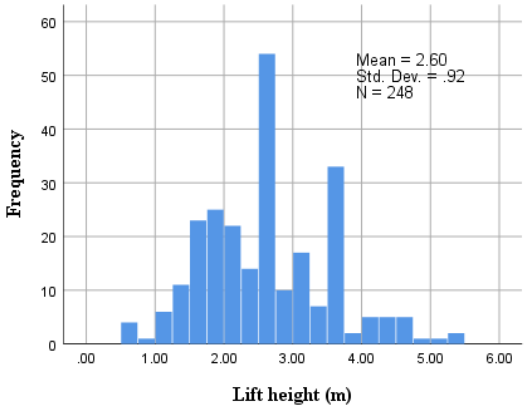

Figure 3-2 Histogram of heights of the lifts of vertical walls

3.2.2 Properties of materials

The range of properties of difference materials used in the vertical walls are summarised in this section. The range for reinforcement ratio was from 0.03 to 0.64 % with mean reinforcement ratio 0.21 % and standard deviation was 0.125. The range of unit cement content was from 282 to 333 kg/m^3 with mean unit cement content 301.04 kg/m^3 and standard deviation was 9.137. The range of water to cement ratio was from 49 to 55% with mean water to cement 53.71 % and standard deviation was 1.525. Among 248 lifts of vertical walls, expansive additive was used only in 5 lifts. The histograms for reinforcement ratio, unit cement content and water to cement ratio are shown in Figures 3-3 and 3-4.

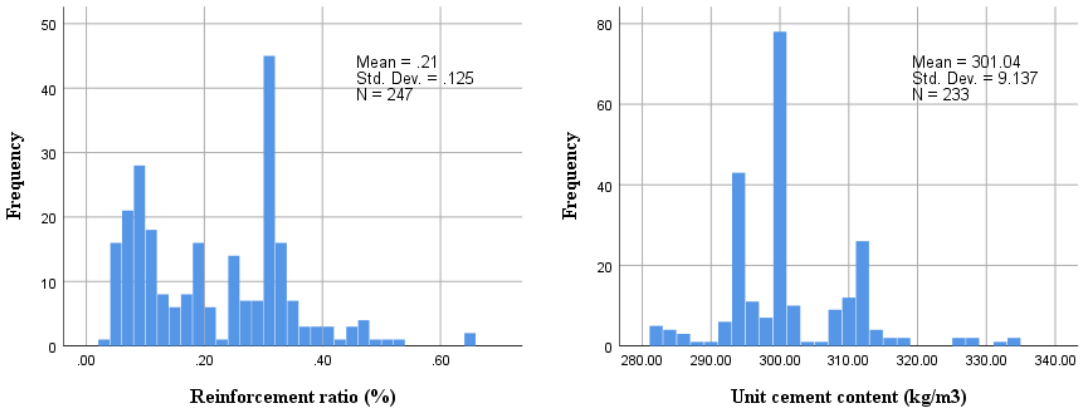

Figure 3-3 Histograms of reinforcement ratio and unit cement content of the lifts of vertical walls

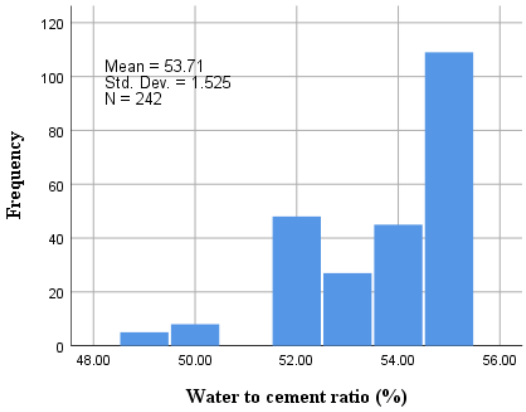

Figure 3-4 Histogram of water to cement ratio of the lifts of vertical walls

3.2.3 Properties of fresh concrete

The properties of fresh concrete are summarised in this section. The range of initial concrete temperature was from 6 to 32 ºC with mean temperature 16.35 ºC and standard deviation was 6.46. The range of slump was from 6 to 10.5 mm with mean slump 8.57 mm and standard deviation was 0.787. The range of air content was from 3.6 to 5.8%, with mean air content 4.73 % and standard deviation was 0.766. The range of chloride content in concrete was from 0.01 to 0.1 %, with mean chloride content 0.03 % and standard deviation was 0.014. the histograms of initial concrete temperature, slum, air content and chloride content are shown in Figures 3-5 and 3-6.

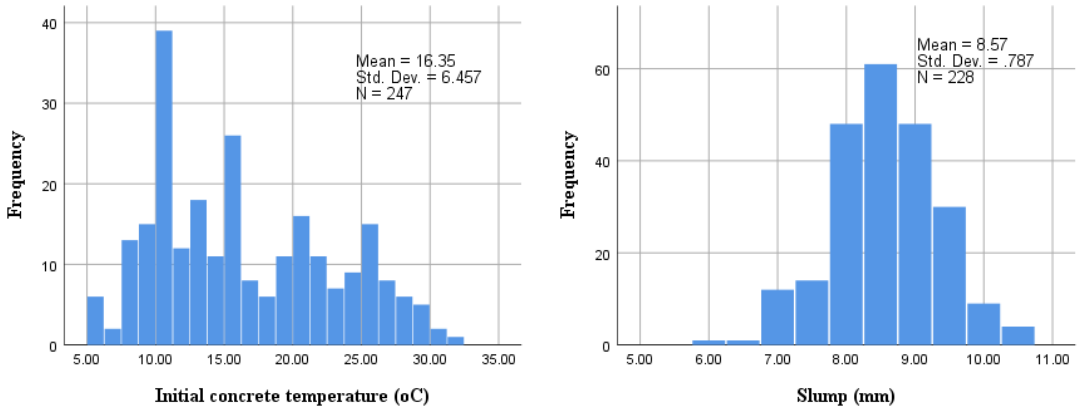

Figure 3-5 Histogram of initial concrete temperature and slump of the lifts of vertical walls

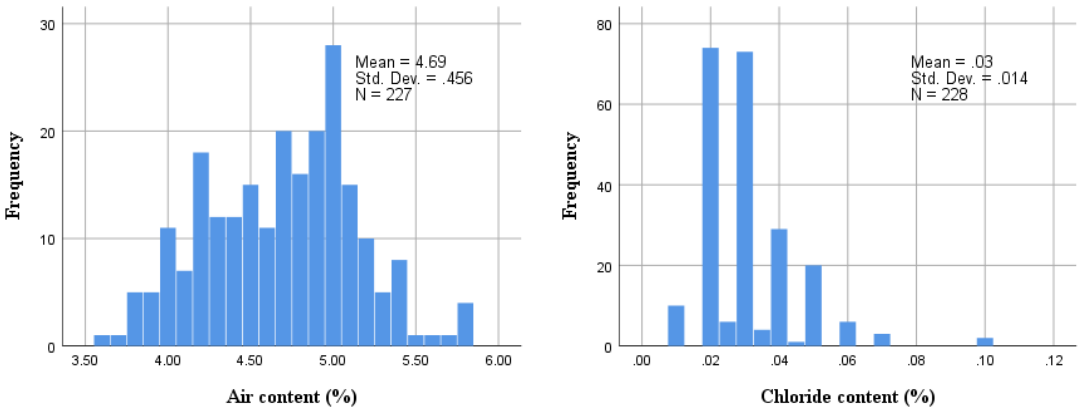

Figure 3-6 Histograms of air content and chloride content of the lifts of vertical walls

3.2.4 Strength properties of concrete

The strength properties of concrete are summarised in this section. The range of 7-day concrete strength was from 16 to 29.7 MPa with mean strength 21.58 MPa and standard

deviation was 2.27. The range of 28-day concrete strength was from 28.1 to 40.9 MPa with mean strength 34.25 MPa and standard deviation was 2.09. The histograms of 7-day concrete strength and 28-day concrete strength are shown in Figure 3-7.

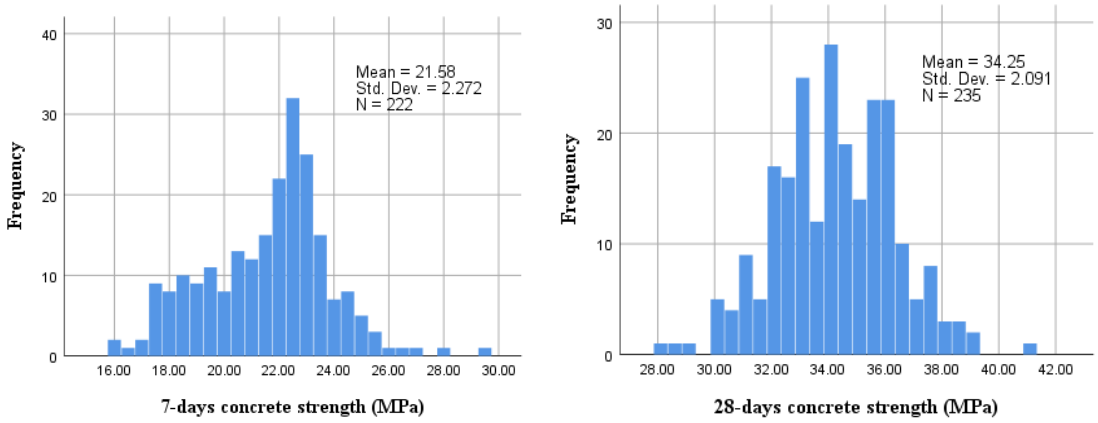

Figure 3-7 Histograms of 7-day and 28-day concrete strength of the lifts of vertical walls

3.2.5 Ambient environmental properties

The ambient environmental properties are summarised in this section. The range of initial ambient temperature was from -1.3 to 31 ^{o}C with mean temperature 13.13 ^{o}C and standard deviation was 7.73. The data contained distributed representation of lifts constructed throughout the year. The number of vertical walls constructed in autumn, spring, summer and winter were 52, 68, 39 and 89, respectively. The histograms for initial ambient temperature and month of construction are shown in Figure 3-8.

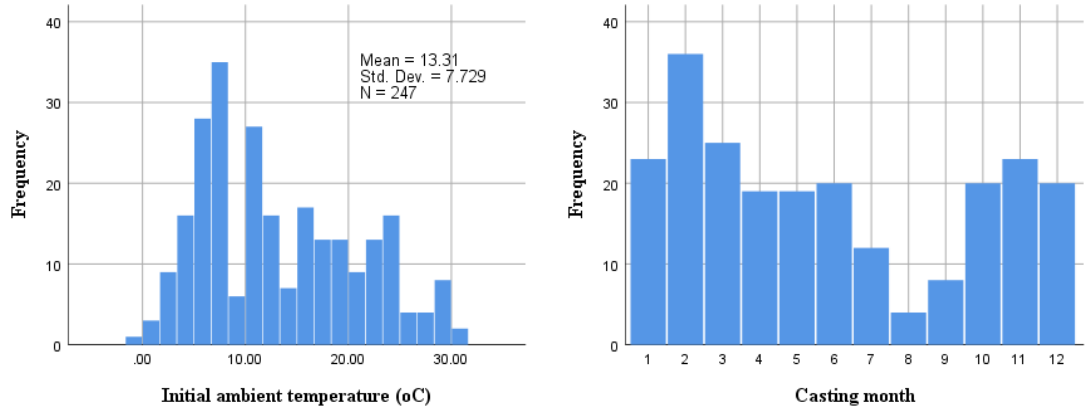

Figure 3-8 Histograms of initial ambient temperature and casting month of the lifts of vertical walls

3.2.6 Temperature properties

Temperature properties are referred to the change in temperature of concrete temperature due to heat of hydration. Temperature was measured at middle thickness of the lift. The range of maximum temperature at middle thickness of lifts was from 16 to 75.5 ^{o}C with mean temperature 52.34 ^{o}C and standard deviation was 11.51. The range of maximum temperature rise at middle thickness of lifts was from 6 to 57.4 ^{o}C with mean temperature rise 35 ^{o}C and standard deviation was 9.1. The range of maximum temperature time at middle thickness of lifts was from 15 to 119 hrs with mean time 59.09 hrs and standard deviation was 19.22. The histograms of maximum temperature in the middle thickness, maximum temperature rise, and maximum temperature time are shown in Figures 3-9 and 3-10.

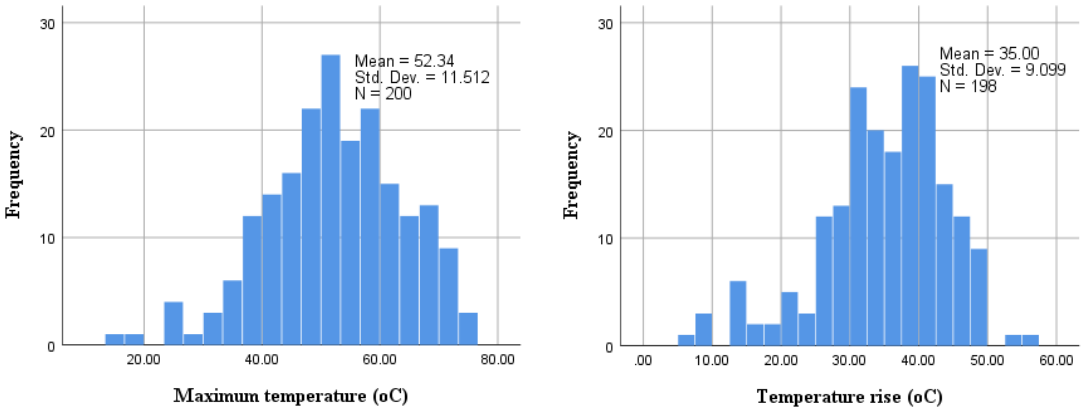

Figure 3-9 Histograms of maximum temperature and temperature rise of the lifts of vertical walls

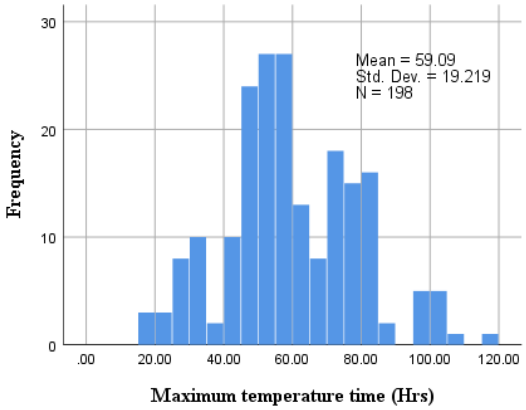

Figure 3-10 Histogram of the maximum temperature time of the lifts of vertical walls

3.2.7 Other properties

Some other properties which were also recorded in the database are summarised in this section. The range of lift interval was from 3 to 139 day with mean time 23.91 day and standard deviation was 18.59. Lift interval was referred to the time gap between two consecutive lifts. The range of form removal time was from 2 to 74 day with mean time 14.95 day and standard deviation was 11.443. The range of curing period was from 1 to 42 day with mean time 9.37 day and standard deviation was 4.528. Curing period is referred to the curing time for top finished surface of lift under consideration. The range of restraint level was from 1 to 7.24 with mean time 2.13 and standard deviation was 1.275. The restraint level is referred to the ratio of area of restraining surface to the area of retrained surface. The histograms of lift interval, form removal time, curing period and restraint level are shown in the Figures 3-11 and 3-12.

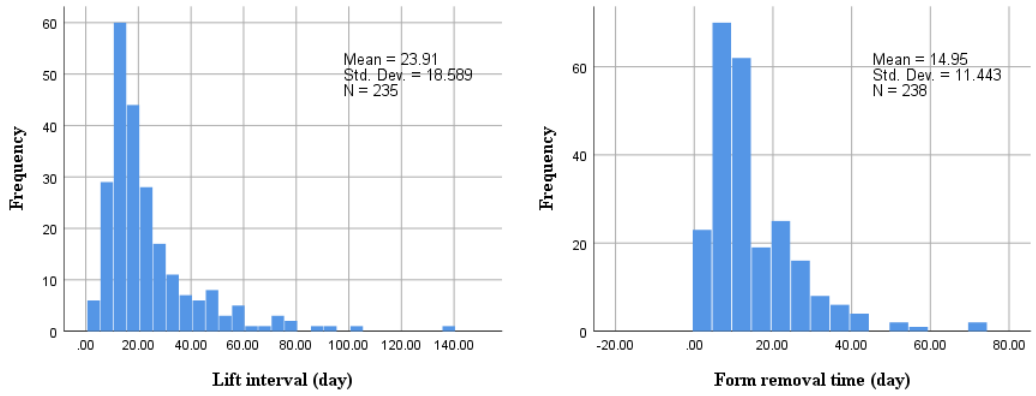

Figure 3-11 Histogram of the lift interval and form removal time of the lifts of vertical walls

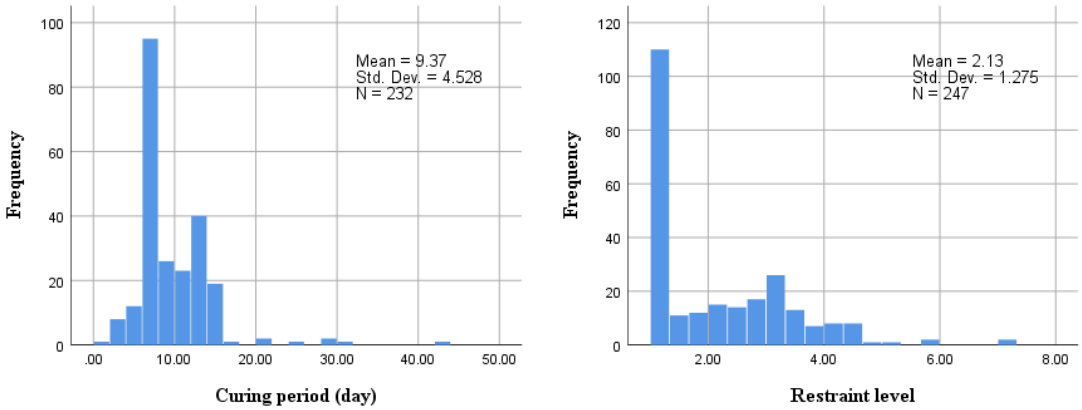

Figure 3-12 Histogram of the curing period and restraint level of the lifts of vertical walls

3.2.8 Cracking condition of the lifts of the vertical walls

In the dataset, among 248 lifts of vertical walls, 94 lifts were cracked whereas 154 lifts were uncracked. The range of maximum thermal crack width was from 0.04 to 0.4 mm with mean maximum crack width 0.06 mm and standard deviation was 0.089. The range of total thermal crack width was from 0.04 to 1.45 mm with mean total crack width 0.12 mm and standard deviation was 0.21. The range of number of cracks was from 1 to 10 cracks. The histograms for maximum crack width, total crack width and number of cracks are shown in Figures 3-13 and 3-14.

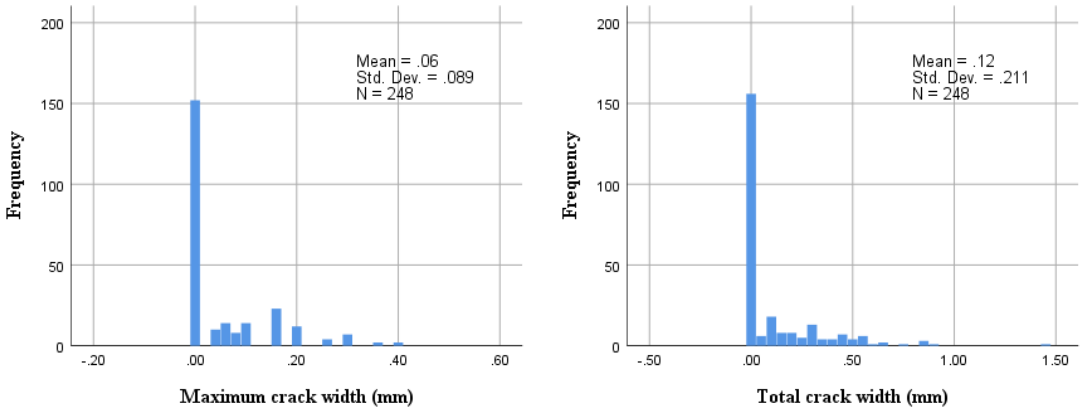

Figure 3-13 Histograms of the maximum crack width and total crack width of the lifts of vertical walls

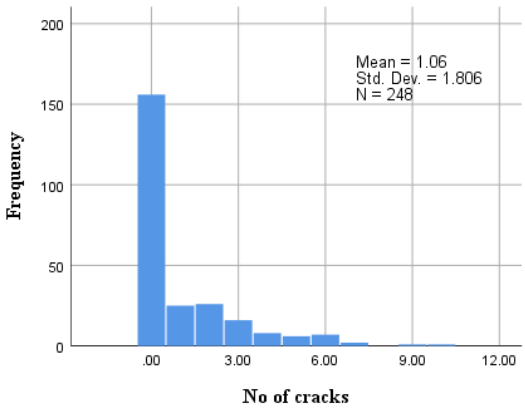

Figure 3-14 Histogram of the number of cracks of the lifts of vertical walls

3.3 Characteristics of parapet walls

3.3.1 Geometric properties

In the dataset, the lifts of parapet walls were 0.4 to 1.5 m thick with mean thickness 0.6 m and standard deviation was 0.195. The width was in the range of 3.1 to 28.5 m with mean width 11.51 m and standard deviation was 4.998. The range of the height of the lifts was 0.5 to 4.3 m with mean height 1.67 m and standard deviation was 0.96. The histograms for thickness, width and the height of the lifts of vertical walls are shown in Figures 3-15 and 3-16

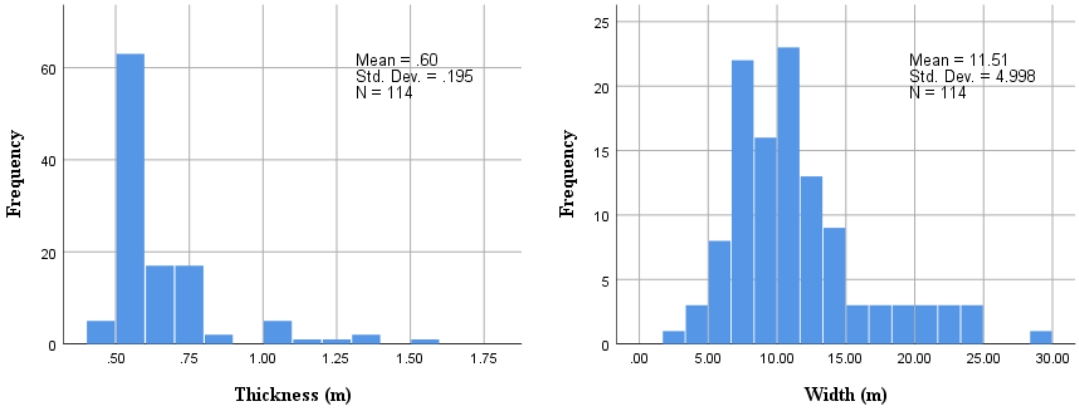

Figure 3-15 Histograms of the thickness and width of the lifts of parapet walls

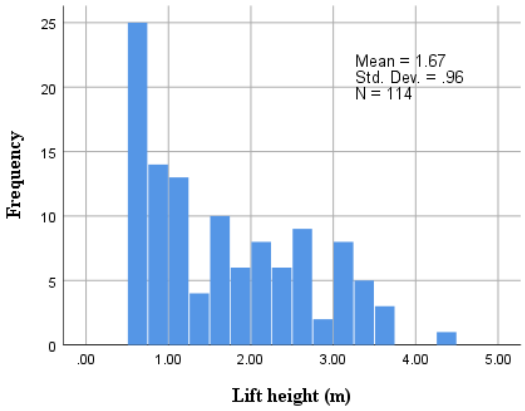

Figure 3-16 Histogram of the height of the lifts of parapet walls

3.3.2 Properties of materials

The range of properties of difference materials used in the vertical walls are summarised in this section. The range for reinforcement ratio was from 0.08 to 1.13 % with mean reinforcement ratio 0.42 % and standard deviation was 0.212. The range of unit cement

content was from 277 to 331 kg/m^3 with mean unit cement content 300.09 kg/m^3 and standard deviation was 9.881. The range of water to cement ratio was from 49 to 55% with mean water to cement 53.67 % and standard deviation was 1.569. Among 248 lifts of vertical walls, expansive additive was used in 15 lifts. The histograms for reinforcement ratio, unit cement content and water to cement ratio are shown in Figures 3-17 and 3-18.

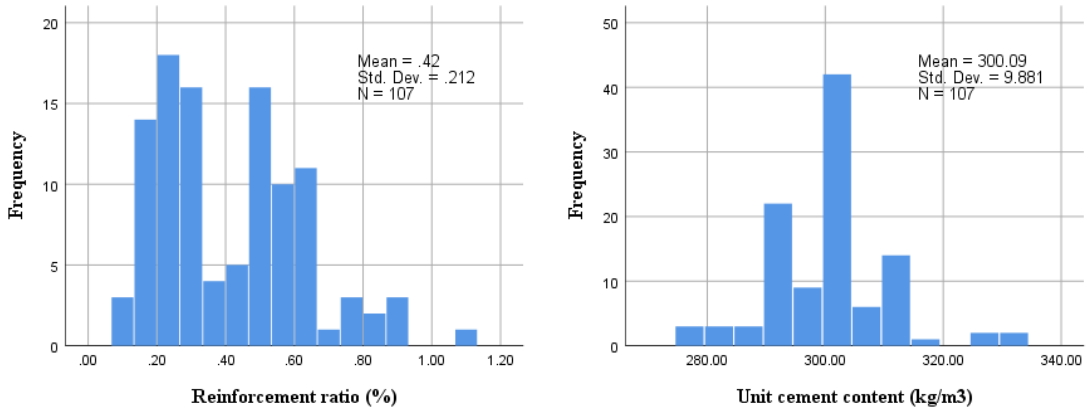

Figure 3-17 Histograms of the reinforcement ratio and unit cement content of the lifts of parapet walls

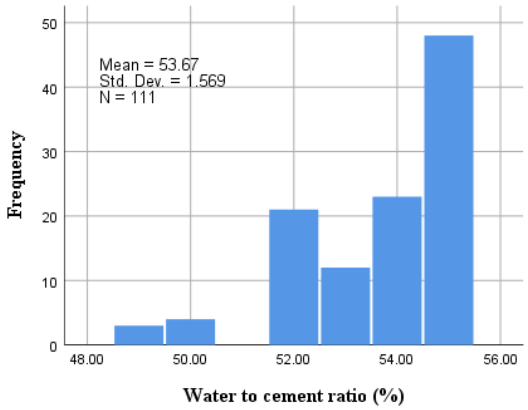

Figure 3-18 Histogram of the water to cement content of the lifts of parapet walls

3.3.3 Properties of fresh concrete

The properties of fresh concrete are summarised in this section. The range of initial concrete temperature was from 6 to 34 ^{o}C with mean temperature 17.72 ^{o}C and standard deviation was 7.332. The range of slump was from 6.5 to 10.0 mm with mean slump 8.38 mm and standard deviation was 0.872. The range of air content was from 3.7 to 5.6%, with mean air content 4.56 % and standard deviation was 0.472. The range of chloride content in concrete was from 0.01 to 0.07 %, with mean chloride content 0.03 % and

standard deviation was 0.012. the histograms of initial concrete temperature, slum, air content and chloride content are shown in Figures 3-19 and 3-20.

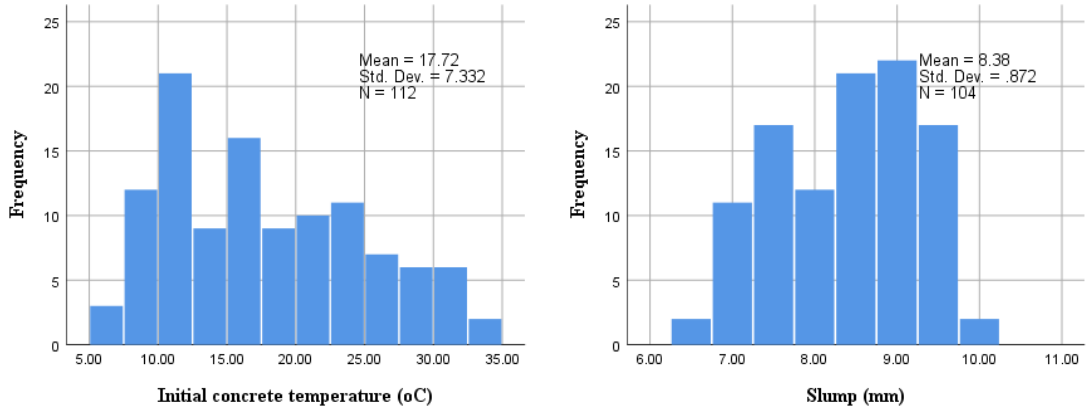

Figure 3-19 Histograms of the initial concrete temperature and slump of the lifts of parapet walls

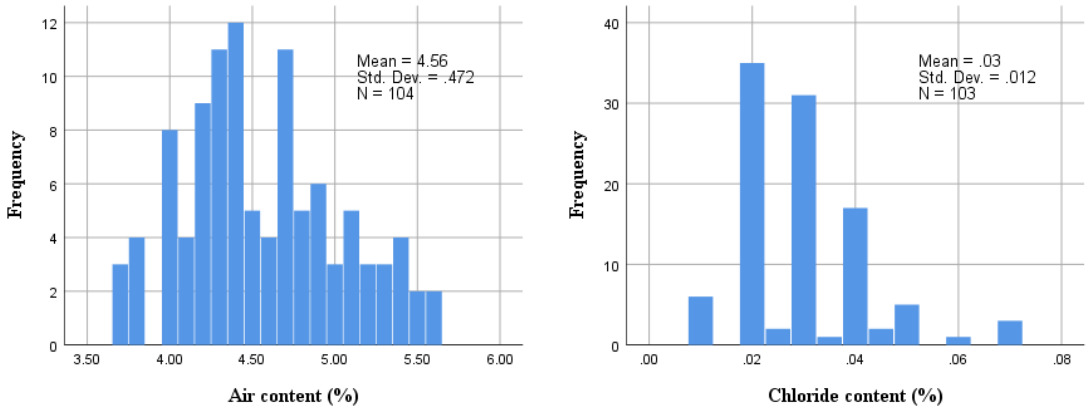

Figure 3-20 Histograms of the air content and chloride content of the lifts of parapet walls

3.3.4 Strength properties of concrete

The strength properties of concrete are summarised in this section. The range of 7-day concrete strength was from 17 to 27.1 MPa with mean strength 21.76 MPa and standard deviation was 2.203. The range of 28-day concrete strength was from 28.9 to 40.8 MPa with mean strength 34.25 MPa and standard deviation was 2.391. The histograms of 7-day concrete strength and 28-day concrete strength are shown in Figure 3-21.

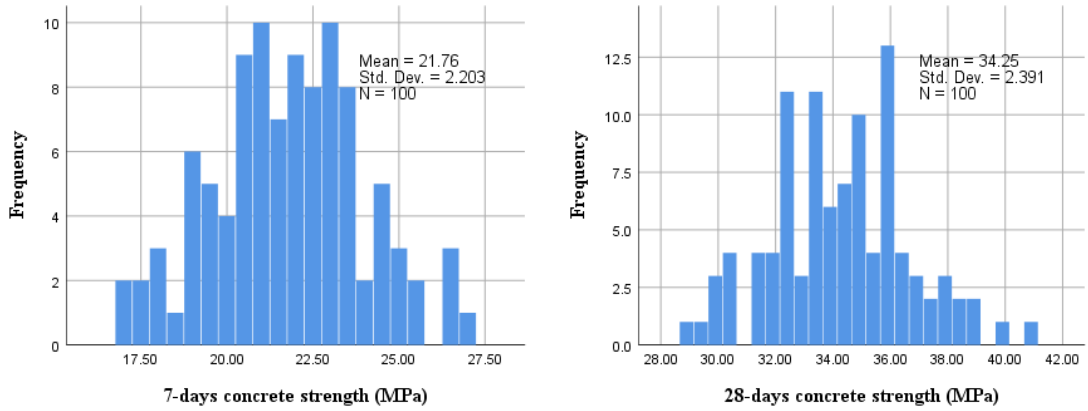

Figure 3-21 Histograms of the 7- day and 28- day concrete strength of the lifts of parapet walls

3.3.5 Ambient environmental properties

The ambient environmental properties are summarised in this section. The range of initial ambient temperature was from 1 to 31 ºC with mean temperature 15.03 ºC and standard deviation was 8.07. The data contained distributed representation of lifts constructed throughout the year. The number of vertical walls constructed in autumn, spring, summer and winter were 20, 34, 28 and 32, respectively. The histograms for initial ambient temperature and month of construction are shown in Figure 3-22.

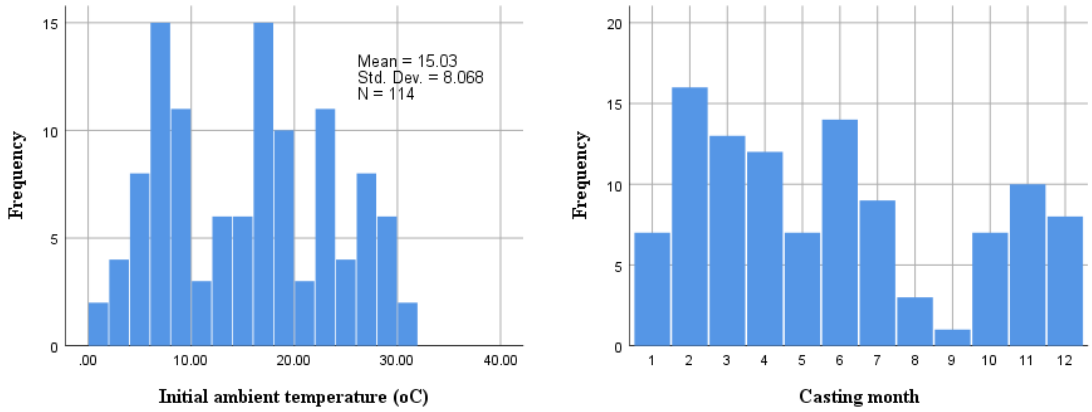

Figure 3-22 Histograms of the initial ambient temperature and casting month of the lifts of parapet walls

3.3.6 Temperature properties

Temperature properties are referred to the change in temperature of concrete temperature due to heat of hydration. Temperature was measured at middle thickness of the lift. The range of maximum temperature at middle thickness of lifts was from 13.6 to 69.1 ºC with

mean temperature 38.96 ºC and standard deviation was 12.58. The range of maximum temperature rise at middle thickness of lifts was from 2.7 to 38.1 ºC with mean temperature rise 20.79 ºC and standard deviation was 9.299. The range of maximum temperature time at middle thickness of lifts was from 5.8 to 106 hrs with mean time 39.03 hrs and standard deviation was 18.149. The histograms of maximum temperature in the middle thickness, maximum temperature rise, and maximum temperature time are shown in Figures 3-23 and 3-24.

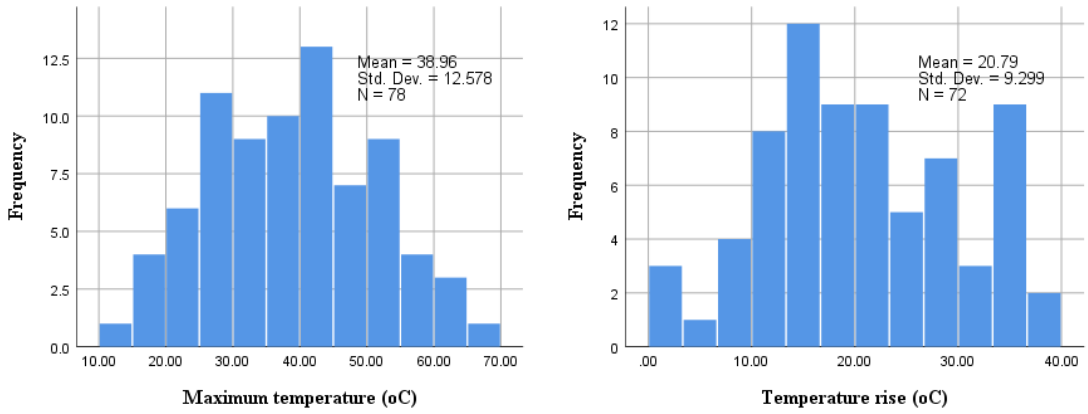

Figure 3-23 Histograms of the maximum temperature and temperature rise of the lifts of parapet walls

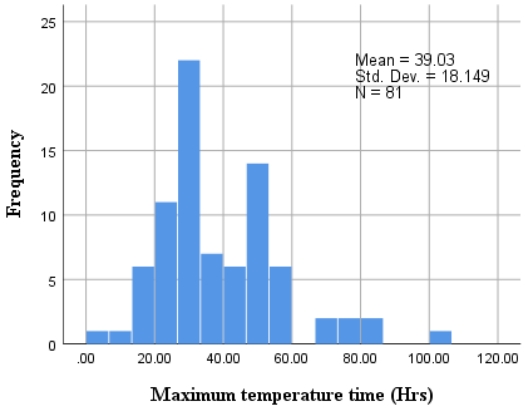

Figure 3-24 Histograms of the maximum temperature time of the lifts of parapet walls

3.3.7 Other properties

Some other properties which were also recorded in the database are summarised in this section. The range of lift interval was from 1 to 94 day with mean time 16.52 day and standard deviation was 15.587. Lift interval was referred to the time gap between two consecutive lifts. The range of form removal time was from 2 to 35 day with mean time 9.79 day and standard deviation was 5.306. The range of curing period was from 1 to 28

day with mean time 8.81 day and standard deviation was 3.7. Curing period is referred to the curing time for top finished surface of lift under consideration. The range of restraint level was from 1 to 7 with mean time 2.95 and standard deviation was 0.914. The restraint level is referred to the ratio of area of restraining surface to the area of retrained surface. The histograms of lift interval, form removal time, curing period and restraint level are shown in the Figures 3-25 and 3-26.

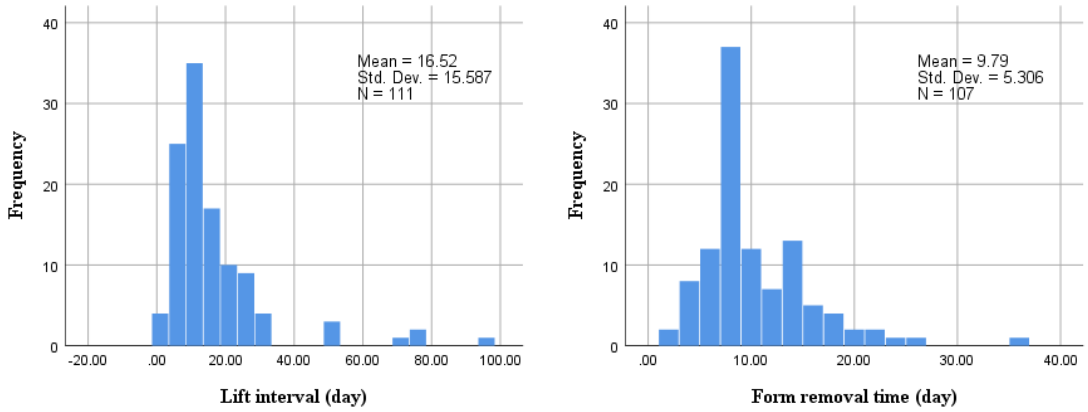

Figure 3-25 Histograms of the lift interval and form removal time of the lifts of parapet walls

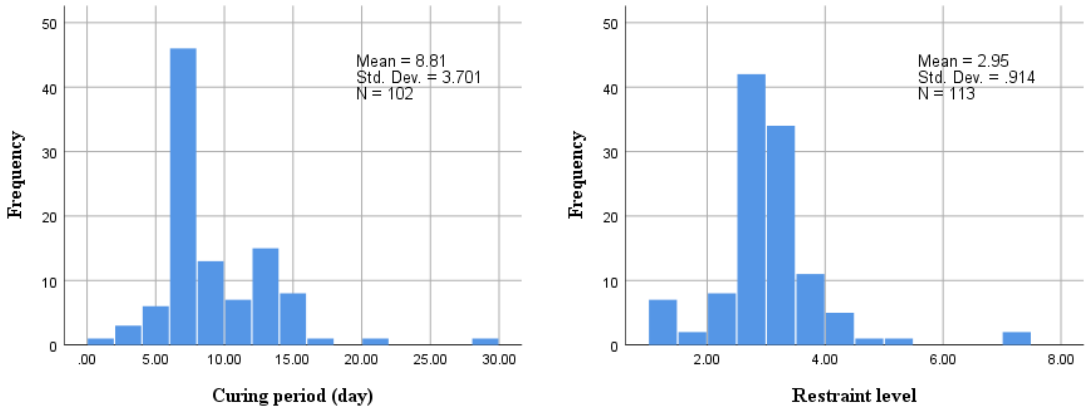

Figure 3-26 Histograms of the curing period and restraint level of the lifts of parapet walls

3.3.8 Cracking condition of the lifts of the parapet walls

In the dataset, among 114 lifts of parapet walls, 23 lifts were cracked whereas 91 lifts were uncracked. The range of maximum thermal crack width was from 0.04 to 0.3 mm with mean maximum crack width 0.03 mm and standard deviation was 0.066. The range of total thermal crack width was from 0.04 to 1.06 mm with mean total crack width 0.07 mm and standard deviation was 0.188. The range of number of cracks was from 1 to 9

cracks. The histograms for maximum crack width, total crack width and number of cracks are shown in Figures 3-27 and 3-28.

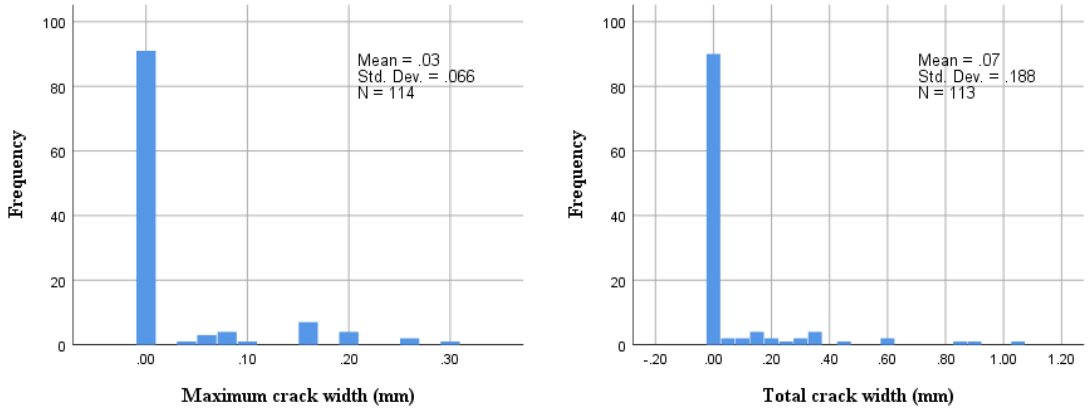

Figure 3-27 Histograms of the maximum crack width and total crack width of the lifts of parapet walls

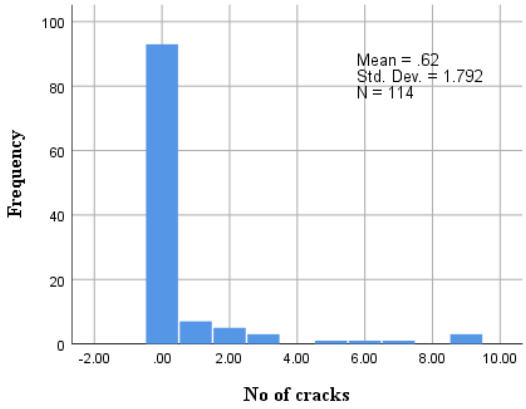

Figure 3-28 Histogram of the number or cracks of the lifts of parapet walls

4 Prediction of occurrence of thermal cracking by artificial neural networks

In this chapter, prediction of occurrence of thermal cracking is explained. In other words, these ANNs give output that whether the wall will be cracked or not. In this study, neural networks for vertical walls and parapet walls were developed separately. The details are categorically described in the following sections.

4.1 Neural networks for vertical walls

In this study, two neural networks for vertical walls were developed. Difference in both ANNs was the number of input parameters.

1st ANN named as ANN-V(a) was developed by substantial number of input parameters available for dataset. Number of nodes in the input layer were 18, 1 for bias and 17 nodes for input parameters. The input parameters were thickness, width, lift height, reinforcement ratio, water to cement ratio, cement content, expansive additive, slump, air content, initial concrete temperature, initial ambient temperature, 28-days concrete strength, lift interval, maximum temperature, maximum temperature time, form removal time and curing period. The summary of the dataset used in all 5-folds of ANN-V(a) is shown in Table 4-1.

Table 4-1 Case processing summary for ANN-V(a)

		Valid	Training	Testing	Holdouts
Sample Size (N)	Fold 1	150	101	21	28
	Fold 2	150	99	21	30
	Fold 3	150	90	32	28
	Fold 4	150	94	24	32
	Fold 5	150	95	23	32

Table 4-2 Efficiency table of ANN-V(a)

		Training	Testing	Holdouts
Prediction Accuracy (%)	Fold 1	89.1	71.4	89.3
	Fold 2	86.9	76.2	76.6
	Fold 3	83.3	84.4	75.0
	Fold 4	87.2	75	81.3
	Fold 5	90.7	95.2	72.0
	Average	87.4	80.4	78.8

Out of 248 lifts of vertical walls, 150 were usable due to elimination of the remaining lifts containing missing or ambiguous inputs entries. In this ANN, 6 number of units were obtained for the hidden layer by hit and trial method. This network was able to predict average 87.4%, 80.4% and 78.8% correct answers for training, testing and validation phase, respectively. The variation in the accuracy of holdout samples was from 72 to 89.3% as shown in Table 4-2. Normalized importance of the input parameters in prediction of occurrence of thermal cracking for fold 1 of ANN-V(a) are summarized in figure 4-1.

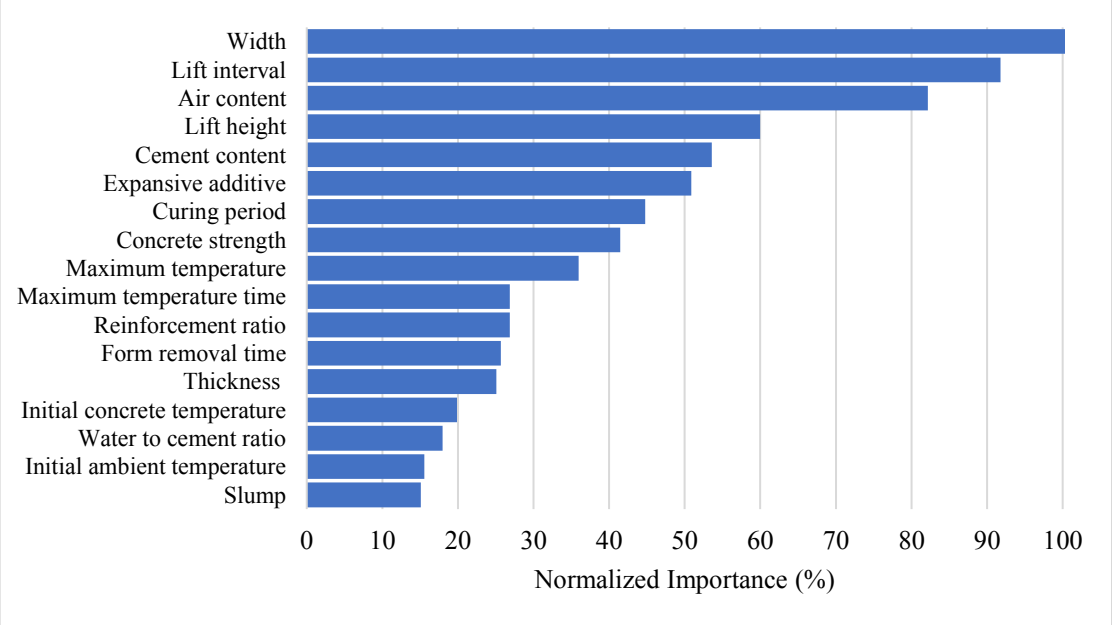

Figure 4-1 Normalized importance of input parameters for ANN-V(a)

It can be observed from figure 4-1 that width, lift interval and air content are the most important whereas water to cement ratio, initial ambient temperature and slump are the least important input parameters for ANN-V(a). As the ANNs are developed by using random initialization of synaptic weights so all of them may produce different normalized importance. In this study, normalized importance given by the most efficient ANNs among other ANNs are reported. The order of the normalized importance might be changed a little bit by retraining of the same ANNs as well. Least important parameters cannot be neglected because sometimes it becomes extremely difficult or impossible to obtain an efficient ANN without inclusion of least important parameters.

ANN-V(a) contained many input parameters which were not easy to obtain in all cases, for example, maximum temperature, maximum temperature time, etc. It also reduced the size of dataset due to many missing values along with the chances of overfitting due to the presence of large number of input parameters. So, an attempt was made to develop an alternative ANN named as ANN-V(b) by using less input parameters from the dataset which were easy to obtain in field and necessary to obtain an efficient network. In this case, the number of nodes in the input layer was 11, 1 for bias and 12 nodes for input parameters. The input parameters were thickness, width, lift height, reinforcement ratio, cement content, initial concrete temperature, initial ambient temperature, lift interval, form removal time and curing period. The lifts with expansive additive were also ignored as there were only 5 such lifts. The summary of the dataset used in all 5-folds of ANN-V(b) is shown in Table 4-3.

Out of 248 lifts of vertical walls, 201 lifts were usable due to elimination of the remaining lifts containing missing or ambiguous inputs entries for many parameters. In this ANN, 6 number of units were obtained for the hidden layer by hit and trial method. This network was able to predict average 85.1%, 76.2% and 81.5% correct answers for training, testing and validation phase, respectively. The variation in the accuracy of holdout samples was from 75 to 89.5% as shown in Table 4-4. ANN-V(b) exhibited nearly the same performance to ANN-V(a) during training and testing phase but ANN-V(b) performed better than ANN-V(a) for holdout samples. Overall, ANN-V(b) should be ranked superior because it used less number of input parameters which were easy to obtain for actual structures and incorporated bigger training and testing dataset.

Table 4-3 Case processing summary for ANN-V(b)

		Valid	Training	Testing	Holdouts
Sample Size (N)	Fold 1	201	132	31	38
	Fold 2	201	120	37	44
	Fold 3	201	135	26	40
	Fold 4	201	135	31	35
	Fold 5	201	131	25	45

Table 4-4 Efficiency table of ANN-V(b)

		Training	Testing	Holdouts
Prediction Accuracy (%)	Fold 1	85.6	76.5	89.5
	Fold 2	83.3	82.5	75.0
	Fold 3	83.7	76.9	80.0
	Fold 4	82.2	73.5	82.8
	Fold 5	90.8	71.4	80.0
	Average	85.1	76.2	81.5

Normalized importance of the input parameters in prediction of occurrence of thermal cracking for fold 1 of ANN-V(b) are summarized in figure 4-2. It can be observed from figure 4-2 that width, lift height and cement content are the most important whereas form removal time, initial ambient temperature and thickness are the least important input parameters for ANN-V(b).

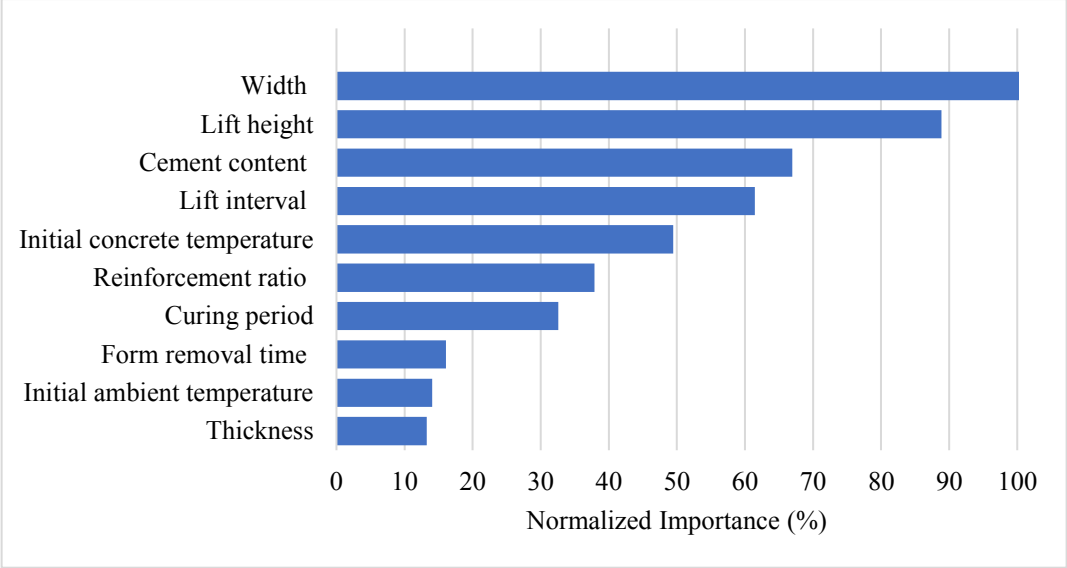

Figure 4-2 Normalized importance of input parameters for ANN-V(b)

4.2 Neural networks for parapet walls

In this study, two neural networks for parapet walls were developed. Difference in the two ANNs is the number of input parameters.

1st ANN named as ANN-P(a) was developed by substantial number of input variables available for dataset. The number of nodes in the input layer were 18, 1 for bias and 17 nodes for input parameters. The input parameters were thickness, width, lift height, reinforcement ratio, water to cement ratio, unit cement content, unit content of expansive additive, slump, air content, initial concrete temperature, initial ambient temperature, 28-days concrete strength, lift interval, maximum temperature, maximum temperature time, form removal time and curing period. The summary of the dataset used in all 5-folds of ANN-P(a) is shown in Table 4-5.

Out of 114 lifts of parapet walls, only 49 lifts were usable due to elimination of the remaining lifts containing missing or ambiguous inputs entries for many parameters. In this ANN, 5 number of units were obtained for the hidden layer by hit and trial method. This network was able to predict average 92.2%, 98% and 92.4% correct answers for training, testing and validation phase, respectively. The variation in the accuracy of holdout samples was from 83.3 to 100% as shown in Table 4-6. Normalized importance of the input parameters in prediction of occurrence of thermal cracking for fold 1 of ANN-P(a) are summarized in figure 4-3.

Table 4-5 Case processing summary for ANN-P(a)

		Valid	Training	Testing	Holdouts
Sample Size (N)	Fold 1	49	34	7	8
	Fold 2	49	29	10	10
	Fold 3	49	34	9	6
	Fold 4	49	31	8	10
	Fold 5	49	32	8	9

Table 4-6 Efficiency table of ANN-P(a)

		Training	Testing	Holdouts
Prediction Accuracy (%)	Fold 1	94.1	100	100
	Fold 2	86.2	90	88.9
	Fold 3	97.1	100	83.3
	Fold 4	93.1	100	90.0
	Fold 5	90.6	100	100
	Average	92.2	98	92.4

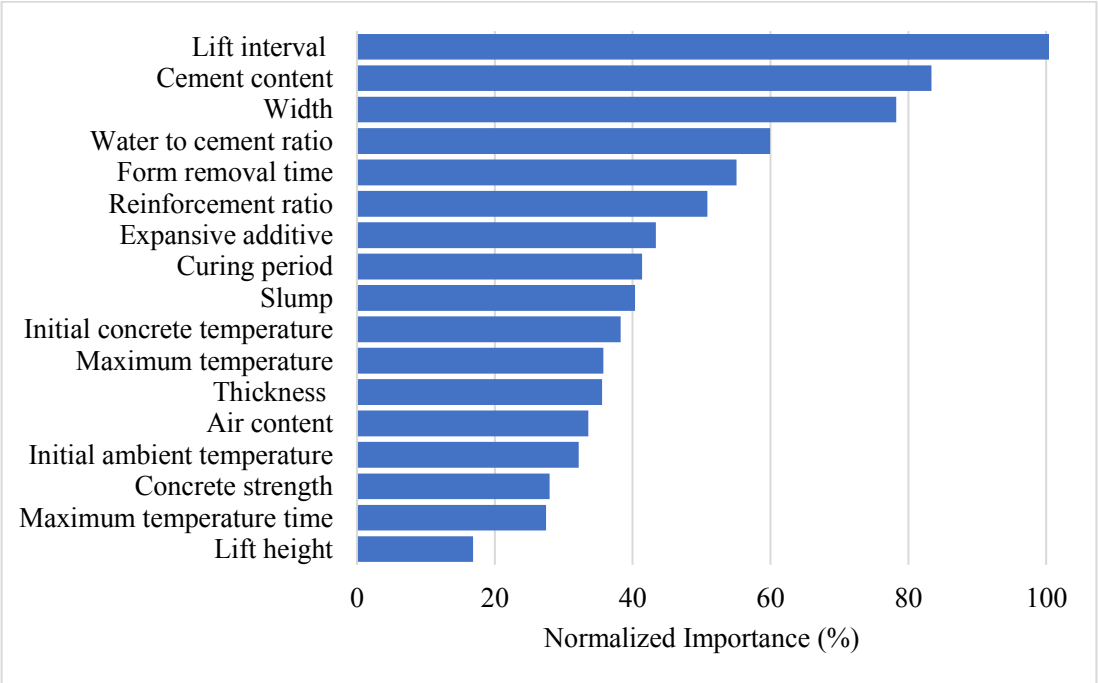

Figure 4-3 Normalized importance of input parameters for ANN-P(a)

It can be observed from figure 4-3 that lift interval, cement content and width are the most important whereas concrete strength maximum temperature time and lift height are the least important input parameters for ANN-P(a).

ANN-P(a) was developed on similar concept as of ANN-V(a). So, an attempt was made to develop an alternative ANN named as ANN-P(b) by using less input variables from the dataset. In this case, the number of nodes in the input layer were 12, 1 for bias and 11 nodes for input parameters. The input parameters were thickness, width, lift height, reinforcement ratio, unit cement content, unit content of expansive additive, initial concrete temperature, initial ambient temperature, lift interval, form removal time and curing period. The summary of the dataset used in all 5-folds of ANN-P(b) is shown in Table 4-7.

Out of 114 lifts of parapet walls, 85 lifts were usable due to elimination of the remaining lifts containing missing or ambiguous inputs entries for many parameters. In this ANN, 6 number of units were obtained for the hidden layer by hit and trial method. This network was able to predict average 96.0%, 98.5% and 87.6% correct answers for training, testing and validation phase, respectively. The variation in the accuracy of holdout samples was from 82.4 to 94.4% as shown in Table 4-8. So, ANN-P(b) exhibited a little better performance for training and testing phase but little lower performance for validation phase than ANN-P(a). Overall, ANN-P(b) should be ranked superior because it used less number of input parameters which were easy to obtain for actual structures and incorporated bigger training and testing dataset.

Table 4-7 Case processing summary for ANN-P(b)

		Valid	Training	Testing	Holdouts
Sample Size (N)	Fold 1	85	54	13	18
	Fold 2	85	53	14	18
	Fold 3	85	57	15	13
	Fold 4	85	55	13	17
	Fold 5	85	55	13	17

Table 4-8 Efficiency table of ANN-P(b)

		Training	Testing	Holdouts
Prediction Accuracy (%)	Fold 1	94.5	100	94.4
	Fold 2	98.2	100	94.0
	Fold 3	96.5	100	84.6
	Fold 4	98.2	100	82.4
	Fold 5	92.7	92.3	82.4
	Average	96.0	98.5	87.6

Normalized importance of the input parameters in prediction of occurrence of thermal cracking for fold 1 of ANN-P(b) are summarized in figure 4-4. It can be observed from figure 4-4 that width, lift interval and thickness are the most important whereas curing period, reinforcement ratio and lift height are the least important input parameters for ANN-P(b).

If we compare the important parameters for ANNs of both vertical walls and parapets, width was an important parameter, and influence of width of the wall is a well-known fact. Lift interval was another common influential factor for all ANNs which is one of the decisive parameters for external restraints for the walls. The influence of unit cement content was also quite pronounced which is a key parameter for maximum temperature rise.

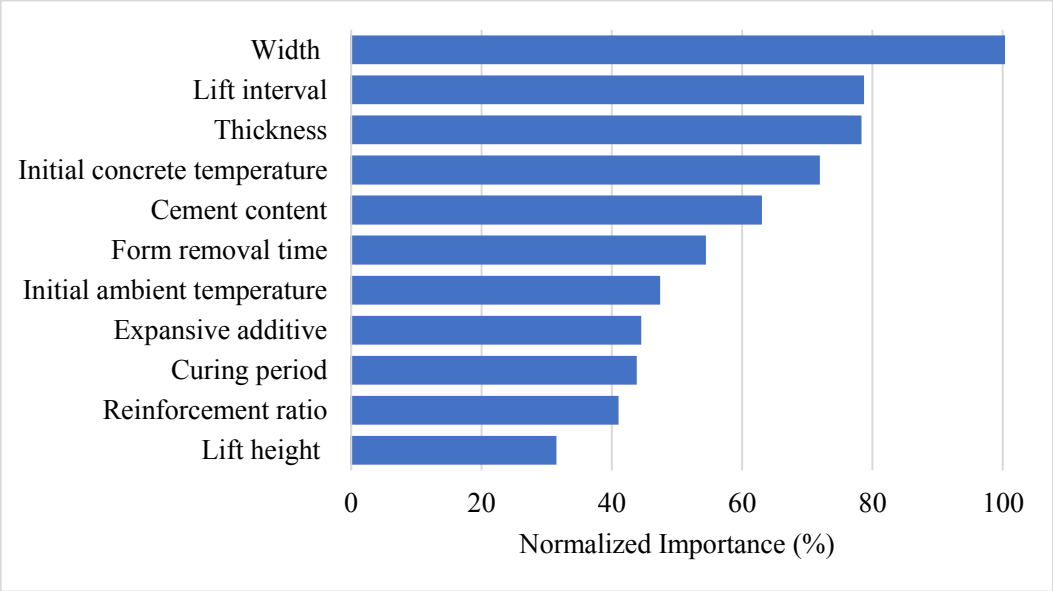

Figure 4-4 Normalized importance of input parameters for ANN-P(b)

4.3 Conclusions

Based on the findings of this study, which was focused on predicting the occurrence of thermal cracking of RC abutments using feedforward multilayer perceptron artificial neural networks and reliable actual construction data, following conclusions are drawn:

(i) Performance of ANNs with less number of input parameters for both vertical walls and parapets was promising, which was a good step towards prediction of occurrence of thermal cracking in RC abutments with basic information such as geometric and material properties, and ambient environmental conditions.

(ii) For vertical walls, ANN-V(b) which was the preferred ANN found in this study showed average accuracy level 81.5% for holdout samples by considering thickness, width, lift height, reinforcement ratio, cement content, initial concrete temperature, initial ambient temperature, lift interval, form removal time and curing period as input parameters.

(iii) For parapet walls, ANN-P(b) which was the preferred ANN found in this study showed average accuracy level 87.6% for holdout samples by considering thickness, width, lift height, reinforcement ratio, cement content, expansive additive, initial concrete temperature, initial ambient temperature, lift interval, form removal time and curing period as input parameters.

5 Prediction of maximum width of thermal cracking by artificial neural networks

In this chapter, prediction of maximum width of thermal cracking is explained. In this study, neural networks for vertical walls and parapet walls were developed separately. The details are categorically described in the following sections.

5.1 Neural networks for vertical walls

In this study, ANNs were developed by using less number of parameters which were easy to obtain in the field. The input parameters were thickness, width, lift height, reinforcement ratio, unit cement content, expansive additive, initial concrete temperature, initial ambient temperature, 28-days concrete strength, lift interval, form removal time and curing period. The size of the network was decided by hit and trial method and that network was selected for which accuracy of holdout samples was maximum among others to avoid overfitting. By performing hit and trial method, 2 hidden layers with 6 nodes in first layer and 3 nodes in second layer were selected. The performance of the selected ANN in terms of relationship between actual and predicted maximum crack width ±0.1 mm allowable error lines and ±0.075 mm allowable error lines is shown in Figures 5-1 and 5-2, respectively.

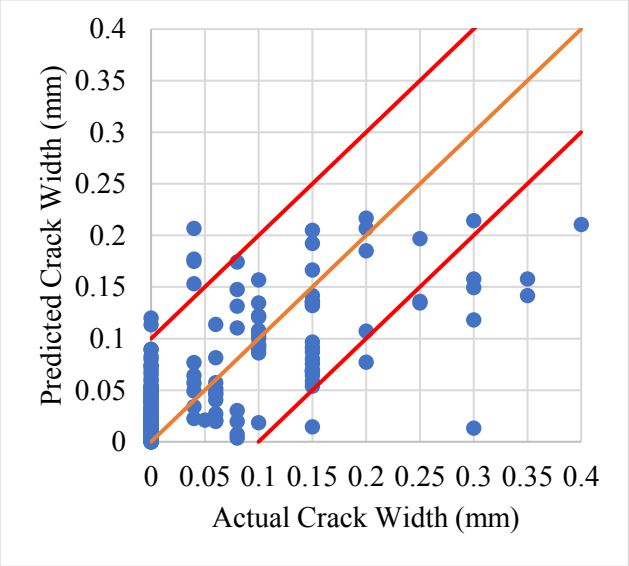

Figure 5-1 Relationship between actual and predicted maximum crack width for selected ANN with ±0.1 mm allowable error lines for vertical walls

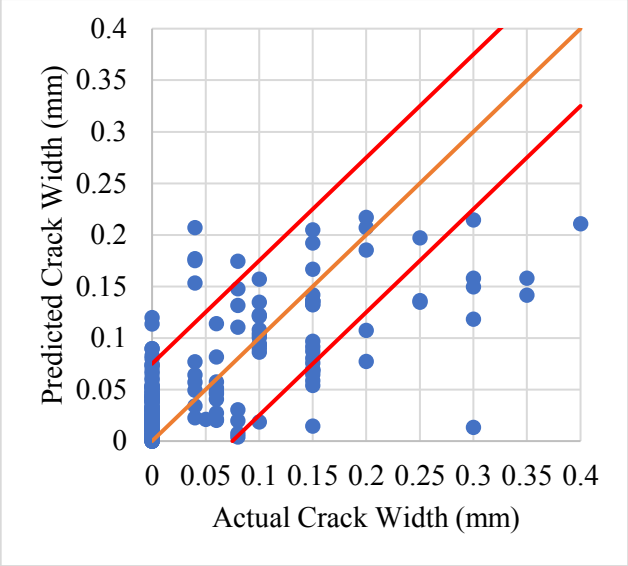

Figure 5-2 Relationship between actual and predicted maximum crack width for selected ANN with ±0.075 mm allowable error lines

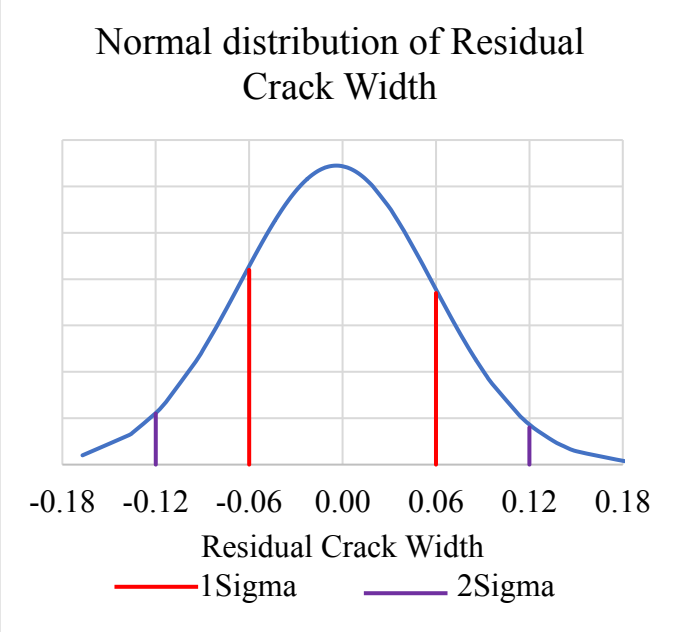

Figure 5-3 Normal distribution of residual crack width with 1sigma and 2sigma lines

It can be observed from Figures 5-1 through 5-3 that in predicting maximum width of thermal cracking, the selected ANN showed the accuracy level of 90.95 % with ±0.1 mm allowable error and 83 % with ±0.075 mm allowable error in residual crack width was achieved.

To avoid overfitting, 5- fold cross validation was also performed. The case processing summary of the dataset used in all 5-folds of ANN-MCW-V(b) is shown in Table 5-1. And the efficiency of the ANN is shown in Table 5-2.

Table 5-1Case processing summary for ANN-MCW-V(b)

Case processing summary for ANN-V(b)			
For All 5 Folds	Valid	Training, Testing and Validation	Holdouts
	188	155	33

Table 5-2 Efficiency table of ANN-MCW-V(b)

Efficiency table of ANN-MCW-V(b)					
		Training, Testing & Validation		Holdouts	
Tolerance Level		0.075 (mm)	0.1 (mm)	0.075 (mm)	0.1 (mm)
Prediction Accuracy (%)	Fold 1	91.3 %	96.00 %	78.94 %	84.21 %
	Fold 2	88.6%	93.96%	79.49 %	87.18 %
	Fold 3	91.95%	95.3%	78.38 %	81.09 %
	Fold 4	89.26%	93.29%	78.38 %	83.78 %
	Fold 5	91.27%	92.62%	75.67 %	83.78 %
	Avg.	90.48%	94.23%	78.17%	84.0 %

It can be observed from Table 5-2 that in predicting maximum width of thermal cracking, the selected ANN showed the average accuracy level of 94.23 % with ±0.1 mm allowable error during training, testing and validation and 84% with ±0.1 mm allowable error during for holdout samples was achieved. The average accuracy level of 90.48 % with ±0.075 mm allowable error during training, testing and validation and 78.17 % with ±0.075 mm allowable error during for holdout samples was achieved.

The performance of ANN for holdouts is shown in the Figure 5-4.

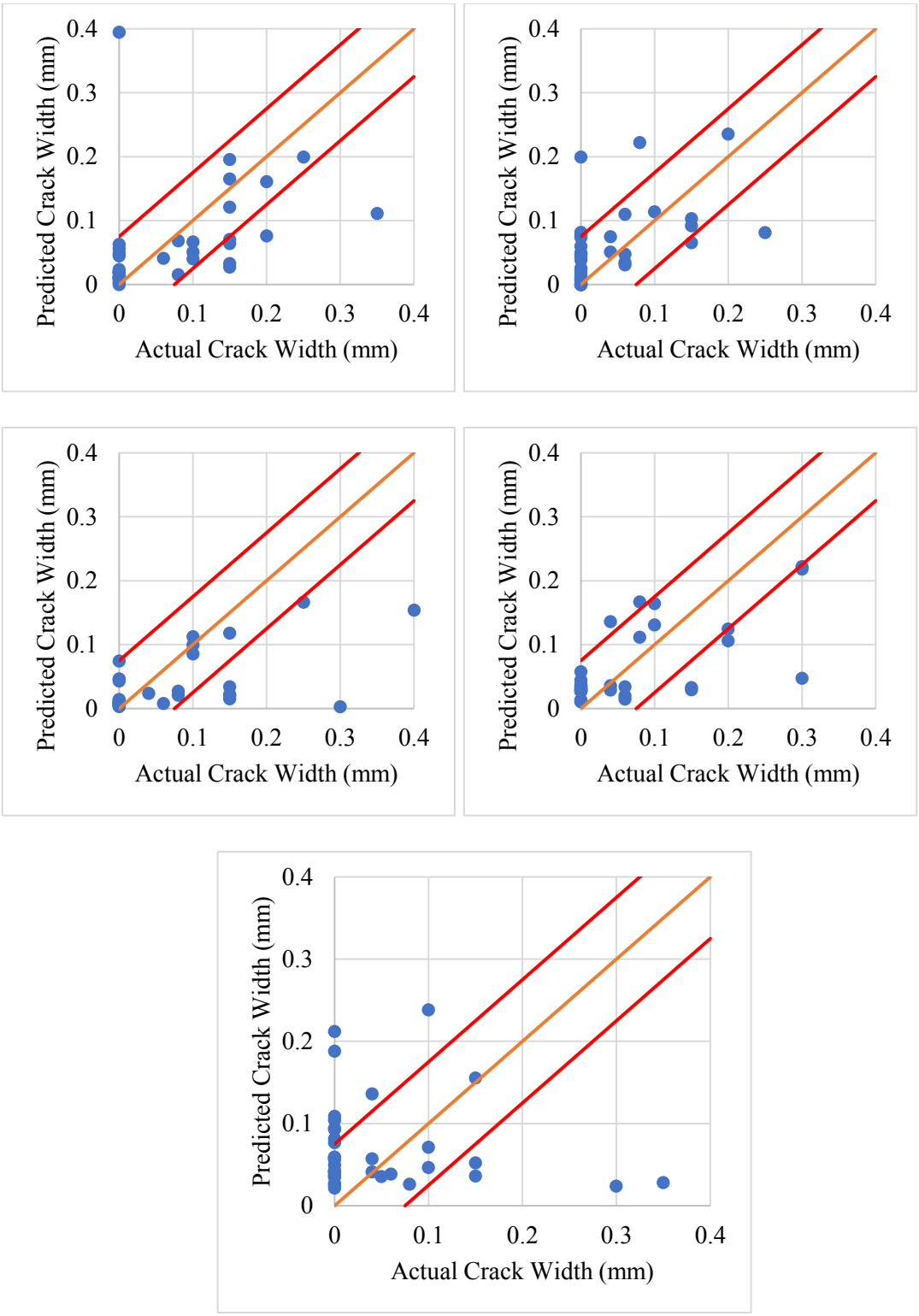

Figure 5-4 Relationship between actual crack width and predicted crack width for 5 Folds for vertical walls

5.2 Neural networks for parapets

In this study, ANNs were developed by using less number of parameters which were easy to obtain in the field. The input parameters were thickness, width, lift height, reinforcement ratio, unit cement content, expansive additive, initial concrete temperature, initial ambient temperature, 28-days concrete strength, lift interval, form removal time and curing period. The size of the network was decided by hit and trial method and that network was selected for which accuracy of holdout samples was maximum among others to avoid overfitting. By performing hit and trial method, 2 hidden layers with 6 nodes in first layer and 3 nodes in second layer were selected. The performance of the selected ANN in terms of relationship between actual is shown in Figures 5-5. It can be seen from Figures 5-5 that the ANN showed a high level of accuracy.

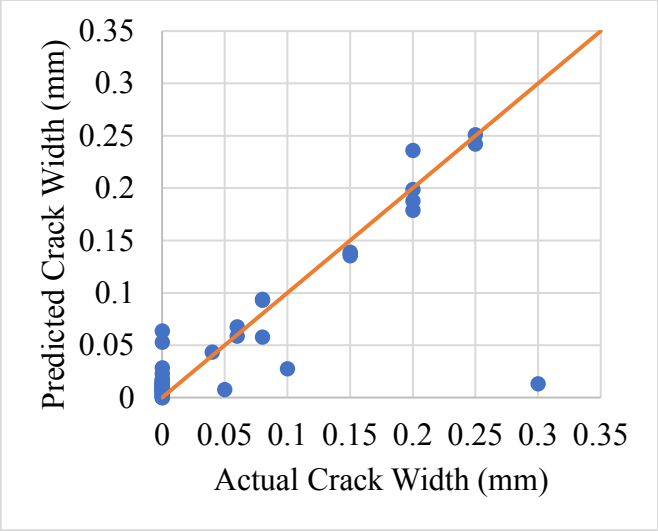

Figure 5-5 Relationship between actual and predicted maximum crack width for selected ANN for parapets

Although ANNs showed high level of accuracy but it is important to validate the ANN for generalized ANN. To avoid overfitting, 5- fold cross validation was also performed. The case processing summary of the dataset used in all 5-folds of ANN-MCW-P(b) is shown in Table 5-3. And the efficiency of the ANN is shown in Table 5-4. It can be observed from Figure 5-6 that despite of high accuracy level the ANN is unable to predict the higher crack widths which implies that ANN is overfitting.

Table 5-3 Case processing summary for ANN-MCW-P(b)

Case processing summary for ANN-V(b)			
For All 5 Folds	Valid	Training, Testing and Validation	Holdouts
	76	61	15

Table 5-4 Efficiency table of ANN-MCW-P(b)

Efficiency table of ANN-MCW-P(b)					
		Training, Testing & Validation		Holdouts	
Tolerance Level		0.075 (mm)	0.1 (mm)	0.075 (mm)	0.1 (mm)
Prediction Accuracy (%)	Fold 1	90 %	93 %	100 %	100%
	Fold 2	91 %	93 %	73.3 %	80 %
	Fold 3	93%	96%	73.3 %	80 %
	Fold 4	95%	98%	80 %	86 %
	Fold 5	95%	98%	80 %	86 %
	Avg.	93%	96%	81%	86%

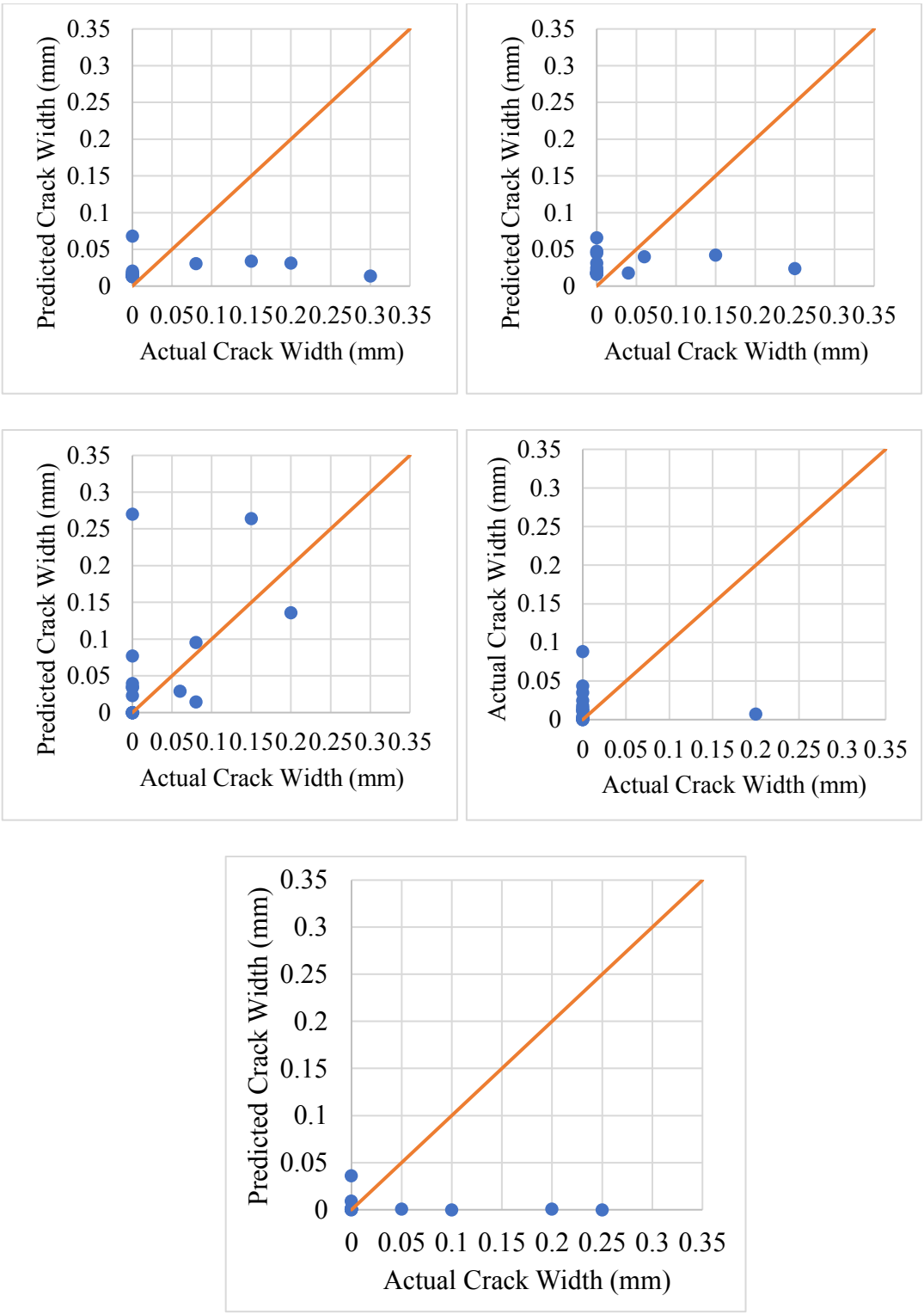

Figure 5-6 Relationship between actual crack width and predicted crack width for 5 Folds for parapets

5.3 Conclusions

Based on the developed ANN to predict maximum width of thermal cracking in vertical walls, following conclusions are drawn;

- Present ANN could predict 90.95 % (171 lifts out of 188) correctly if the permissible error in prediction is considered as ± 0.1 mm.
- 16 lifts out of 17 lifts for which prediction error was more than ± 0.1 mm were constructed from 2007 to 2009.
- If ± 0.075 mm is considered as permissible error in prediction, then prediction accuracy was 83 % (156 lifts out of 188 were correctly predicted).
- If ± 0.05 mm is considered as permissible error in prediction, then prediction accuracy was 69 % (130 lifts out of 188 were correctly predicted).
- ANNs are potential candidates to perform this type of complex problems by using reliable data.

Based on the developed ANN to predict maximum width of thermal cracking in parapets, following conclusions are drawn;

- Present ANN could predict 94.74 % (72 lifts out of 76) correctly if the permissible error in prediction is considered as ± 0.1 mm.
- If ± 0.075 mm is considered as permissible error in prediction, then prediction accuracy was 93.42 % (71 lifts out of 76 were correctly predicted).
- If ± 0.05 mm is considered as permissible error in prediction, then prediction accuracy was 90.8 % (69 lifts out of 76 were correctly predicted).
- Although accuracy level of prediction is high, but this high accuracy is for small crack widths as the ANN is unable to predict larger crack width for holdout samples. The possible reasons are as follows;
    - The dataset is very small, so it is insufficient to build an appropriate ANN.
    - There are very few number of lifts with larger crack widths which are causing insufficiency in data with larger crack widths.

6 Parametric studies on influential parameters

In this chapter, influential parameters on thermal crack width are categorically explained for vertical walls.

6.1 Parametric studies on influential parameters for vertical walls

In this section, influential parameters on thermal crack width are categorically explained for vertical walls. Parametric studies were conducted at different seasonal conditions i.e., cold, normal and hot weather. To simulate cold weather, initial ambient temperature was kept as 0^{o}C and initial concrete temperature as 10^{o}C. To simulate normal weather, initial ambient temperature was kept as 20^{o}C and initial concrete temperature as 20^{o}C. To simulate hot weather, initial ambient temperature was kept as 30^{o}C and initial concrete temperature as 30^{o}C. All the studies were carried out at varying level of unit cement content which was from 280 to 330 kg/m^{3}.

6.1.1 Effect of cement content and thickness of the lift

Parametric studies were conducted to observe the effect of thickness of the lift at different amount of unit cement content. This study was conducted on three different widths of the wall i.e., 10 m, 15 m and 25 m which represent relatively small, medium and relatively larger width walls, respectively. The results of different width lifts are categorically explained below. Other input values used in this parametric study are summarized in the following table.

Lift Height	Rebar Ratio	Expansive Additives	28 Days Strength	Lift Interval	Formwork Removal Time	Curing Period
3 m	0.3 %	0	25 MPa	7 Day	7 Day	7 Day

For 10 m wide wall:

The results for parametric studies about the effect of thickness of the lift in cold weather, normal weather and hot weather are shown in Figures 6-1 through 6-3 for 10 m wide lifts. It can observe from Figures 6-1 that in cold weather, cement content is very influential in determining maximum crack width (MCW) as by increasing cement content from 280

kg/m^3 to 330 kg/m^3, the maximum crack width may increase from 0 mm to around 0.05 mm and from 0 mm to 0.07 mm for 0.5 m thick lift and 3 m thick lift, respectively.

Increase in thickness of the wall is also little influential as it can increase MCW up to around 0.02 mm, but this increase is not considerably high. But in all cases, MCW is considerably less than 0.15 mm which is the threshold value for MCW.

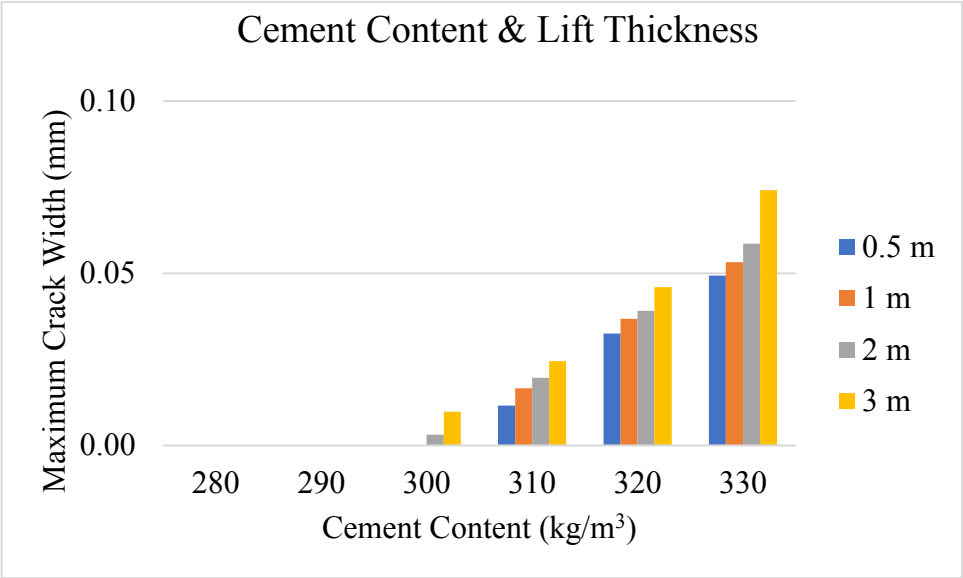

Figure 6-1 Effect of the lift thickness in cold weather for 10 m wide lift

It can observe from Figures 6-2 that in normal weather, cement content is very influential in determining maximum crack width (MCW) as by increasing cement content from 280 kg/m^3 to 330 kg/m^3, the maximum crack width may increase from 0 mm to around 0.05 mm and from 0 mm to 0.11 mm for 0.5 m thick lift and 3 m thick lift, respectively.

Increase in thickness of the wall is also more influential than that in cold weather as it can increase MCW up to around 0.06 mm when cement content is high, which is a considerable increase in MCW. But in all cases, MCW is considerably less than 0.15 mm which is the threshold value for MCW.

It can observe from Figures 6-3 that in hot weather, cement content is very influential in determining maximum crack width (MCW) as by increasing cement content from 280 kg/m^3 to 330 kg/m^3, the maximum crack width may increase from 0 mm to around 0.05 mm and from 0 mm to 0.10 mm for 0.5 m thick lift and 3 m thick lift, respectively.

Increase in thickness of the wall is also more influential than that in cold weather as it can increase MCW up to around 0.05 mm when cement content is high, which is a

considerable increase in MCW. But in all cases, MCW is considerably less than 0.15 mm which is the threshold value for MCW.

Overall, the effect of the thickness of the wall is considerably influential when high cement content is used whereas this effect can be neglected at low and normal cement content. But in all conditions as mentioned in this section, MCW is less than 0.15 mm.

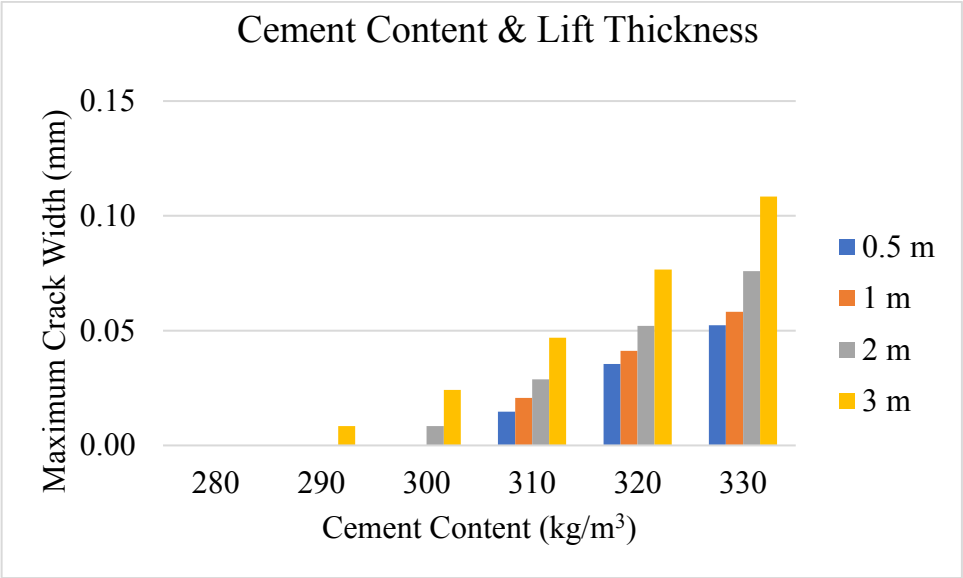

Figure 6-2 Effect of the lift thickness in normal weather for 10 m wide lift

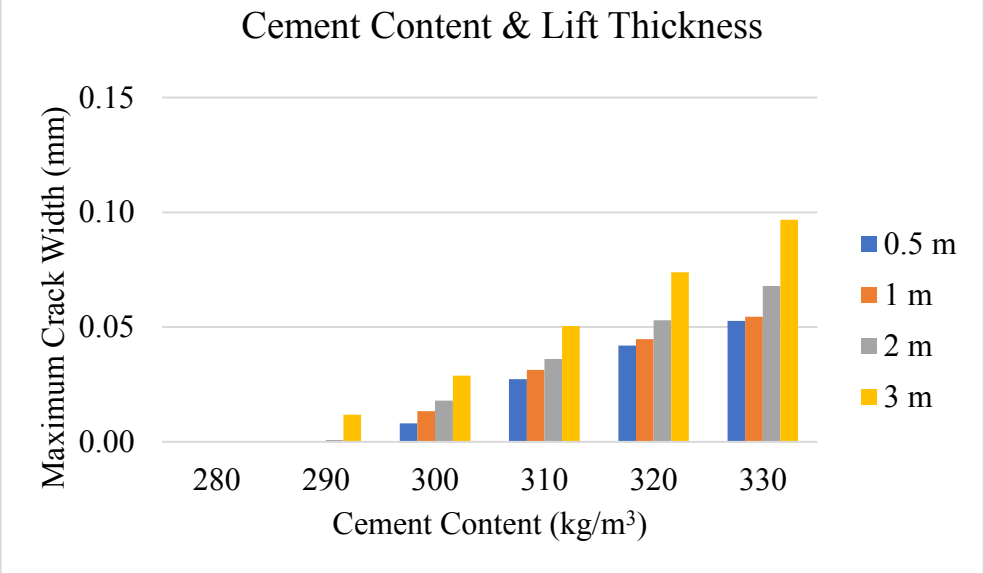

Figure 6-3 Effect of the lift thickness in hot weather for 10 m wide lift

For 15 m wide wall:

The results for parametric studies about the effect of thickness of the lift in cold weather, normal weather and hot weather are shown in Figures 6-4 through 6-6 for 15 m wide lifts.

It can observe from Figures 6-4 that in cold weather, cement content is very influential in determining maximum crack width (MCW) as by increasing cement content from 280 kg/m^3 to 330 kg/m^3, the maximum crack width may increase from 0 mm to around 0.04 mm and from 0 mm to 0.12 mm for 0.5 m thick lift and 3 m thick lift, respectively.

Increase in thickness of the wall is also influential as it can increase MCW up to around 0.05 mm and 0.08 mm for normal unit cement content and high unit cement content, respectively, and this increase is considerably high. But in all cases, MCW is considerably less than 0.15 mm which is the threshold value for MCW.

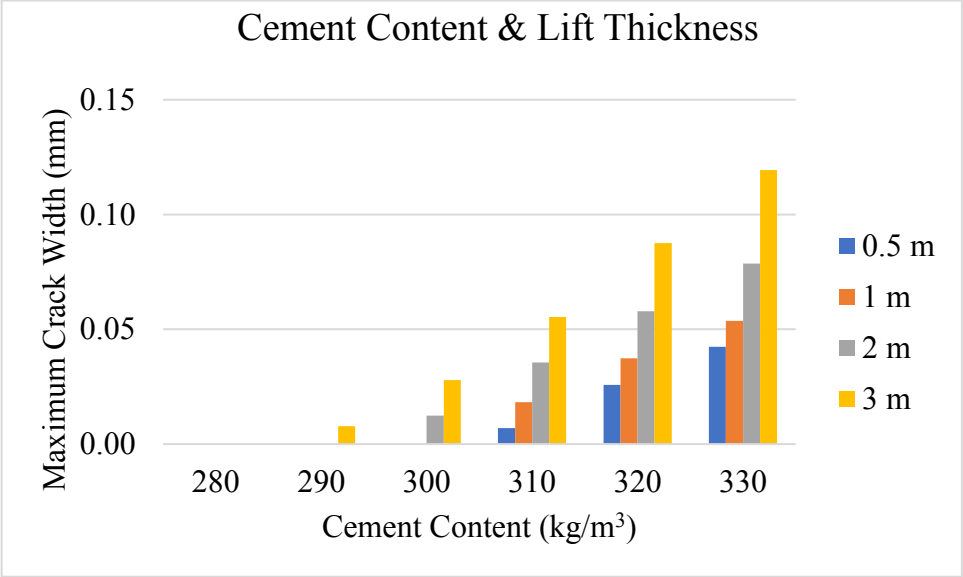

Figure 6-4 Effect of the lift thickness in cold weather for 15 m wide lift

It can observe from Figures 6-5 that in normal weather, cement content is very influential in determining maximum crack width (MCW) as by increasing cement content from 280 kg/m^3 to 330 kg/m^3, the maximum crack width may increase from 0 mm to around 0.05 mm and from 0.01 mm to 0.16 mm for 0.5 m thick lift and 3 m thick lift, respectively.

Increase in thickness of the wall is also influential as it can increase MCW up to around 0.06 mm and 0.11 mm for normal unit cement content and high unit cement content, respectively, and this increase is considerably high. In these scenarios, if the lift thickness is greater than 2 m, then cement content greater than 310 kg/m^3 may cause harmful cracking.

It can observe from Figures 6-6 that in hot weather, cement content is very influential in determining maximum crack width (MCW) as by increasing cement content from 280

kg/m^3 to 330 kg/m^3, the maximum crack width may increase from 0 mm to around 0.06 mm and from 0.03 mm to 0.17 mm for 0.5 m thick lift and 3 m thick lift, respectively.

Increase in thickness of the wall is also influential as it can increase MCW up to around 0.09 mm for both normal unit cement content and high unit cement content, and this increase is considerably high. In these scenarios, if the lift thickness is greater than 2 m, then cement content greater than 310 kg/m^3 may cause harmful cracking.

Overall, the effect of the thickness of the wall is considerably high. For 15 m wide lift udder the conditions mentioned earlier, if the lift thickness is greater than 2 m, then cement content greater than 310 kg/m^3 may cause harmful cracking.

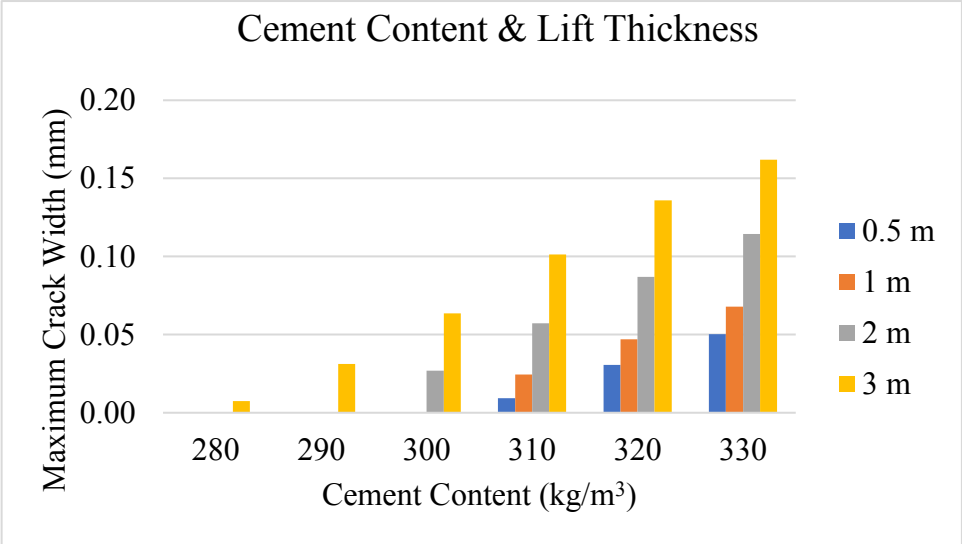

Figure 6-5 Effect of the lift thickness in normal weather for 15 m wide lift

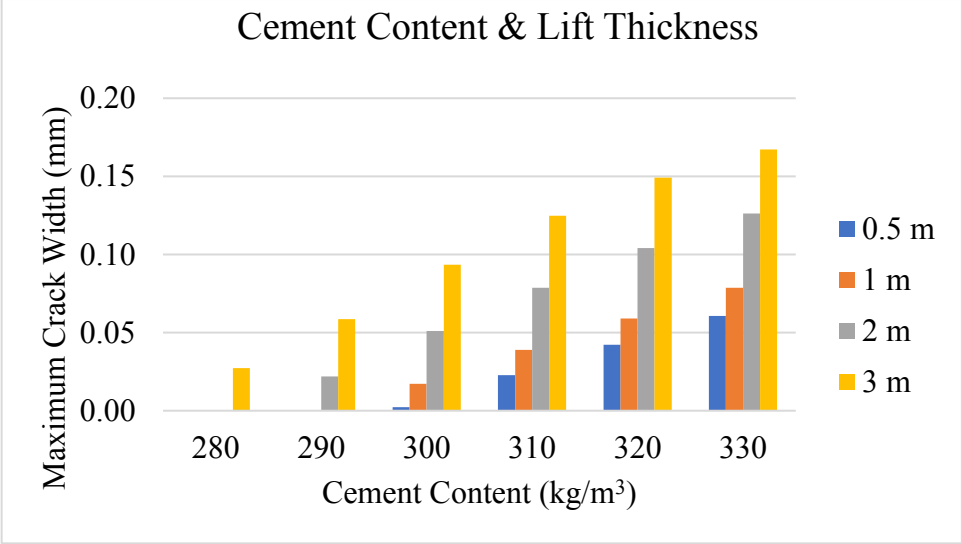

Figure 6-6 Effect of the lift thickness in hot weather for 15 m wide lift

For 25 m wide lifts:

The results for parametric studies about the effect of thickness of the lift in cold weather, normal weather and hot weather for 25 m wide lifts are shown in Figures 6-7 through 6-9.

It can observe from Figures 6-7 that in cold weather, cement content is very influential in determining maximum crack width (MCW) as by increasing cement content from 280 kg/m^3 to 330 kg/m^3, the maximum crack width may increase from 0 mm to around 0.02 mm and from 0.02 mm to 0.18 mm for 0.5 m thick lift and 3 m thick lift, respectively.

Increase in thickness of the wall is also influential as it can increase MCW up to around 0.1 mm and 0.16 mm for normal unit cement content and high unit cement content, respectively, and this increase is considerably high. In these scenarios, if the lift thickness is greater than 2 m, then cement content greater than 300 kg/m^3 may cause harmful cracking.

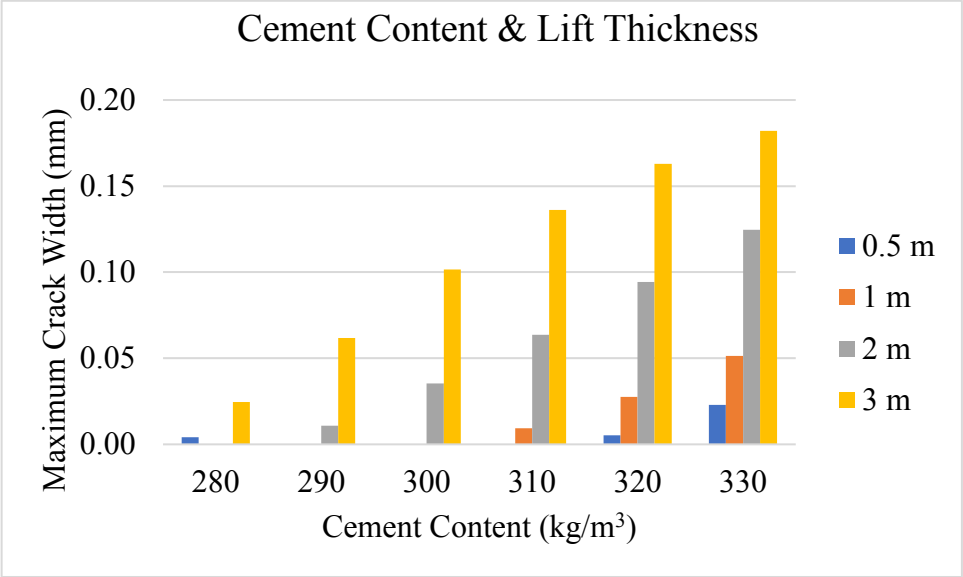

Figure 6-7 Effect of the lift thickness in cold weather for 25 m wide lift

It can observe from Figures 6-8 that in normal weather, cement content is very influential in determining maximum crack width (MCW) as by increasing cement content from 280 kg/m^3 to 330 kg/m^3, the maximum crack width may increase from 0 mm to around 0.05 mm and from 0.08 mm to 0.21 mm for 0.5 m thick lift and 3 m thick lift, respectively.

Increase in thickness of the wall is also influential as it can increase MCW up to around 0.16 mm for both normal unit cement content and high unit cement content, and this increase is considerably high. In these scenarios, if the lift thickness is greater than 2 m,

then cement content equal to or greater than 300 kg/m^3 may cause harmful cracking. Even for 2 m thick lift, unit cement content greater than 300 kg/m^3 may cause harmful cracking.

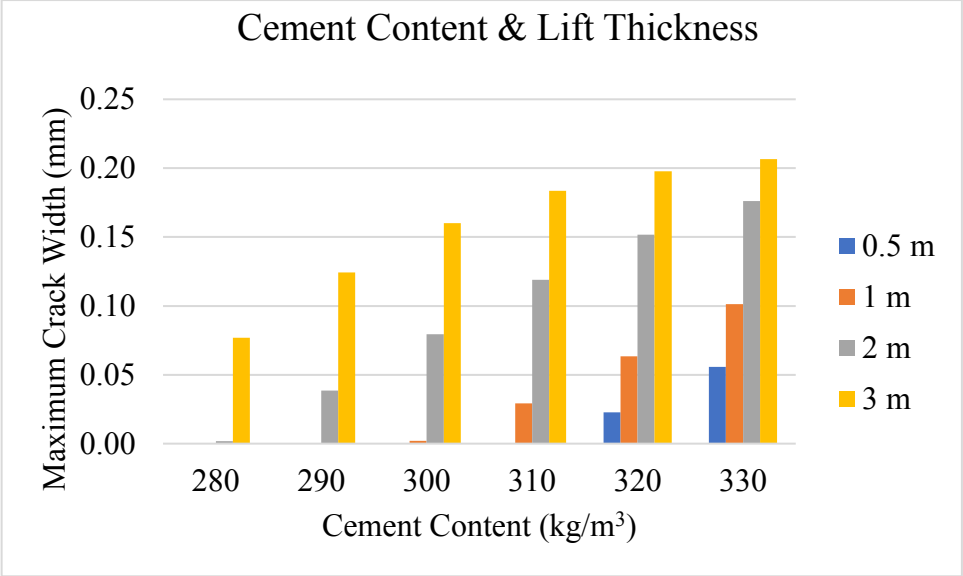

Figure 6-8 Effect of the lift thickness in normal weather for 25 m wide lift

It can observe from Figure 6-9 that in hot weather, cement content is very influential in determining maximum crack width (MCW) as by increasing cement content from 280 kg/m^3 to 330 kg/m^3, the maximum crack width may increase from 0 mm to around 0.09 mm and from 0.13 mm to 0.21 mm for 0.5 m thick lift and 3 m thick lift, respectively.

Increase in thickness of the wall is also influential as it can increase MCW up to around 0.19 mm and 0.12 mm for normal unit cement content and high unit cement content, respectively, and this increase is considerably high. In these scenarios, if the lift thickness is greater than 2 m, then even a low unit cement content may cause harmful cracking. Even for 2 m thick lift, unit cement content greater than 300 kg/m^3 may cause harmful cracking.

Overall, the effect of the thickness of the wall is considerably high. For 25 m wide lift udder the conditions mentioned earlier, if the lift thickness is greater than 2 m, then cement content greater than 300 kg/m^3 for cold weather, 290 kg/m^3 for normal weather may cause harmful cracking. For hot weather, even a low unit cement content may cause harmful cracking.

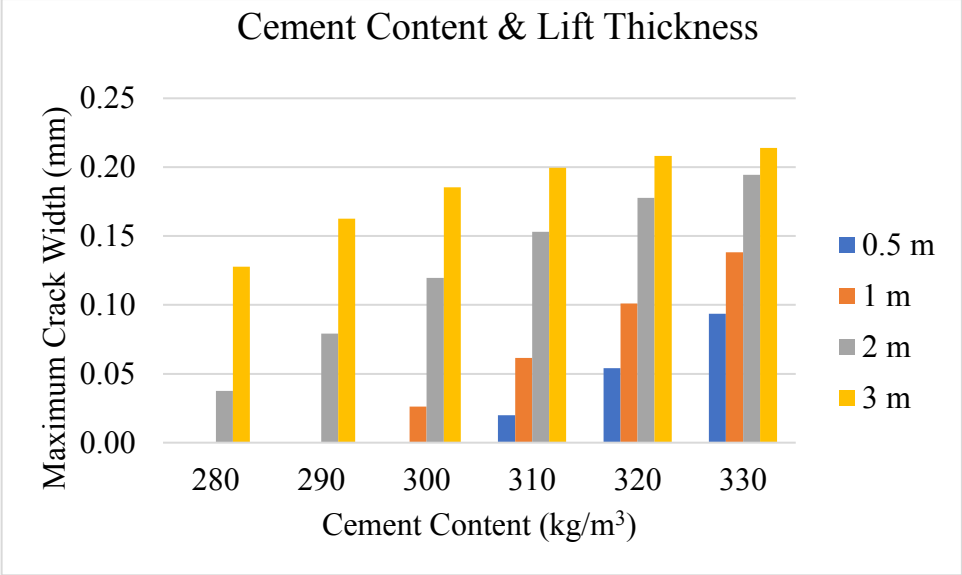

Figure 6-9 Effect of the lift thickness in hot weather for 25 m wide lift

6.1.2 Effect of cement content and width of the lift

Parametric studies were conducted to observe the effect of width of the lift at different amount of unit cement content. This study was conducted on four different ratios of reinforcement of the wall i.e., 0.05%, 0.1%, 0.3% and 0.5% which represent very small, relatively small, normal and relatively larger reinforcement amount, respectively. The results of different width lifts are categorically explained below. Other input values used in this parametric study are summarized in the following table.

Thickness	Lift Height	Expansive Additives	28 Days Strength	Lift Interval	Formwork Removal Time	Curing Period
2 m	3 m	0	25 MPa	7 Day	7 Day	7 Day

For 0.05% Reinforcement Ratio:

The results for parametric studies about the effect of width of the lifts in cold weather, normal weather and hot weather for 0.05% reinforcement ratio are shown in Figures 6-10 through 6-12.

It can observe from Figure 6-10 that in cold weather, cement content is very influential in determining maximum crack width (MCW) as by increasing cement content from 280

kg/m^3 to 330 kg/m^3, the maximum crack width may increase from 0 mm to around 0.06 mm and from 0.12 mm to 0.18 mm for 5 m wide lift and 25 m wide lift, respectively.

Increase in width of the wall is also influential as it can increase MCW up to around 0.12 mm for all low, normal and high unit cement content, and this increase is considerably high. In these scenarios, if the lift width is greater than 15 m, then unit cement content greater than 300 kg/m^3 may cause harmful cracking.

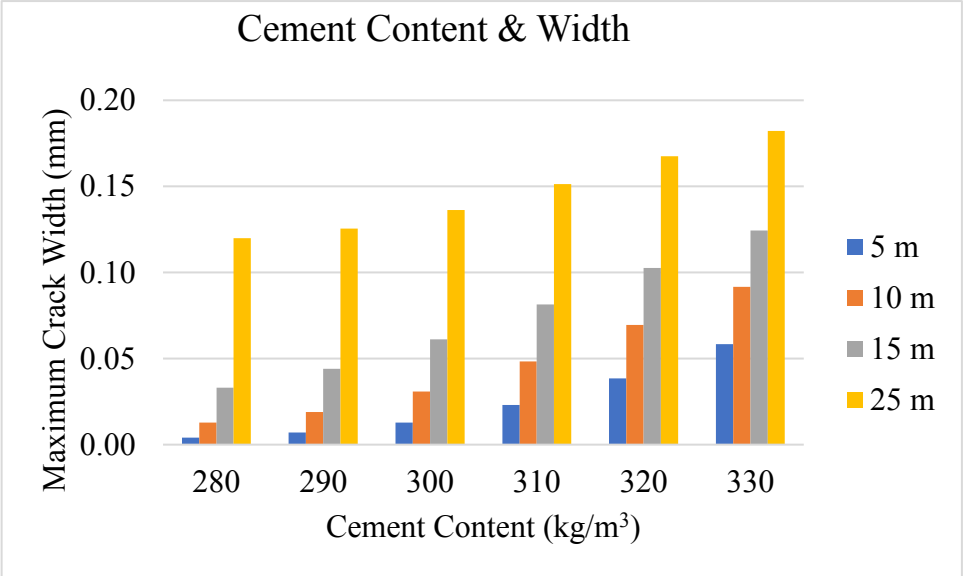

Figure 6-10 Effect of the width of the lift with 0.05% reinforcement ratio in cold weather

It can observe from Figure 6-11 that in normal weather, cement content is very influential in determining maximum crack width (MCW) as by increasing cement content from 280 kg/m^3 to 330 kg/m^3, the maximum crack width may increase from 0 mm to around 0.09 mm and from 0.13 mm to 0.21 mm for 5 m and 25 m wide lift, respectively.

Increase in width of the wall is also influential as it can increase MCW up to around 0.12 mm for all low, normal and high unit cement content, and this increase is considerably high. In these scenarios, if the lift width is large as 25 m, then even relatively low unit cement content may cause harmful cracking. If the lift width is 15 m, then unit cement content greater than 300 kg/m^3 may cause harmful cracking.

It can observe from Figure 6-12 that in hot weather, cement content is very influential in determining maximum crack width (MCW) as by increasing cement content from 280 kg/m^3 to 330 kg/m^3, the maximum crack width may increase from 0.1 mm to around 0.1 mm and from 0.15 mm to 0.21 mm for 5 m and 25 m wide lift, respectively.

Increase in width of the wall is also influential as it can increase MCW up to around 0.12 mm for all low, normal and high unit cement content, and this increase is considerably high. In these scenarios, if the lift width is 15 m, then unit cement content greater than 300 kg/m^3 may cause harmful cracking. If the lift width is 25 m, then even at a small amount of unit cement content level may cause harmful cracking.

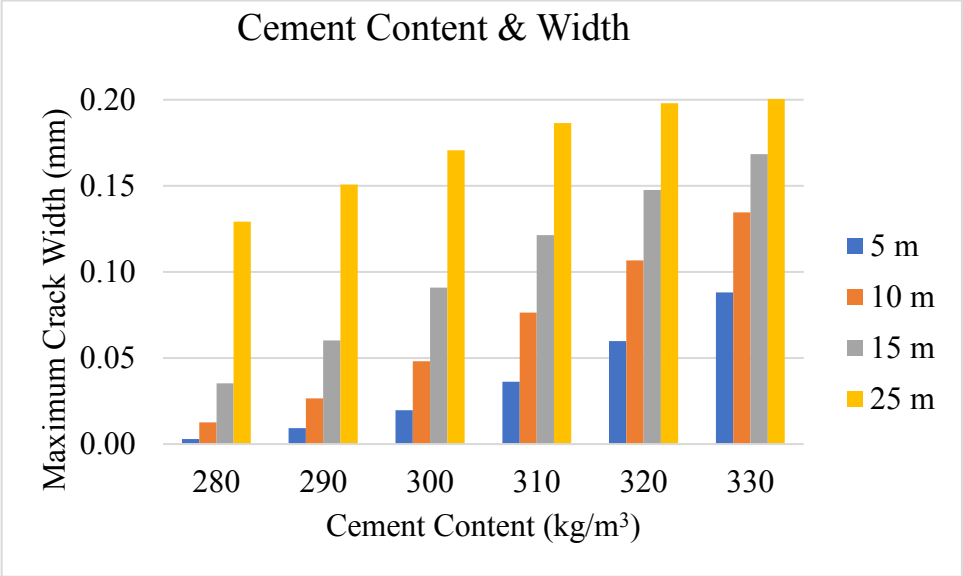

Figure 6-11 Effect of the width of the lift with 0.05% reinforcement ratio in normal weather

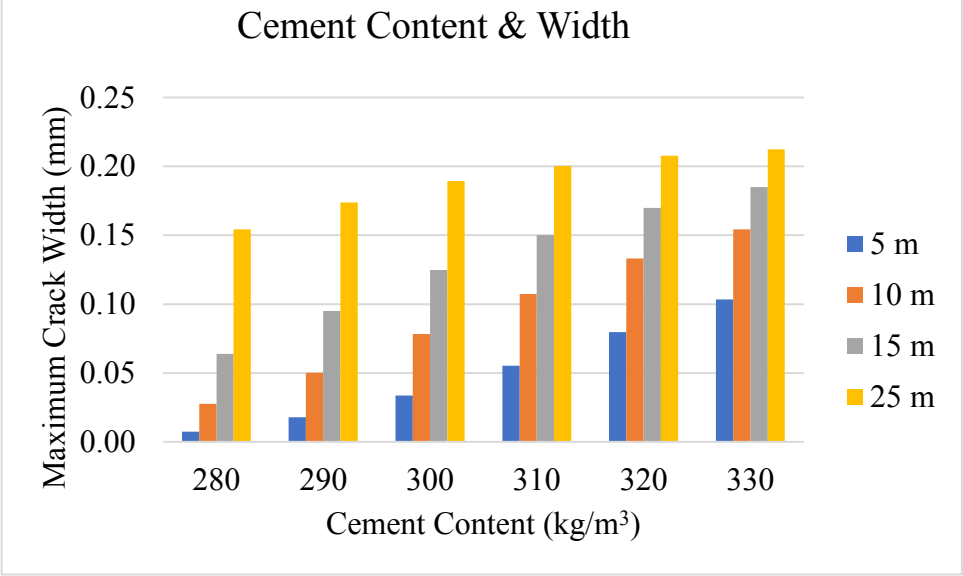

Figure 6-12 Effect of the width of the lift with 0.05% reinforcement ratio in hot weather

For 0.1% Reinforcement Ratio:

The results for parametric studies about the effect of width of the lifts in cold weather, normal weather and hot weather for 0.1% reinforcement ratio are shown in Figures 6-13 through 6-15.

It can observe from Figure 6-13 that in cold weather, cement content is very influential in determining maximum crack width (MCW) as by increasing cement content from 280 kg/m^3 to 330 kg/m^3, the maximum crack width may increase from 0 mm to around 0.05 mm and from 0.09 mm to 0.17 mm for 5 m and 25 m wide lift, respectively.

Increase in width of the wall is also influential as it can increase MCW up to around 0.09 to 0.12 mm for all low, normal and high unit cement content, and this increase is considerably high. In these scenarios, if the lift width is 25 m, then unit cement content greater than 310 kg/m^3 may cause harmful cracking.

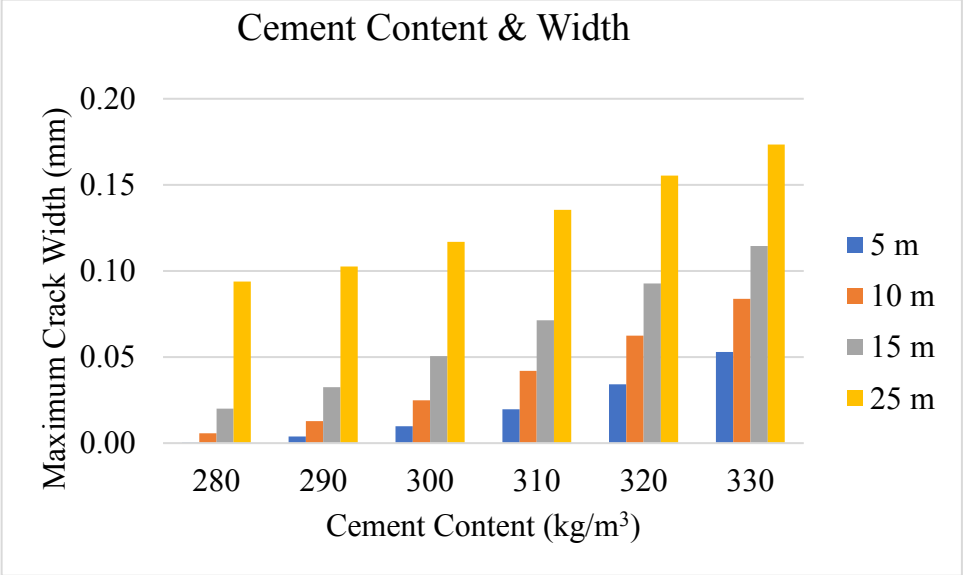

Figure 6-13 Effect of the width of the lift with 0.1% reinforcement ratio in cold weather

It can observe from Figure 6-14 that in normal weather, cement content is very influential in determining maximum crack width (MCW) as by increasing cement content from 280 kg/m^3 to 330 kg/m^3, the maximum crack width may increase from 0 mm to around 0.08 mm and from 0.1 mm to 0.2 mm for 5 m and 25 m wide lift, respectively.

Increase in width of the wall is also influential as it can increase MCW up to around 0.12 to 0.15 mm for all low, normal and high unit cement content, and this increase is considerably high. In these scenarios, if the lift width is 15 m, then unit cement content

greater than 320 kg/m^3 may cause harmful cracking. If the lift width is 25 m, then even at a small amount of unit cement content level may cause harmful cracking.

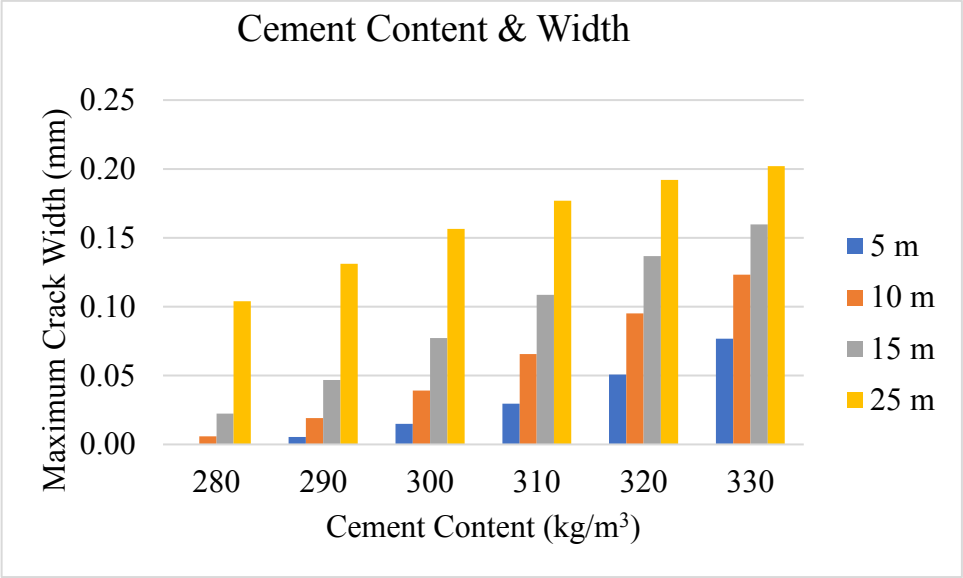

Figure 6-14 Effect of the width of the lift with 0.1% reinforcement ratio in normal weather

It can observe from Figure 6-15 that in hot weather, cement content is very influential in determining maximum crack width (MCW) as by increasing cement content from 280 kg/m^3 to 330 kg/m^3, the maximum crack width may increase from 0 mm to around 0.08 mm and from 0.13 mm to 0.21 mm for 5 m and 25 m wide lift, respectively.

Increase in width of the wall is also influential as it can increase MCW up to around 0.13 to 0.16 mm for all low, normal and high unit cement content, and this increase is considerably high. In these scenarios, if the lift width is 15 m, then unit cement content greater than 310 kg/m^3 may cause harmful cracking. If the lift width is 25 m, then even at a small amount of unit cement content level may cause harmful cracking.

For 0.3 % Reinforcement Ratio:

The results for parametric studies about the effect of width of the lifts in cold weather, normal weather and hot weather for 0.3% reinforcement ratio are shown in Figures 6-16 through 6-18.

It can observe from Figure 6-16 that in cold weather, cement content is very influential in determining maximum crack width (MCW) as by increasing cement content from 280 kg/m^3 to 330 kg/m^3, the maximum crack width may increase from 0 mm to around 0.04 mm and from 0 mm to 0.12 mm for 5 m and 25 m wide lift, respectively.

Increase in width of the wall is also influential as it can increase MCW up to around 0.06 mm for all high unit cement content, and this increase is considerably high. In these scenarios, there is no potential for harmful cracking.

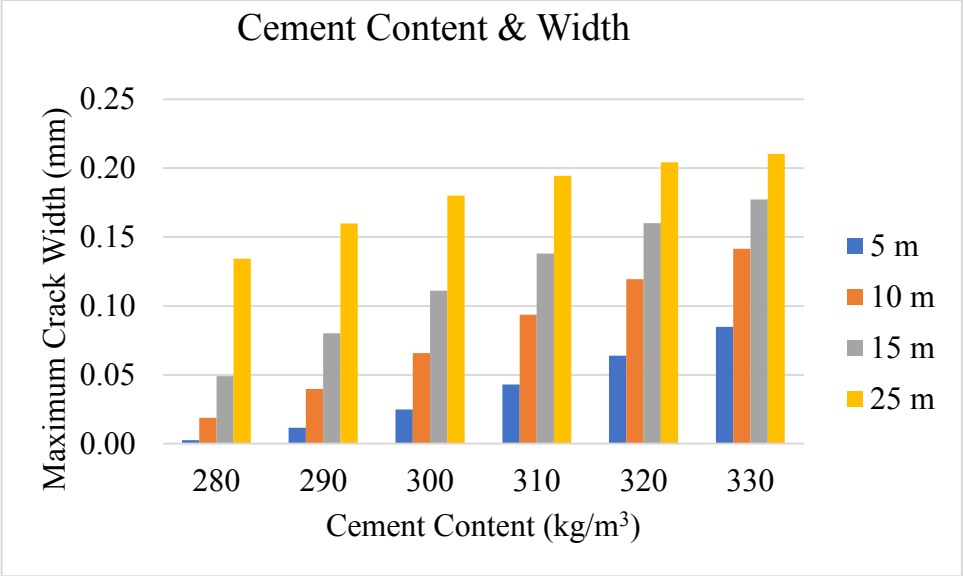

Figure 6-15 Effect of the width of the lift with 0.1% reinforcement ratio in hot weather

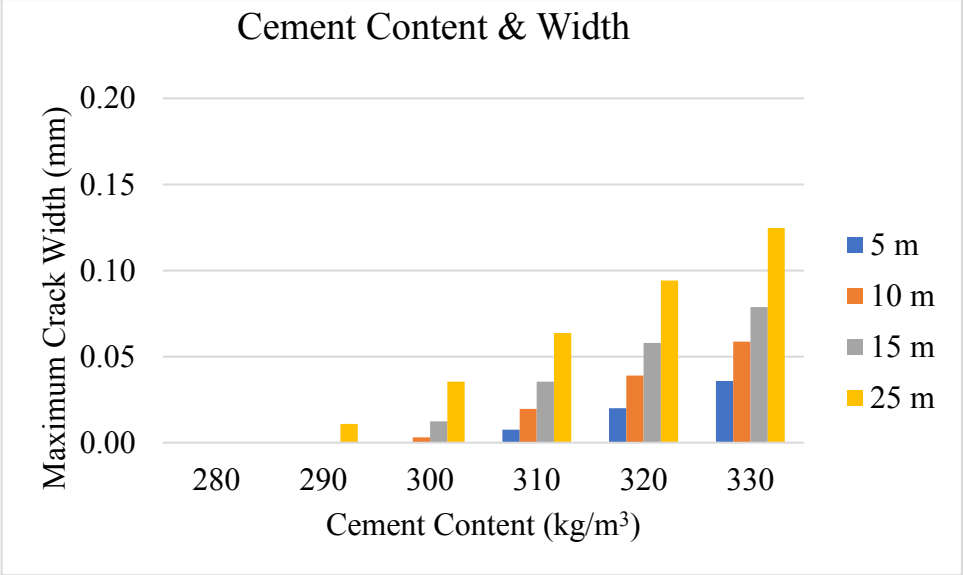

Figure 6-16 Effect of the width of the lift with 0.3% reinforcement ratio in cold weather

It can observe from Figure 6-17 that in normal weather, cement content is quite influential in determining maximum crack width (MCW) as by increasing cement content from 280 kg/m^3 to 330 kg/m^3, the maximum crack width may increase from 0 mm to around 0.03 mm and from 0 mm to 0.18 mm for 5 m and 25 m wide lift, respectively.

Increase in width of the wall is also influential as it can increase MCW up to around 0.15 mm for high unit cement content, and this increase is considerably high. In these scenarios, if the lift width is till 15 m, then there is not much potential for harmful cracking. If the lift width is 25 m, then unit cement content greater than 310 kg/m^3 level may cause harmful cracking.

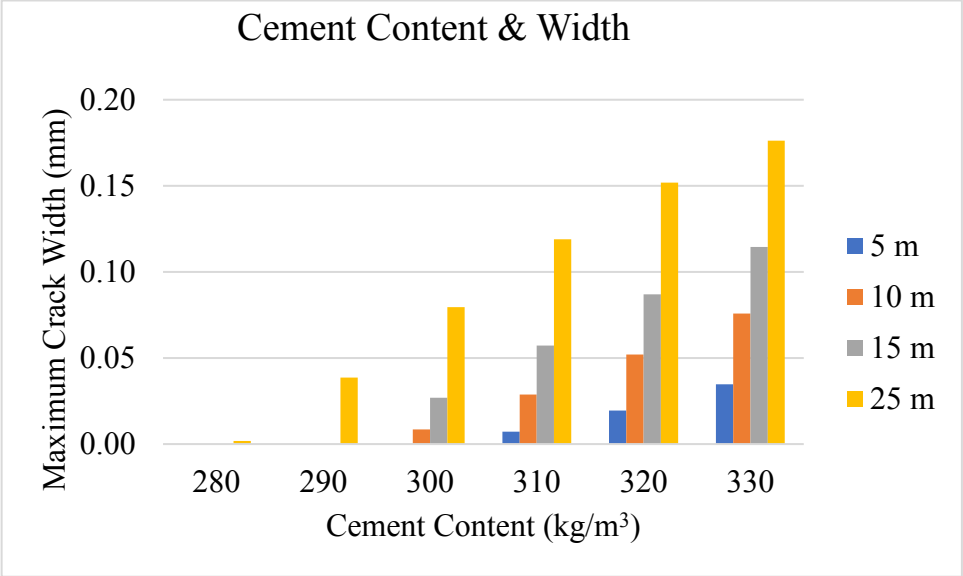

Figure 6-17 Effect of the width of the lift with 0.3% reinforcement ratio in normal weather

It can observe from Figure 6-18 that in hot weather, cement content is quite influential in case of larger width lifts in determining maximum crack width (MCW) as by increasing cement content from 280 kg/m^3 to 330 kg/m^3, the maximum crack width may increase from 0 mm to 0.19 mm for 25 m wide lift.

Increase in width of the wall is also influential as it can increase MCW up to around 0.19 mm for high unit cement content, and this increase is considerably high. In these scenarios, if the lift width is till 15 m, then there is not much potential for harmful cracking. If the lift width is 25 m, then unit cement content greater than 300 kg/m^3 level may cause harmful cracking.

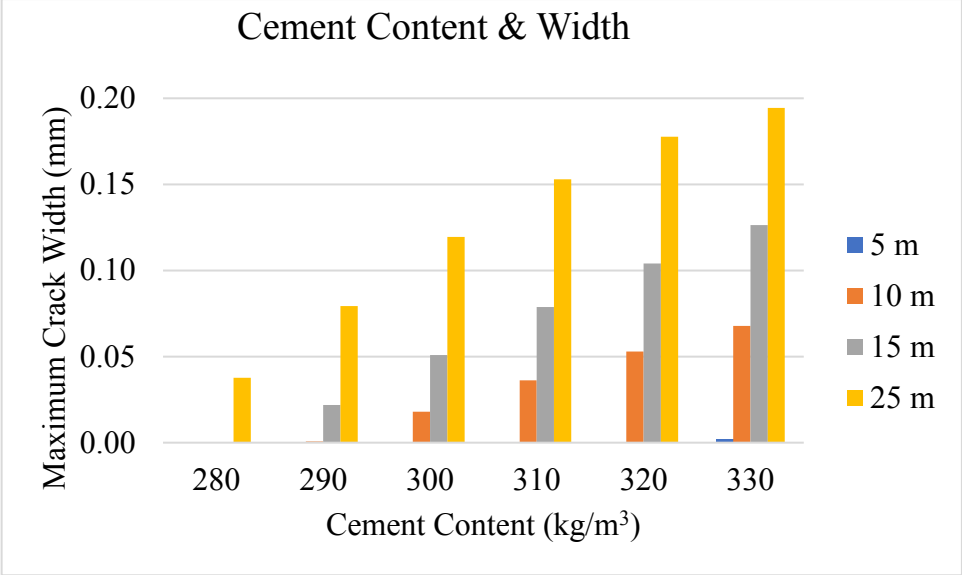

Figure 6-18 Effect of the width of the lift with 0.3% reinforcement ratio in hot weather

For 0.5 % Reinforcement Ratio:

The results for parametric studies about the effect of width of the lifts in cold weather, normal weather and hot weather for 0.5% reinforcement ratio are shown in Figures 6-19 through 6-21.

It can observe from Figure 6-19 that in cold weather, cement content is little influential for larger width walls in determining maximum crack width (MCW) as by increasing cement content from 280 kg/m^3 to 330 kg/m^3, the maximum crack width may increase from 0 mm to 0.06 mm for 25 m wide lift.

Increase in width of the wall is not so influential as it can increase MCW up to around 0.04 mm for high unit cement content, and this increase is negligible. In these scenarios, for all lifts, there is not much potential for harmful cracking.

It can observe from Figure 6-20 that in normal weather, cement content is quite influential for larger width lifts in determining maximum crack width (MCW) as by increasing cement content from 280 kg/m^3 to 330 kg/m^3, the maximum crack width may increase from 0 mm to 0.12 mm for 25 m wide lift.

Increase in width of the wall is also influential as it can increase MCW up to around 0.12 mm for high unit cement content, and this increase is considerably high. In these scenarios, for all lifts, then there is not much potential for harmful cracking.

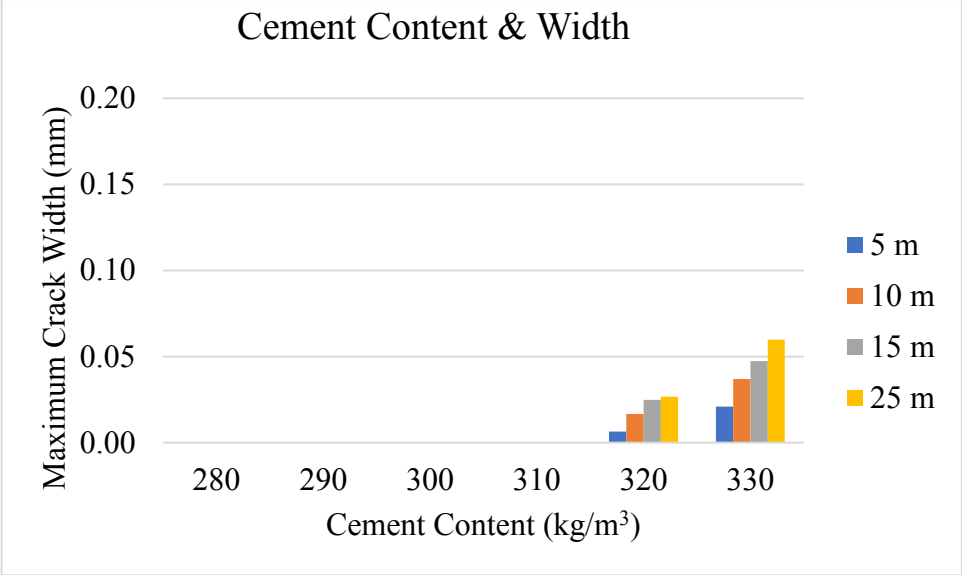

Figure 6-19 Effect of the width of the lift with 0.5% reinforcement ratio in cold weather

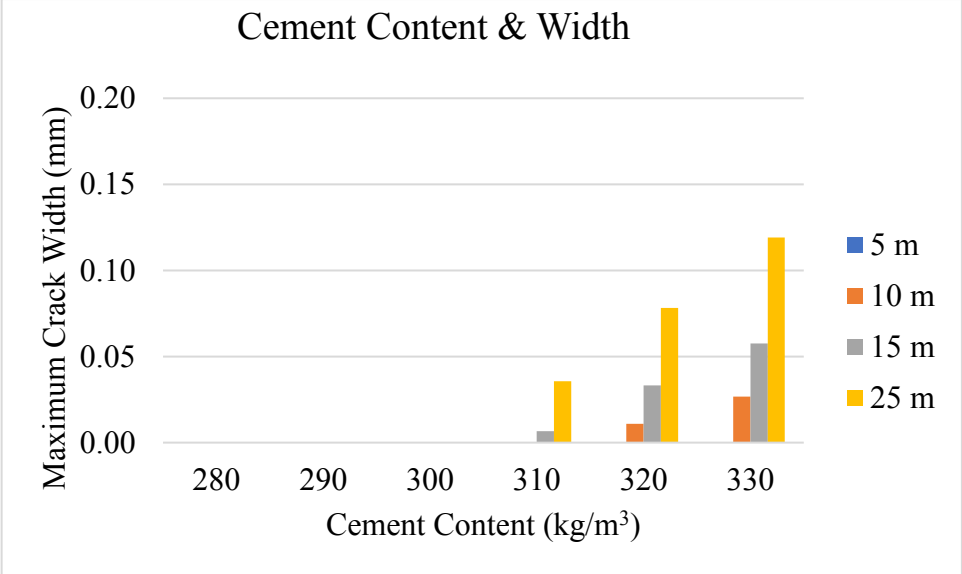

Figure 6-20 Effect of the width of the lift with 0.5% reinforcement ratio in normal weather

It can observe from Figure 6-21 that in hot weather, cement content is quite influential for larger width lifts in determining maximum crack width (MCW) as by increasing cement content from 280 kg/m^3 to 330 kg/m^3, the maximum crack width may increase from 0 mm to 0.15 mm for 25 m wide lift.

Increase in width of the wall is also influential as it can increase MCW up to around 0.15 mm for high unit cement content, and this increase is considerably high. In these scenarios, for all lifts, there is not much potential for harmful cracking except 25 m long lifts with 330 kg/m^3 unit cement content.

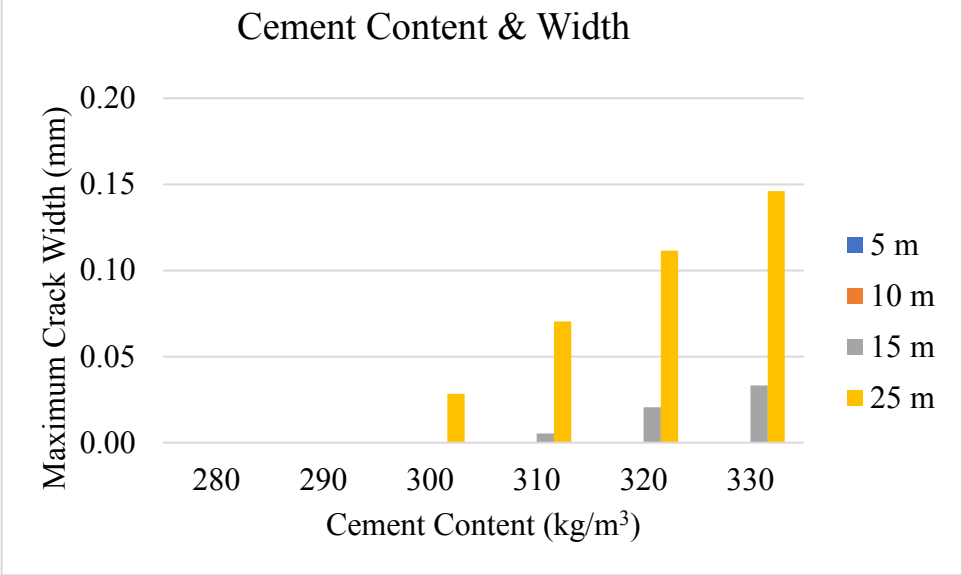

Figure 6-21 Effect of the width of the lift with 0.5% reinforcement ratio in hot weather

6.1.3 Effect of cement content and height of the lift

Parametric studies were conducted to observe the effect of height of the lift at different amount of unit cement content. This study was conducted on three different widths of the wall i.e., 10 m, 15 m and 25 m which represent relatively small, medium and relatively larger width walls, respectively. The results of different width lifts are categorically explained below. Other input values used in this parametric study are summarized in the following table.

Thickness	Rebar Ratio	Expansive Additives	28 Days Strength	Lift Interval	Formwork Removal Time	Curing Period
2 m	0.3 %	0	25 MPa	7 Day	7 Day	7 Day

For 10 m wide wall:

The results for parametric studies about the effect of height of the lift in cold weather, normal weather and hot weather are shown in Figures 6-22 through 6-24 for 10 m wide lifts. It can observe from Figures 6-22 that in cold weather, cement content is very influential in case of larger lift height in determining maximum crack width (MCW) as by increasing cement content from 280 kg/m^3 to 330 kg/m^3, the maximum crack width may increase from 0 mm to 0.08 mm for 4 m lift height.

Increase in lift height is also influential at high unit cement content as it can increase MCW up to around 0.05 mm. But in all cases, MCW is considerably less than 0.15 mm which is the threshold value for MCW.

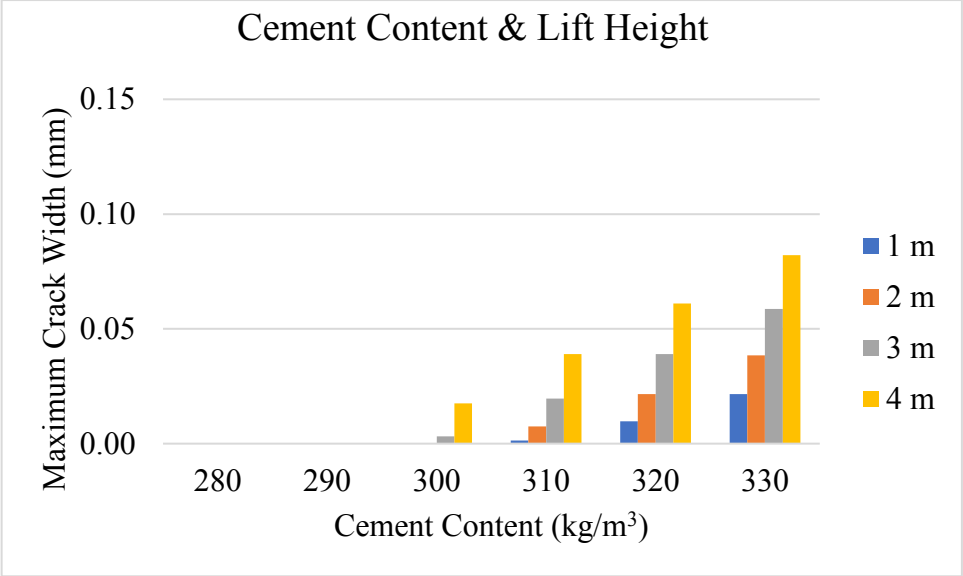

Figure 6-22 Effect of the lift height in cold weather for 10 m wide lift

It can observe from Figures 6-23 that in normal weather, cement content is very influential in case of larger lift height in determining maximum crack width (MCW) as by increasing cement content from 280 kg/m^3 to 330 kg/m^3, the maximum crack width may increase from 0 mm to 0.11 mm for 4 m lift height.

Increase in lift height is also influential at high unit cement content as it can increase MCW up to around 0.06 mm. But in all cases, MCW is considerably less than 0.15 mm which is the threshold value for MCW.

It can observe from Figures 6-24 that in hot weather, cement content is very influential in case of larger lift height in determining maximum crack width (MCW) as by increasing cement content from 280 kg/m^3 to 330 kg/m^3, the maximum crack width may increase from 0 mm to 0.09 mm for 4 m lift height.

Increase in lift height is also little influential at high unit cement content as it can increase MCW up to around 0.04 mm. But in all cases, MCW is considerably less than 0.15 mm which is the threshold value for MCW.

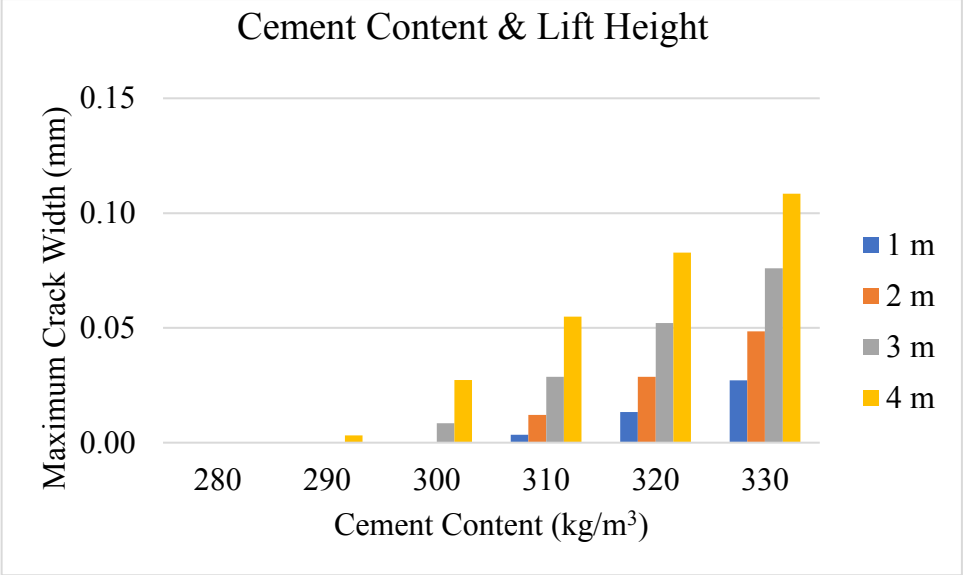

Figure 6-23 Effect of the lift height in normal weather for 10 m wide lift

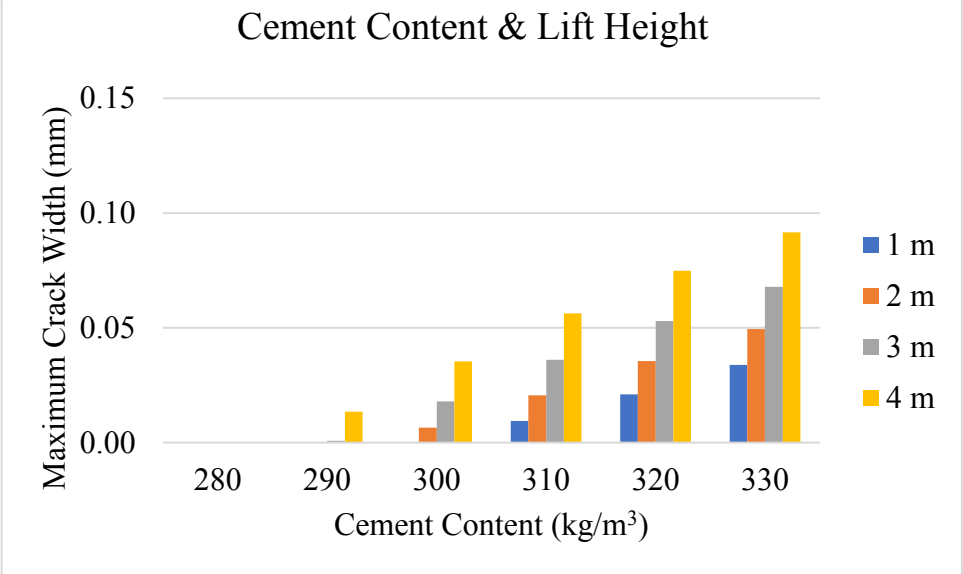

Figure 6-24 Effect of the lift height in hot weather for 10 m wide lift

For 15 m wide wall:

The results for parametric studies about the effect of height of the lift in cold weather, normal weather and hot weather are shown in Figures 6-25 through 6-27 for 15 m wide lifts. It can observe from Figures 6-25 that in cold weather, cement content is very influential in case of larger lift height in determining maximum crack width (MCW) as by increasing cement content from 280 kg/m^3 to 330 kg/m^3, the maximum crack width may increase from 0 mm to 0.11 mm for 4 m lift height.

Increase in lift height is also influential at high unit cement content as it can increase MCW up to around 0.05 mm. But in all cases, MCW is considerably less than 0.15 mm which is the threshold value for MCW.

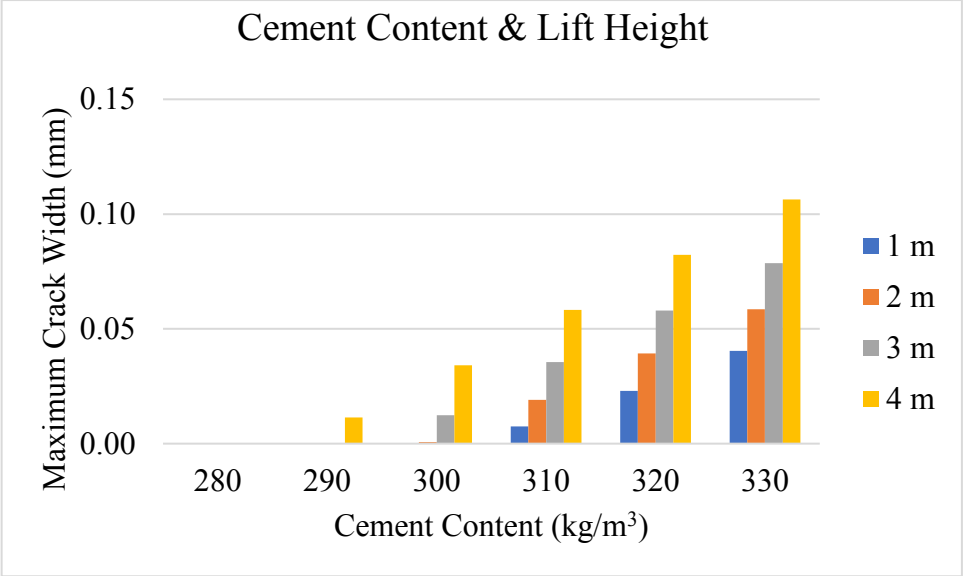

Figure 6-25 Effect of the lift height in cold weather for 15 m wide lift

It can observe from Figures 6-26 that in normal weather, cement content is quite influential in determining maximum crack width (MCW) as by increasing cement content from 280 kg/m^3 to 330 kg/m^3, the maximum crack width may increase from 0 mm to 0.05 mm and 0 to 0.15 mm for 1 m lift height and 4 m lift height, respectively.

Increase in lift height is also influential at high unit cement content as it can increase MCW up to around 0.1 mm. But in all cases, MCW is considerably less than 0.15 mm which is the threshold value for MCW except 4 m high lift at high cement content for which MCW is 0.15mm.

It can observe from Figures 6-27 that in hot weather, cement content is quite influential in determining maximum crack width (MCW) as by increasing cement content from 280 kg/m^3 to 330 kg/m^3, the maximum crack width may increase from 0 mm to 0.07 mm and 0 to 0.16 mm for 1 m and 4 m lift height, respectively.

Increase in lift height is also influential at high unit cement content as it can increase MCW up to around 0.09 mm. But in all cases till 3 m high lifts, MCW is less than 0.15 mm which is the threshold value for MCW. But for 4 m high lift at high cement content MCW is more than 0.15mm.

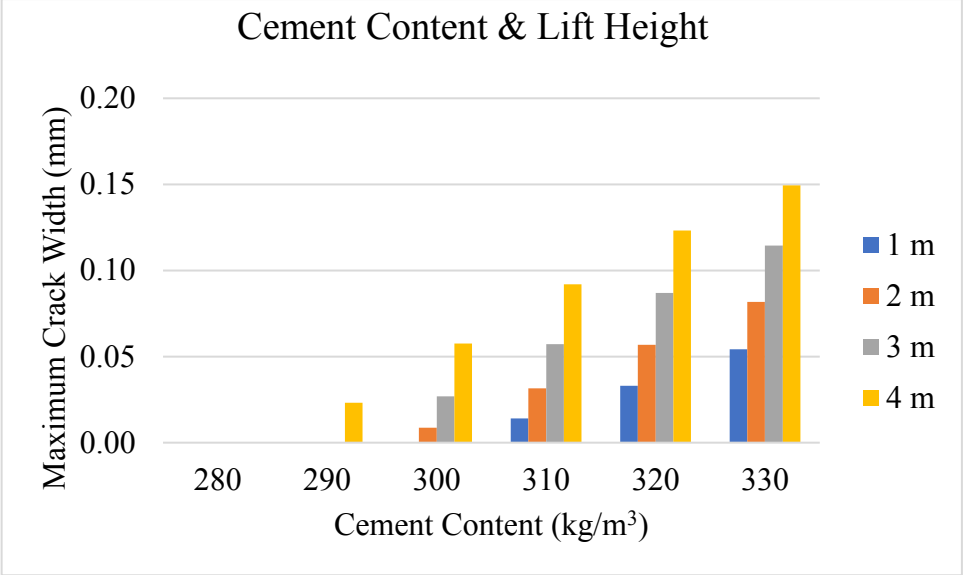

Figure 6-26 Effect of the lift height in normal weather for 15 m wide lift

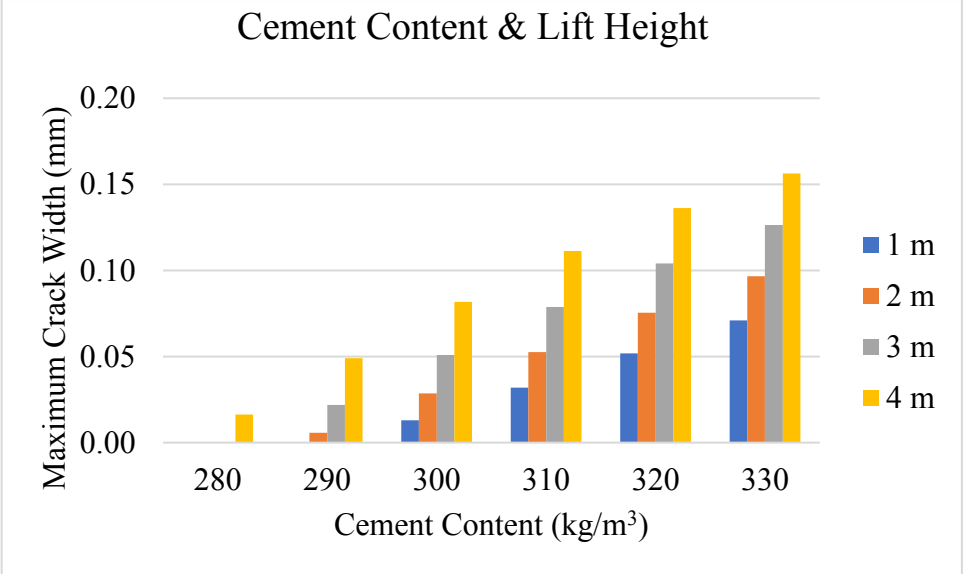

Figure 6-27 Effect of the lift height in hot weather for 15 m wide lift

For 25 m wide wall:

The results for parametric studies about the effect of height of the lift in cold weather, normal weather and hot weather are shown in Figures 6-28 through 6-30 for 25 m wide lifts. It can observe from Figures 6-28 that in cold weather, cement content is quite influential in determining maximum crack width (MCW) as by increasing cement content from 280 kg/m^3 to 330 kg/m^3, the maximum crack width may increase from 0 mm to 0.07 mm and 0 to 0.16 mm for 1 m and 4 m lift height, respectively.

Increase in lift height is also influential as it can increase MCW up to around 0.09 mm. But in all cases till 3 m high lifts, MCW is less than 0.15 mm which is the threshold value for MCW. But for 4 m high lift at high cement content MCW is more than 0.15mm.

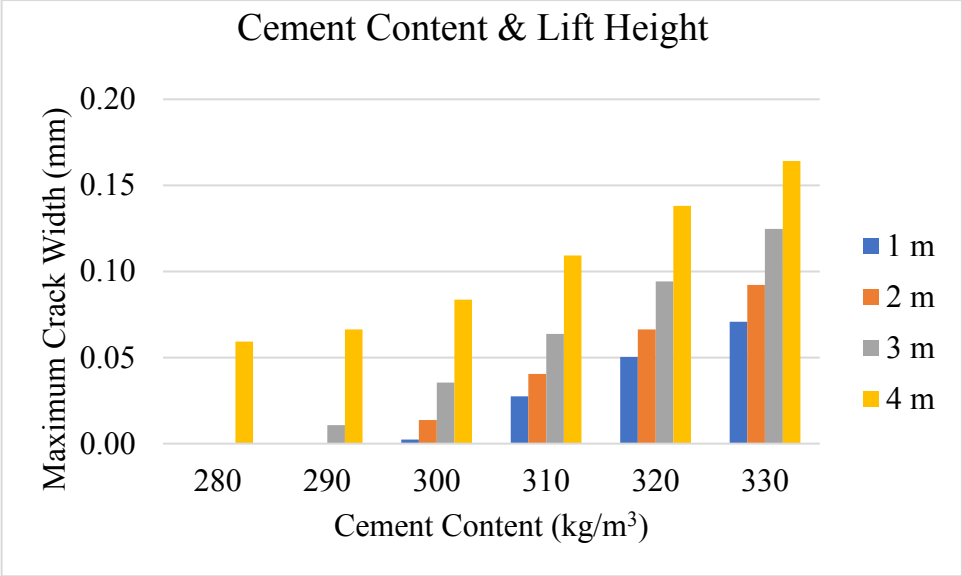

Figure 6-28 Effect of the lift height in cold weather for 25 m wide lift

It can observe from Figures 6-29 that in normal weather, cement content is quite influential in determining maximum crack width (MCW) as by increasing cement content from 280 kg/m^3 to 330 kg/m^3, the maximum crack width may increase from 0 mm to 0.14 mm and 0 to 0.2 mm for 1 m and 4 m lift height, respectively.

Increase in lift height is also influential as it can increase MCW up to around 0.12 mm. But in all cases till 2 m high lifts, MCW is less than 0.15 mm which is the threshold value for MCW. But for 3 m and 4 m high lift at cement content higher than 310 kg/m^{3,} MCW is greater than 0.15mm.

It can observe from Figures 6-30 that in hot weather, cement content is quite influential in determining maximum crack width (MCW) as by increasing cement content from 280 kg/m^3 to 330 kg/m^3, the maximum crack width may increase from 0 mm to 0.17 mm and 0 to 0.22 mm for 1 m and 4 m lift height, respectively.

Increase in lift height is also influential as it can increase MCW up to around 0.11 mm. For 1 m high lifts, MCW is greater than 0.15 mm which is the threshold value for MCW for unit cement content higher than 310 kg/m3. But for 4 m high lift even at unit cement content higher than 290 kg/m^3, MCW is greater than 0.15mm.

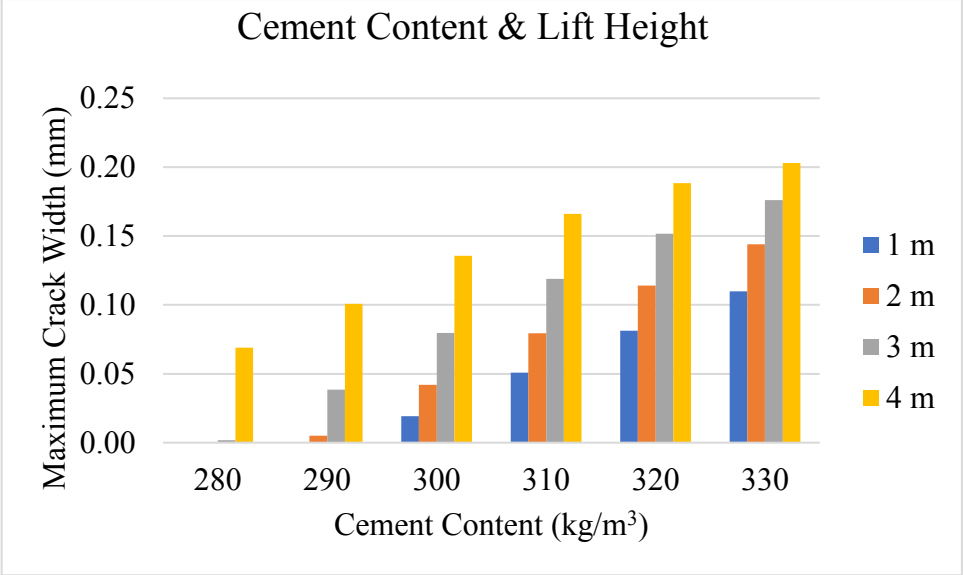

Figure 6-29 Effect of the lift height in normal weather for 25 m wide lift

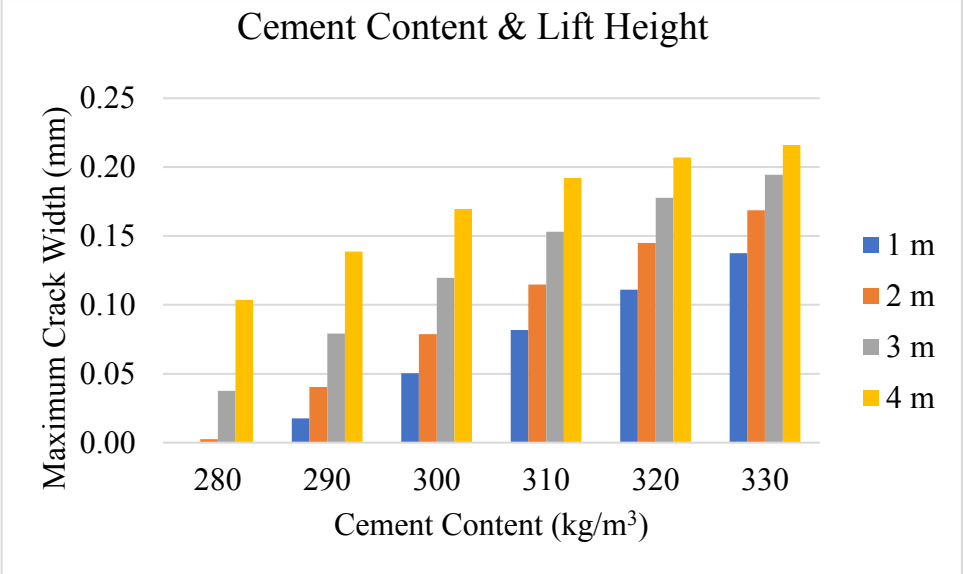

Figure 6-30 Effect of the lift height in hot weather for 25 m wide lift

6.1.4 Effect of cement content and reinforcement ratio

Parametric studies were conducted to observe the effect of reinforcement ratio at different amount of unit cement content. This study was conducted on three different widths of the wall i.e., 10 m, 15 m and 25 m which represent relatively small, medium and relatively larger width walls, respectively. The results of different width lifts are categorically explained below. Other input values used in this parametric study are summarized in the following table.

Thickness	Height	Expansive Additives	28 Days Strength	Lift Interval	Formwork Removal Time	Curing Period
2 m	3 m	0	25 MPa	7 Day	7 Day	7 Day

For 10 m wide wall:

The results for parametric studies about the effect of the reinforcement ratio in cold weather, normal weather and hot weather are shown in Figures 6-31 through 6-33 for 10 m wide lifts. It can observe from Figures 6-31 that in cold weather, cement content is quite influential in case of very low reinforcement ratio in determining maximum crack width (MCW) as by increasing cement content from 280 kg/m^3 to 330 kg/m^3, the maximum crack width may increase from 0.03 mm to 0.15 mm for 0.05% reinforcement ratio.

Increase in reinforcement ratio is also influential at it can reduce MCW up to around 0.15 mm by increasing reinforcement ratio from 0.05% to 0.5%. MCW is less than 0.15 mm which is the threshold value for MCW when reinforcement ration is 0.1% or higher.

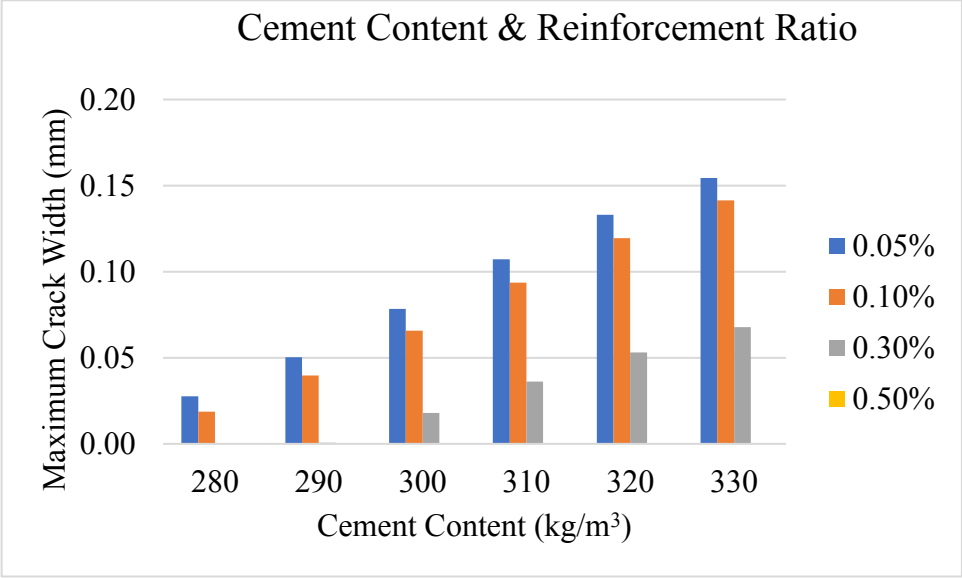

Figure 6-31 Effect of the reinforcement ratio in cold weather for 10 m wide lift

It can observe from Figures 6-32 that in normal weather, cement content is quite influential in case of very low reinforcement ratio in determining maximum crack width (MCW) as by increasing cement content from 280 kg/m^3 to 330 kg/m^3, the maximum crack width may increase from 0.01 mm to 0.12 mm for 0.05% reinforcement ratio.

Increase in reinforcement ratio is also influential at it can reduce MCW up to around 0.10 mm by increasing reinforcement ratio from 0.05% to 0.5% at high cement content. MCW is less than 0.15 mm which is the threshold value for MCW for all cases.

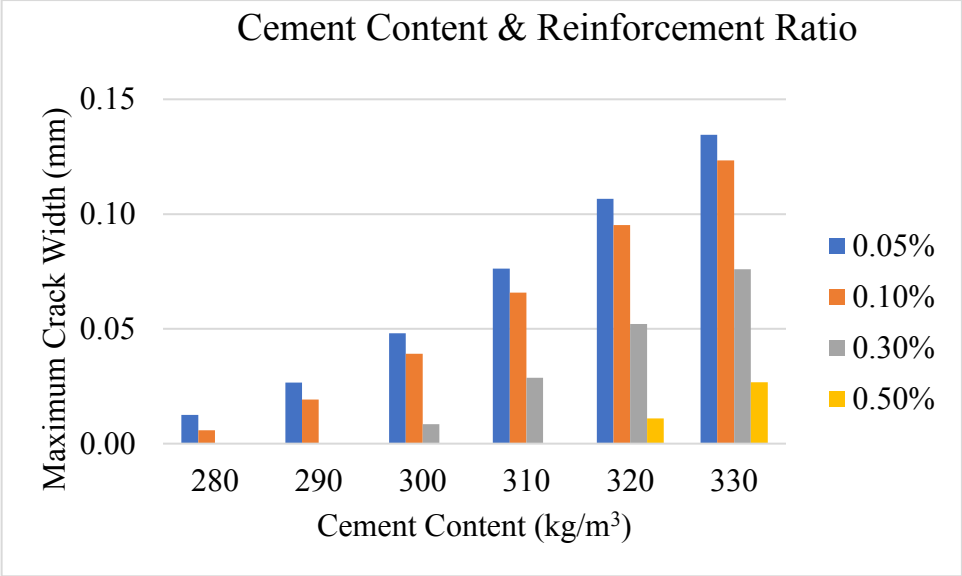

Figure 6-32 Effect of the reinforcement ratio in normal weather for 10 m wide lift

It can observe from Figures 6-33 that in hot weather, cement content is quite influential in case of very low reinforcement ratio in determining maximum crack width (MCW) as by increasing cement content from 280 kg/m^3 to 330 kg/m^3, the maximum crack width may increase from 0.03 mm to 0.15 mm for 0.05% reinforcement ratio.

Increase in reinforcement ratio is also influential at it can reduce MCW up to around 0.15 mm by increasing reinforcement ratio from 0.05% to 0.5%. MCW is less than 0.15 mm which is the threshold value for MCW when reinforcement ration is 0.1% or higher even at high unit cement content.

For 15 m wide wall:

The results for parametric studies about the effect of the reinforcement ratio in cold weather, normal weather and hot weather are shown in Figures 6-34 through 6-36 for 15 m wide lifts. It can observe from Figures 6-34 that in cold weather, cement content is quite influential in case of very low reinforcement ratio in determining maximum crack width (MCW) as by increasing cement content from 280 kg/m^3 to 330 kg/m^3, the maximum crack width may increase from 0.03 mm to 0.12 mm for 0.05% reinforcement ratio.

Increase in reinforcement ratio is also influential at it can reduce MCW up to around 0.07 mm by increasing reinforcement ratio from 0.05% to 0.5%. MCW is less than 0.15 mm which is the threshold value for MCW in all cases.

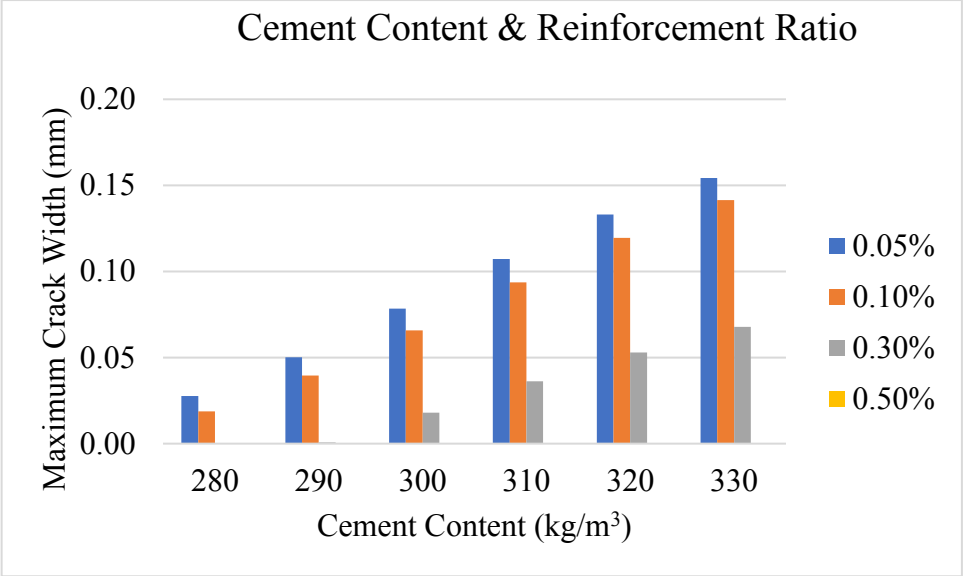

Figure 6-33 Effect of the reinforcement ratio in hot weather for 10 m wide lift

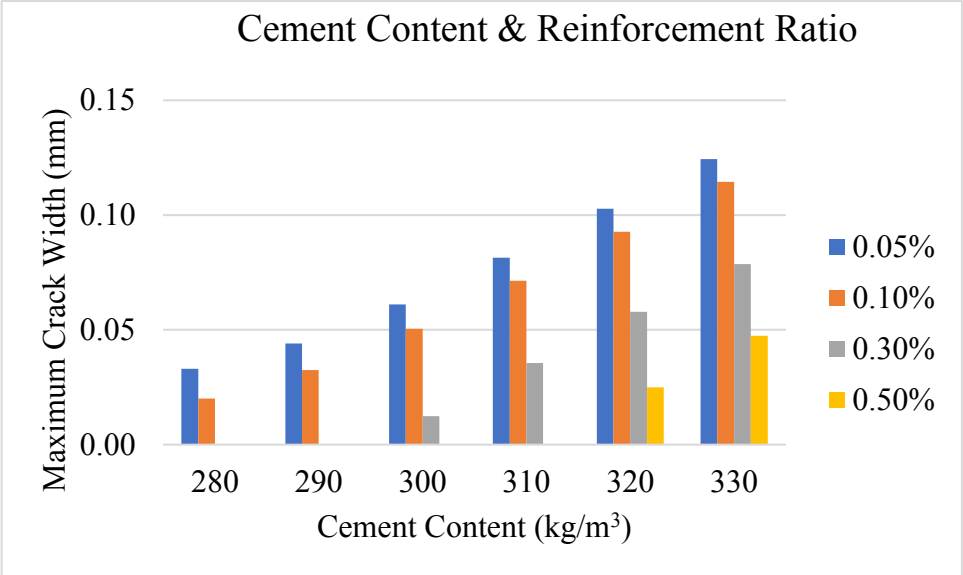

Figure 6-34 Effect of the reinforcement ratio in cold weather for 15 m wide lift

It can observe from Figures 6-35 that in normal weather, cement content is quite influential in case of very low reinforcement ratio in determining maximum crack width (MCW) as by increasing cement content from 280 kg/m^3 to 330 kg/m^3, the maximum crack width may increase from 0.04 mm to 0.17 mm for 0.05% reinforcement ratio.

Increase in reinforcement ratio is also influential at it can reduce MCW up to around 0.11 mm by increasing reinforcement ratio from 0.05% to 0.5%. MCW is less than 0.15 mm

which is the threshold value for MCW when reinforcement ration is 0.3% or higher in all cases. MCW is less than 0.15 mm in all cases when cement content is 320 kg/m^3 or less.

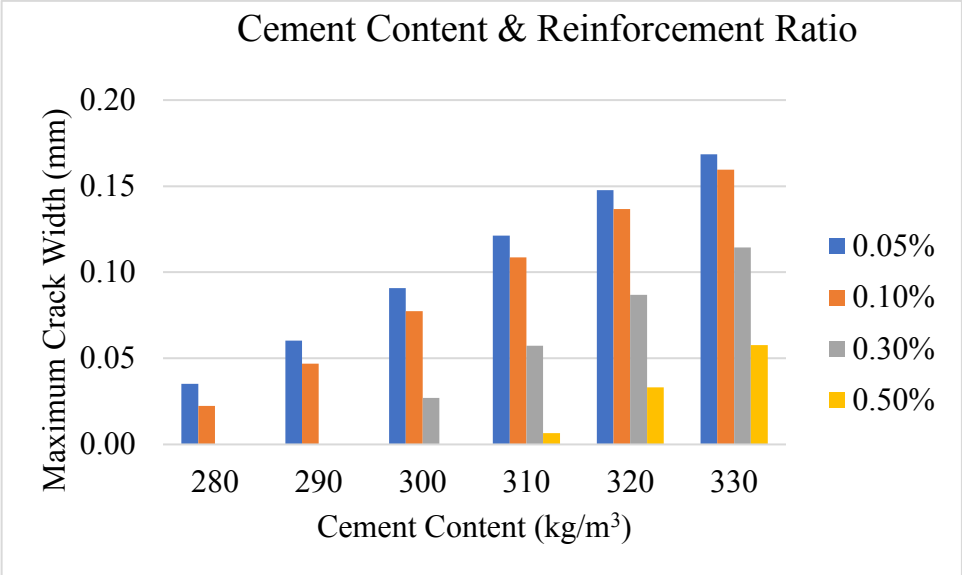

Figure 6-35 Effect of the reinforcement ratio in normal weather for 15 m wide lift

It can observe from Figures 6-36 that in hot weather, cement content is quite influential in case of very low reinforcement ratio in determining maximum crack width (MCW) as by increasing cement content from 280 kg/m^3 to 330 kg/m^3, the maximum crack width may increase from 0.06 mm to 0.18 mm for 0.05% reinforcement ratio.

Increase in reinforcement ratio is also influential at it can reduce MCW up to around 0.16 mm by increasing reinforcement ratio from 0.05% to 0.5% at high level of cement content. MCW is less than 0.15 mm which is the threshold value for MCW when reinforcement ration is 0.3% or higher in all cases. MCW is less than 0.15 mm in all cases when cement content is 300 kg/m^3 or less.

For 25 m wide wall:

The results for parametric studies about the effect of the reinforcement ratio in cold weather, normal weather and hot weather are shown in Figures 6-37 through 6-39 for 25 m wide lifts. It can observe from Figures 6-37 that in cold weather, cement content is quite influential in case of very low reinforcement ratio in determining maximum crack width (MCW) as by increasing cement content from 280 kg/m^3 to 330 kg/m^3, the maximum crack width may increase from 0.12 mm to 0.18 mm for 0.05% reinforcement ratio.

Increase in reinforcement ratio is also influential at it can reduce MCW up to around 0.15 mm by increasing reinforcement ratio from 0.05% to 0.5% % at medium level of cement content. MCW is less than 0.15 mm which is the threshold value for MCW when reinforcement ration is 0.3% or higher in all cases. MCW is less than 0.15 mm in all cases when cement content is 300 kg/m^3 or less.

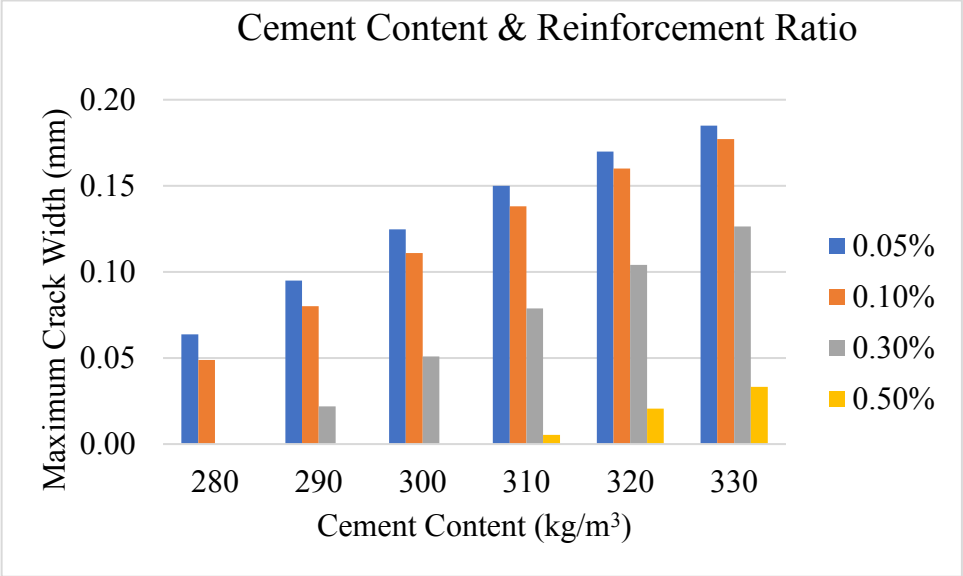

Figure 6-36 Effect of the reinforcement ratio in hot weather for 15 m wide lift

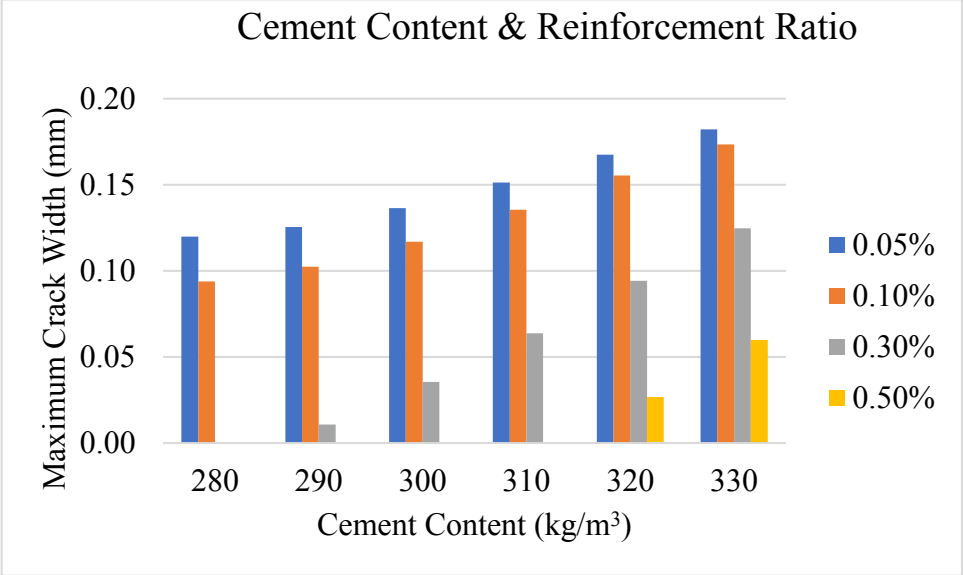

Figure 6-37 Effect of the reinforcement ratio in cold weather for 25 m wide lift

It can observe from Figures 6-38 that in normal weather, cement content is quite influential in case of very low reinforcement ratio in determining maximum crack width (MCW) as by increasing cement content from 280 kg/m^3 to 330 kg/m^3, the maximum crack width may increase from 0.13 mm to 0.21 mm for 0.05% reinforcement ratio.

Increase in reinforcement ratio is also influential at it can reduce MCW up to around 0.16 mm by increasing reinforcement ratio from 0.05% to 0.5% % at medium level of cement content. MCW is less than 0.15 mm which is the threshold value for MCW when reinforcement ration is 0.3% or higher in all cases.

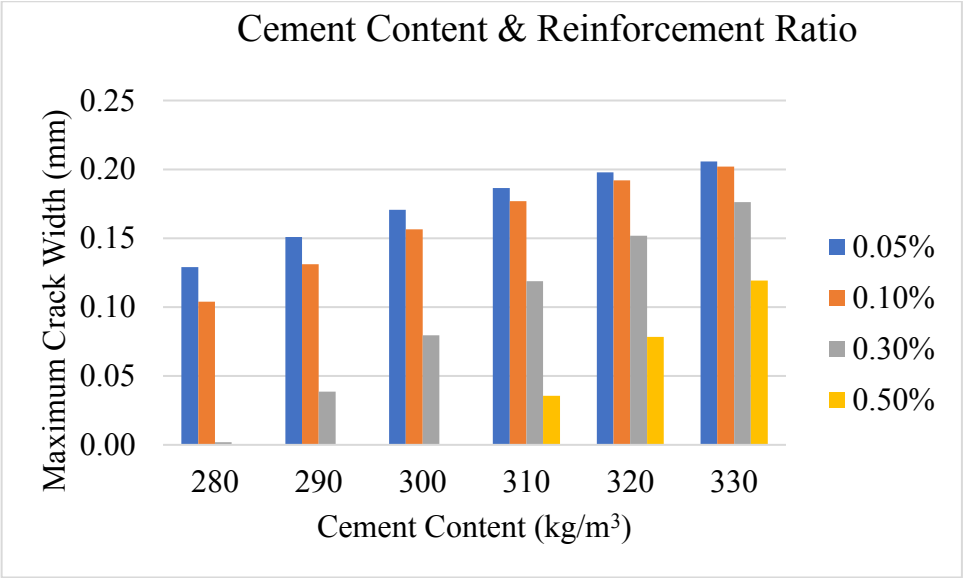

Figure 6-38 Effect of the reinforcement ratio in normal weather for 25 m wide lift

It can observe from Figures 6-39 that in hot weather, cement content is quite influential in case of very low reinforcement ratio in determining maximum crack width (MCW) as by increasing cement content from 280 kg/m^3 to 330 kg/m^3, the maximum crack width may increase from 0.15 mm to 0.21 mm for 0.05% reinforcement ratio.

Increase in reinforcement ratio is also influential at it can reduce MCW up to around 0.15 mm by increasing reinforcement ratio from 0.05% to 0.5% % at medium level of cement content. MCW is less than 0.15 mm which is the threshold value for MCW when reinforcement ration is 0.5% or higher in all cases. MCW is less than 0.15 mm in all cases when cement content is 300 kg/m^3 or less. In this scenario, MCW can be controlled more efficiently by controlling cement content.

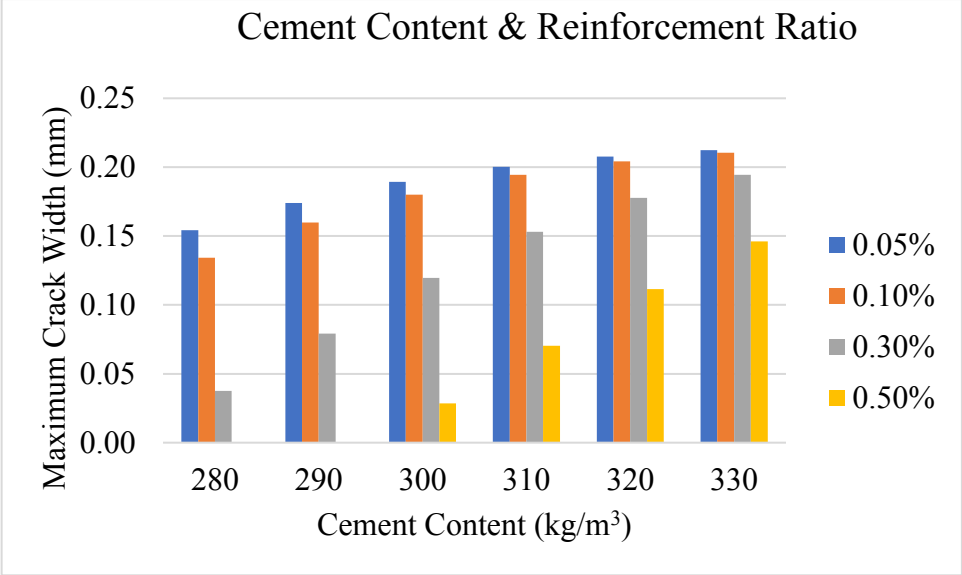

Figure 6-39 Effect of the reinforcement ratio in hot weather for 25 m wide lift

6.1.5 Effect of cement content and lift interval

Parametric studies were conducted to observe the effect of lift interval at different amount of unit cement content. This study was conducted on three different widths of the wall i.e., 10 m, 15 m and 25 m which represent relatively small, medium and relatively larger width walls, respectively. The results of different width lifts are categorically explained below. Other input values used in this parametric study are summarized in the following table.

Thickness	Height	Expansive Additives	28 Days Strength	Lift Interval	Formwork Removal Time	Curing Period
2 m	3 m	0	25 MPa	7 Day	7 Day	7 Day

For 10 m wide wall:

The results for parametric studies about the effect of lift interval in cold weather, normal weather and hot weather are shown in Figures 6-40 through 6-42 for 10 m wide lifts. It can observe from Figures 6-40 that in cold weather, cement content is very influential in determining maximum crack width (MCW) as by increasing cement content from 280 kg/m^3 to 330 kg/m^3, the maximum crack width may increase from 0 mm to around 0.06 mm and from 0 mm to 0.08 mm for 3 day and 28 day lift interval, respectively.

Increase in lift interval is also little influential as it can increase MCW up to around 0.02 mm, but this increase is not considerably high. But in all cases, MCW is considerably less than 0.15 mm which is the threshold value for MCW.

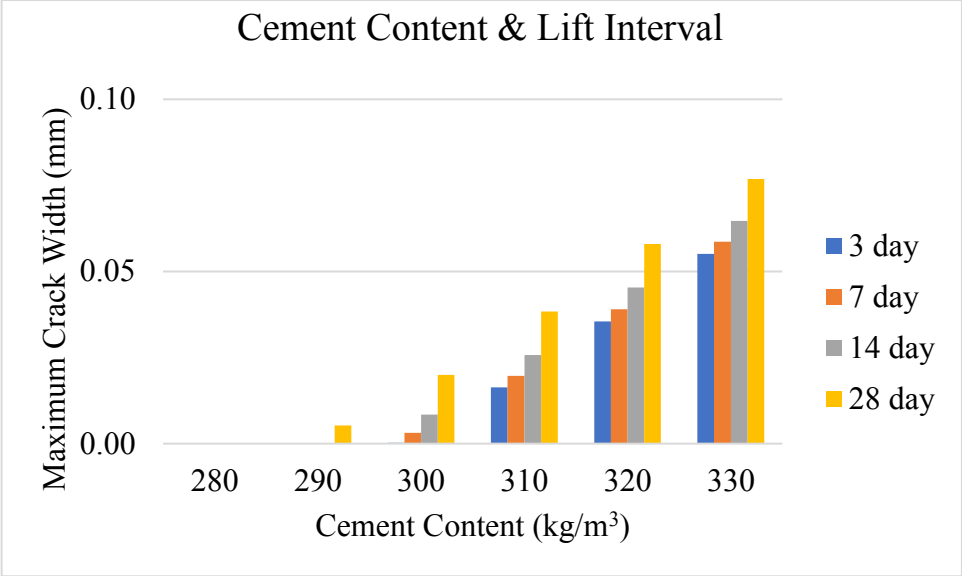

Figure 6-40 Effect of the lift interval in hot weather for 10 m wide lift

It can observe from Figures 6-41 that in normal weather, cement content is very influential in determining maximum crack width (MCW) as by increasing cement content from 280 kg/m^3 to 330 kg/m^3, the maximum crack width may increase from 0 mm to around 0.08 mm and from 0 mm to 0.11 mm for 3 day and 28 day lift interval, respectively.

Increase in lift interval is also little influential as it can increase MCW up to around 0.03 mm, but this increase is not considerably high. But in all cases, MCW is considerably less than 0.15 mm which is the threshold value for MCW.

It can observe from Figures 6-42 that in hot weather, cement content is very influential in determining maximum crack width (MCW) as by increasing cement content from 280 kg/m^3 to 330 kg/m^3, the maximum crack width may increase from 0 mm to around 0.06 mm and from 0 mm to 0.12 mm for 3 day and 28 day lift interval, respectively.

Increase in lift interval is also little influential as it can increase MCW up to around 0.06 mm, but this increase is not considerably high. But in all cases, MCW is considerably less than 0.15 mm which is the threshold value for MCW.

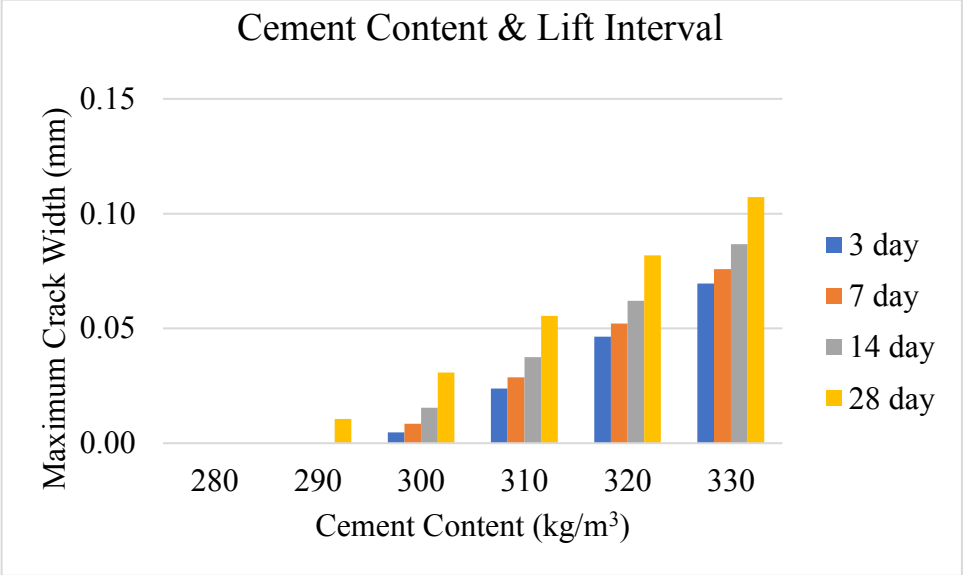

Figure 6-41 Effect of the lift interval in normal weather for 10 m wide lift

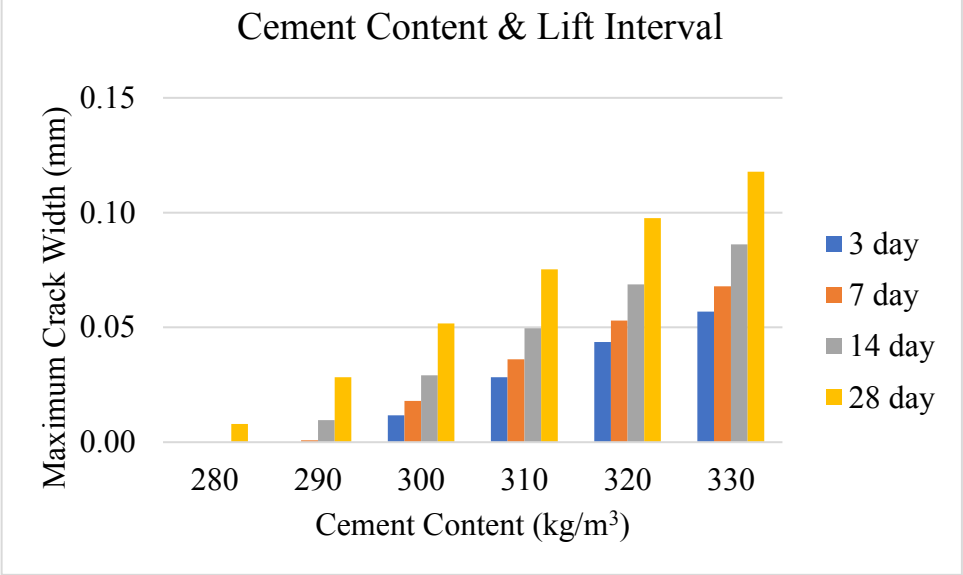

Figure 6-42 Effect of the lift interval in hot weather for 10 m wide lift

For 15 m wide wall:

The results for parametric studies about the effect of lift interval in cold weather, normal weather and hot weather are shown in Figures 6-43 through 6-45 for 15 m wide lifts. It can observe from Figures 6-43 that in cold weather, cement content is very influential in determining maximum crack width (MCW) as by increasing cement content from 280 kg/m^3 to 330 kg/m^3, the maximum crack width may increase from 0 mm to around 0.07 mm and from 0 mm to 0.1 mm for 3 day and 28 day lift interval, respectively.

Increase in lift interval is also little influential as it can increase MCW up to around 0.02 mm, but this increase is not considerably high. But in all cases, MCW is considerably less than 0.15 mm which is the threshold value for MCW.

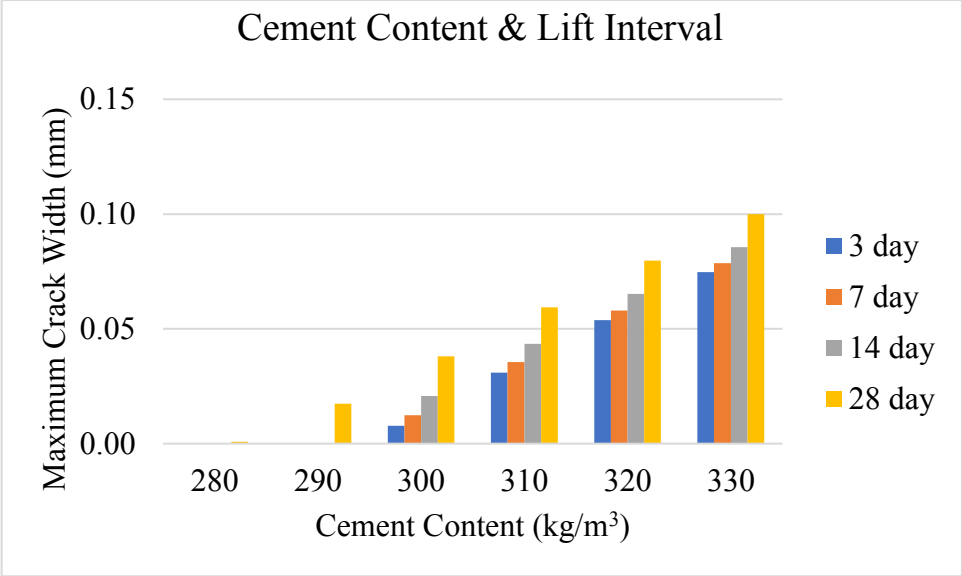

Figure 6-43 Effect of the lift interval in cold weather for 15 m wide lift

It can observe from Figures 6-44 that in normal weather, cement content is very influential in determining maximum crack width (MCW) as by increasing cement content from 280 kg/m^3 to 330 kg/m^3, the maximum crack width may increase from 0 mm to around 0.11 mm and from 0 mm to 0.14 mm for 3 day and 28 day lift interval, respectively.

Increase in lift interval is also little influential as it can increase MCW up to around 0.03 mm, but this increase is not considerably high. But in all cases, MCW is considerably less than 0.15 mm which is the threshold value for MCW.

It can observe from Figures 6-45 that in hot weather, cement content is very influential in determining maximum crack width (MCW) as by increasing cement content from 280 kg/m^3 to 330 kg/m^3, the maximum crack width may increase from 0 mm to around 0.12 mm and from 0 mm to 0.16 mm for 3 day and 28 day lift interval, respectively.

Increase in lift interval is also little influential as it can increase MCW up to around 0.03 mm, but this increase is not considerably high. But in all cases, MCW is less than 0.15 mm which is the threshold value for MCW except for a lift with 28 day interval at high cement content.

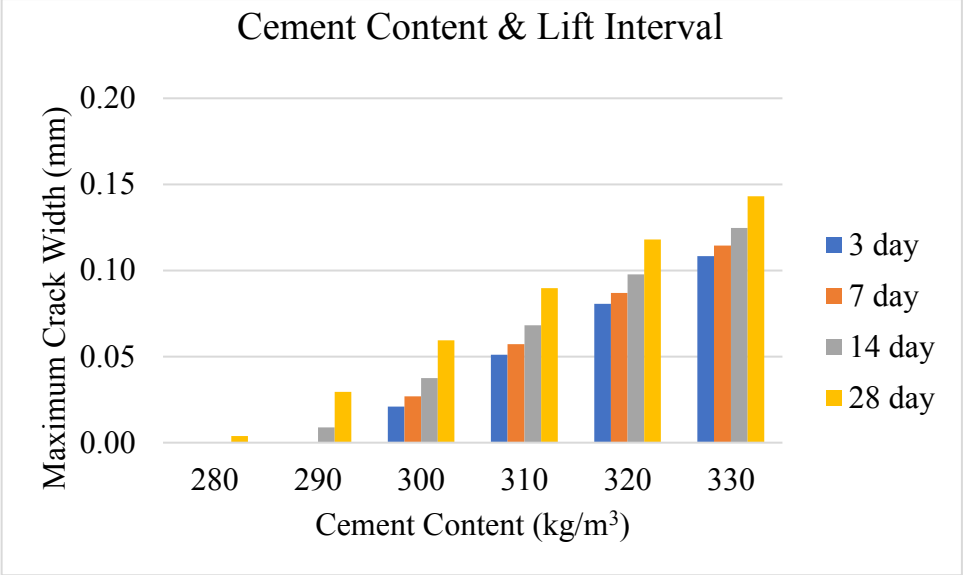

Figure 6-44 Effect of the lift interval in normal weather for 15 m wide lift

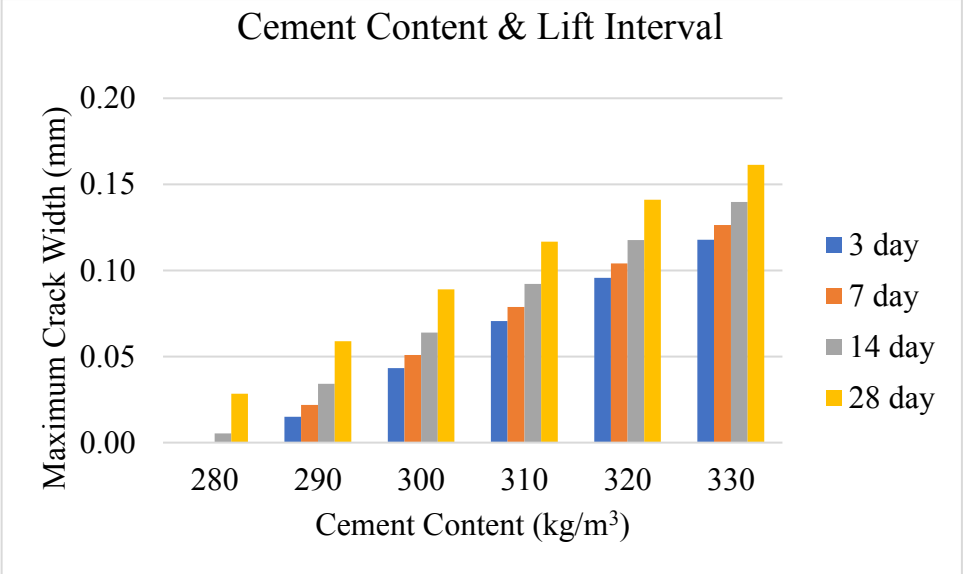

Figure 6-45 Effect of the lift interval in hot weather for 15 m wide lift

For 25 m wide wall:

The results for parametric studies about the effect of lift interval in cold weather, normal weather and hot weather are shown in Figures 6-46 through 6-48 for 25 m wide lifts. It can observe from Figures 6-46 that in cold weather, cement content is very influential in determining maximum crack width (MCW) as by increasing cement content from 280 kg/m^3 to 330 kg/m^3, the maximum crack width may increase from 0 mm to around 0.12 mm and from 0 mm to 0.15 mm for 3 day and 28 day lift interval, respectively.

Increase in lift interval is also little influential as it can increase MCW up to around 0.03 mm, but this increase is not considerably high. But in all cases, MCW is less than 0.15

mm which is the threshold value for MCW except for a lift with 28 day interval at high cement content.

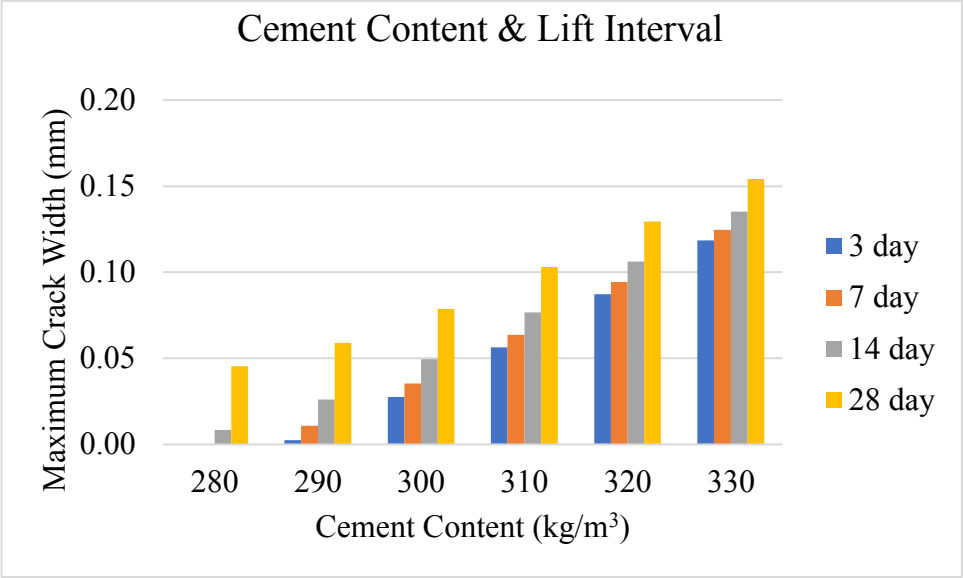

Figure 6-46 Effect of the lift interval in cold weather for 25 m wide lift

It can observe from Figures 6-47 that in cold weather, cement content is very influential in determining maximum crack width (MCW) as by increasing cement content from 280 kg/m^3 to 330 kg/m^3, the maximum crack width may increase from 0 mm to around 0.17 mm and from 0.06 mm to 0.19 mm for 3 day and 28 day lift interval, respectively.

Increase in lift interval is also little influential as it can increase MCW up to around 0.02 mm, but this increase is not considerably high. MCW is less than 0.15 mm which is the threshold value for MCW when unit cement content is 300 kg/m^3 or less.

It can observe from Figures 6-48 that in hot weather, cement content is very influential in determining maximum crack width (MCW) as by increasing cement content from 280 kg/m^3 to 330 kg/m^3, the maximum crack width may increase from 0.03 mm to around 0.19 mm and from 0.09 mm to 0.21 mm for 3 day and 28 day lift interval, respectively.

Increase in lift interval is also little influential as it can increase MCW up to around 0.03 mm, but this increase is not considerably high. But in all cases, MCW is greater than 0.15 mm which is the threshold value for MCW when unit cement content is 300 kg/m^3 or more

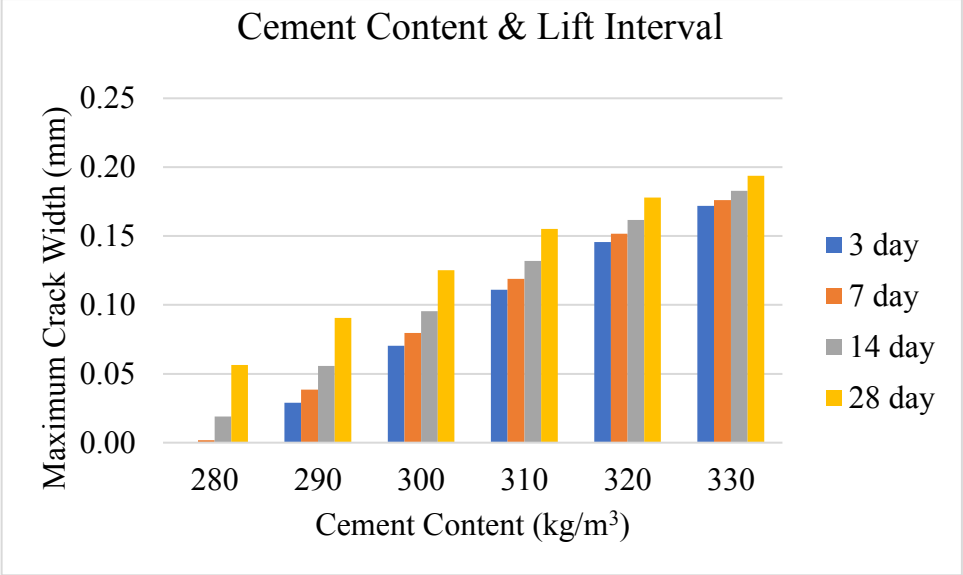

Figure 6-47 Effect of the lift interval in normal weather for 25 m wide lift

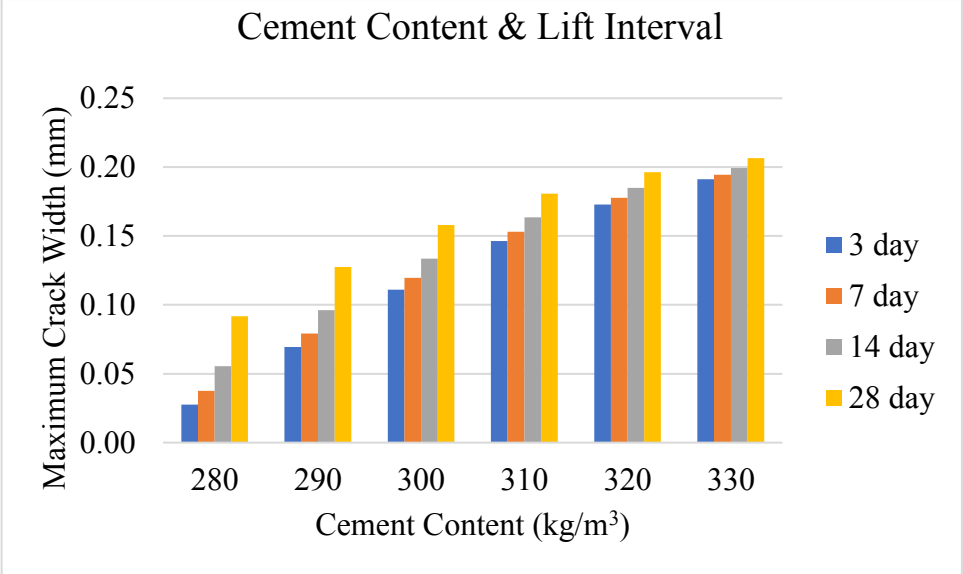

Figure 6-48 Effect of the lift interval in hot weather for 25 m wide lift

6.1.6 Effect of cement content and initial concrete temperature

Parametric studies were conducted to observe the effect of initial concrete temperature at different amount of unit cement content. This study was conducted in three different seasonal variations i.e., when initial ambient temperature is 0°C, 20°C and 30°C which represent cold weather, normal weather and hot weather, respectively. The results are categorically explained below. Other input values used in this parametric study are summarized in the following table.

Thickness	Height	Width	Expansive Additives	28 Days Strength	Lift Interval	Formwork Removal Time	Curing Period
2 m	3 m	15 m	0	25 MPa	7 Day	7 Day	7 Day

The results for parametric studies about the effect of initial concrete temperature in cold weather, normal weather and hot weather are shown in Figures 6-49 through 6-51 for 15 m wide lifts. It can observe from Figures 6-49 that in cold weather, cement content is very influential in determining maximum crack width (MCW) as by increasing cement content from 280 kg/m^3 to 330 kg/m^3, the maximum crack width may increase from 0 mm to around 0.07 mm and from 0.01 mm to 0.09 mm for 5^{o}C and 20^{o}C initial concrete temperature, respectively.

Increase in initial concrete temperature is also little influential as it can increase MCW up to around 0.04 mm, but this increase is not considerably high. But in all cases, MCW is considerably less than 0.15 mm which is the threshold value for MCW.

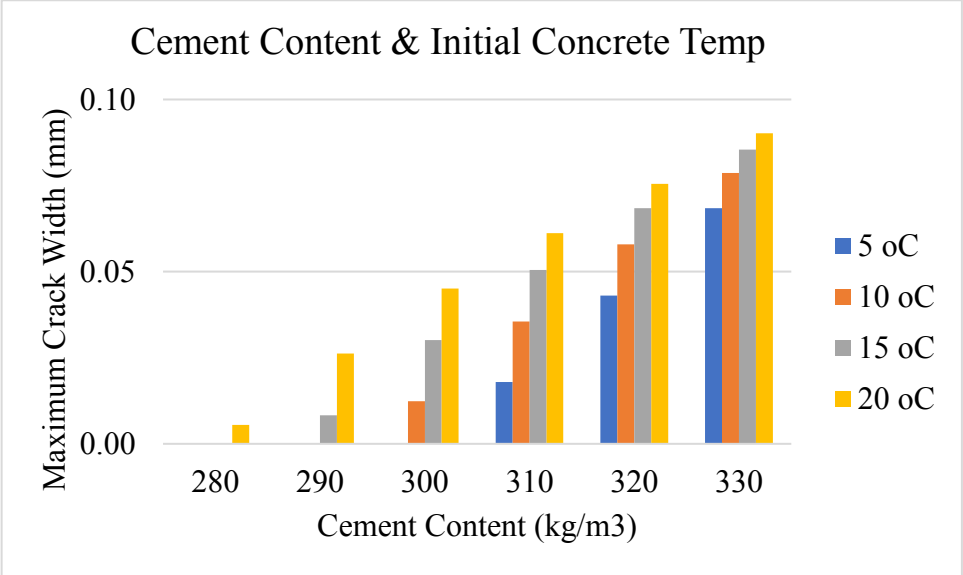

Figure 6-49 Effect of the initial concrete temperature in cold weather for 15 m wide lift

It can observe from Figures 6-50 that in normal weather, cement content is very influential in determining maximum crack width (MCW) as by increasing cement content from 280 kg/m^3 to 330 kg/m^3, the maximum crack width may increase from 0 mm to around 0.1 mm and from 0.01 mm to 0.12 mm for 10^{o}C and 30^{o}C initial concrete temperature, respectively.

Increase in initial concrete temperature is also influential as it can increase MCW up to around 0.05 mm, but this increase is not considerably high. But in all cases, MCW is considerably less than 0.15 mm which is the threshold value for MCW.

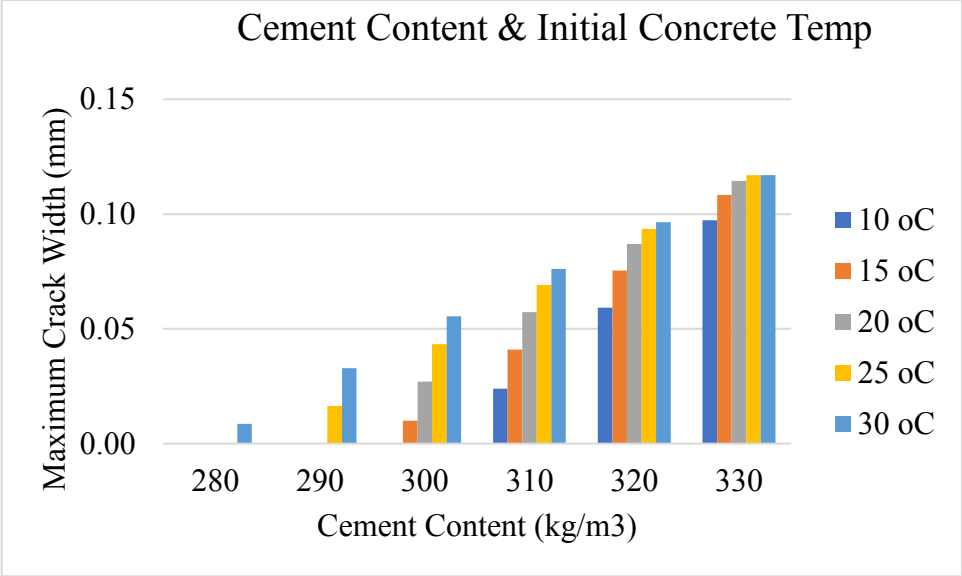

Figure 6-50 Effect of the initial concrete temperature in normal weather for 15 m wide lift

It can observe from Figures 6-51 that in hot weather, cement content is very influential in determining maximum crack width (MCW) as by increasing cement content from 280 kg/m^3 to 330 kg/m^3, the maximum crack width may increase from 0 mm to around 0.07 mm and from 0 mm to 0.13 mm for both 15^{o}C and 30^{o}C initial concrete temperature.

Increase in initial concrete temperature is also little influential as it can increase MCW up to around 0.04 mm, but this increase is not considerably high. But in all cases, MCW is considerably less than 0.15 mm which is the threshold value for MCW.

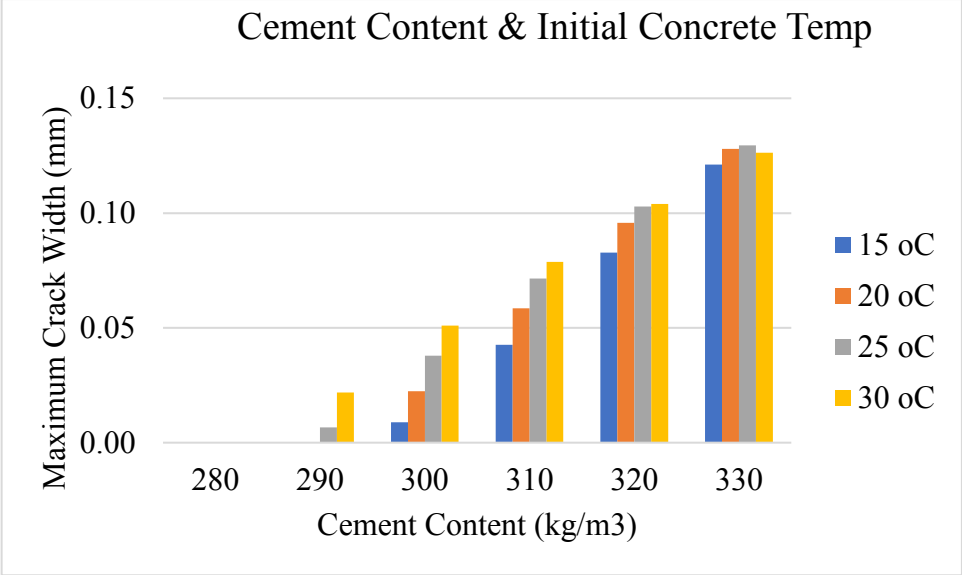

Figure 6-51 Effect of the initial concrete temperature in hot weather for 15 m wide lift

6.1.7 Effect of cement content and 28 day concrete strength

Parametric studies were conducted to observe the effect of concrete strength at different amount of unit cement content. This study was conducted in three different seasonal variations i.e., when initial ambient temperature is 0°C, 20°C and 30°C which represent cold weather, normal weather and hot weather, respectively. The results are categorically explained below. Other input values used in this parametric study are summarized in the following table.

Thickness	Height	Width	Expansive Additives	Rebar ratio	Lift Interval	Formwork Removal Time	Curing Period
2 m	3 m	15 m	0	0.3 %	7 Day	7 Day	7 Day

The results for parametric studies about the effect of concrete strength in cold weather, normal weather and hot weather are shown in Figures 6-52 through 6-54 for 15 m wide lifts. It can observe from Figures 6-52 that in cold weather, cement content is very influential in determining maximum crack width (MCW) as by increasing cement content from 280 kg/m^3 to 330 kg/m^3, the maximum crack width may increase from 0 mm to around 0.08 mm and from 0.02 mm to 0.13 mm for 25MPa and 40 MPa concrete strength, respectively.

Increase in concrete strength is also influential as it can increase MCW up to around 0.05 mm. But in all cases, MCW is considerably less than 0.15 mm which is the threshold value for MCW.

It can observe from Figures 6-53 that in normal weather, cement content is very influential in determining maximum crack width (MCW) as by increasing cement content from 280 kg/m^3 to 330 kg/m^3, the maximum crack width may increase from 0 mm to around 0.11 mm and from 0.03 mm to 0.16 mm for 25MPa and 40 MPa concrete strength, respectively.

Increase in concrete strength is also influential as it can increase MCW up to around 0.05 mm. But in all cases, MCW is considerably less than 0.15 mm which is the threshold value for MCW except for the case when 40MPa concrete with high cement content is used.

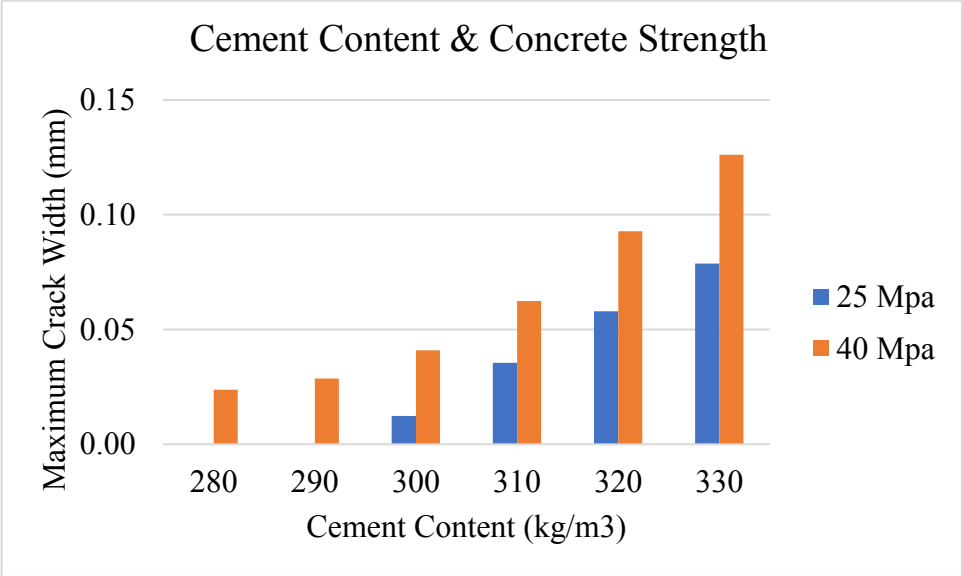

Figure 6-52 Effect of the 28 day concrete strength in cold weather for 15 m wide lift with 0.3% reinforcement ratio

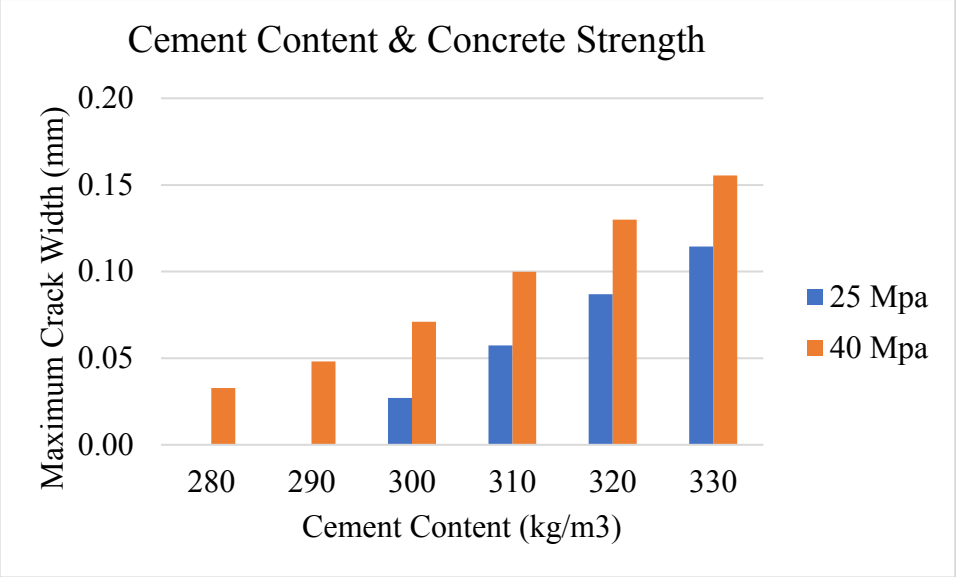

Figure 6-53 Effect of the 28 day concrete strength in normal weather for 15 m wide lift with 0.3% reinforcement ratio

It can observe from Figures 6-54 that in hot weather, cement content is very influential in determining maximum crack width (MCW) as by increasing cement content from 280 kg/m^3 to 330 kg/m^3, the maximum crack width may increase from 0 mm to around 0.13 mm and from 0.03 mm to 0.16 mm for 25MPa and 40 MPa concrete strength, respectively.

Increase in concrete strength is also influential as it can increase MCW up to around 0.04 mm. But in all cases, MCW is considerably less than 0.15 mm which is the threshold value for MCW except for the case when 40MPa concrete with high cement content is used.

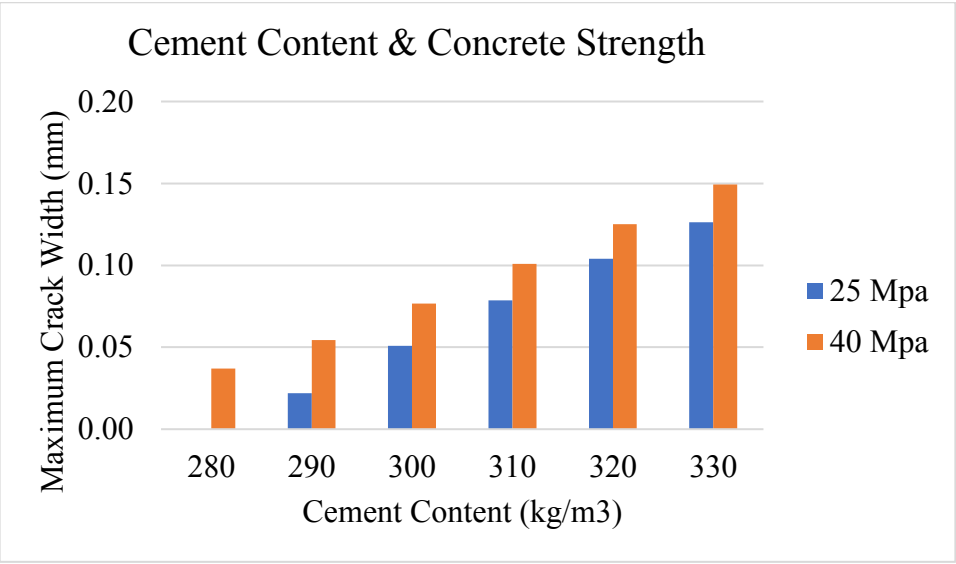

Figure 6-54 Effect of the 28 day concrete strength in hot weather for 15 m wide lift with 0.3% reinforcement ratio

6.2 Conclusions on parametric studies on vertical walls

Based on the parametric studies for vertical walls using previously trained ANN, following conclusions are drawn.

- ANNs are very useful tools to establish systematic relationship among different parameters which influence maximum crack width.
- The increase in cement content is very influential in every condition as it can significantly increase maximum crack width.
- In hotter weather, the tendency of increasing maximum crack width is more as compared to colder weather.
- The increase in thickness of the lift is quite significant as increase in thickness can increase maximum crack width. This effect is more pronounces in wider lifts.
- The increase in height of the lift is quite significant as increase in height can increase maximum crack width. This effect is more pronounces in wider lifts.
- The increase in width of the lift is very significant as increase in width can increase maximum crack width significantly. This effect is more pronounces in the lifts with less reinforcement ratio.
- The increase in reinforcement ratio of the lift is very significant as increase in reinforcement ratio can reduce maximum crack width significantly.
- The increase in lift interval is little significant as increase in lift interval can increase maximum crack width. This effect is more pronounces in the hotter season.
- The increase in initial concrete temperature is little significant as increase in initial concrete temperature can increase maximum crack width. This effect is more pronounces when unit cement content is in the normal range.
- The increase in concrete strength is also significant as increase in concrete strength can increase maximum crack width.
- These studies will provide the threshold limits for input parameters to control harmful thermal cracking.

7 Conclusions

In this chapter, conclusions obtained from different parts of the research are categorically explained.

7.1 Prediction of occurrence of thermal cracking by artificial neural networks

Based on the findings of this study, which was focused on predicting the occurrence of thermal cracking of RC abutments using feedforward multilayer perceptron artificial neural networks and reliable actual construction data, following conclusions are drawn:

i. Performance of ANNs with less number of input parameters for both vertical walls and parapets was promising, which was a good step towards prediction of occurrence of thermal cracking in RC abutments with basic information such as geometric and material properties, and ambient environmental conditions.
ii. For vertical walls, ANN-V(b) which was the preferred ANN found in this study showed average accuracy level 81.5% for holdout samples by considering thickness, width, lift height, reinforcement ratio, cement content, initial concrete temperature, initial ambient temperature, lift interval, form removal time and curing period as input parameters.
iii. For parapet walls, ANN-P(b) which was the preferred ANN found in this study showed average accuracy level 87.6% for holdout samples by considering thickness, width, lift height, reinforcement ratio, cement content, expansive additive, initial concrete temperature, initial ambient temperature, lift interval, form removal time and curing period as input parameters.

7.2 Prediction of maximum width of thermal cracking by artificial neural networks

Based on the developed ANN to predict maximum width of thermal cracking, following conclusions are drawn;

i. Present ANN could predict 90.95 % (171 lifts out of 188) correctly if the permissible error in prediction is considered as ± 0.1 mm.

ii. 16 lifts out of 17 lifts for which prediction error was more than ± 0.1 mm were constructed from 2007 to 2009.
iii. If ± 0.075 mm is considered as permissible error in prediction, then prediction accuracy was 83 % (156 lifts out of 188 were correctly predicted).
iv. If ± 0.05 mm is considered as permissible error in prediction, then prediction accuracy was 69 % (130 lifts out of 188 were correctly predicted).
v. ANNs are potential candidates to perform this type of complex problems by using reliable data.

Based on the developed ANN to predict maximum width of thermal cracking in parapets, following conclusions are drawn;

i. Present ANN could predict 94.74 % (72 lifts out of 76) correctly if the permissible error in prediction is considered as ± 0.1 mm.
ii. If ± 0.075 mm is considered as permissible error in prediction, then prediction accuracy was 93.42 % (71 lifts out of 76 were correctly predicted).
iii. If ± 0.05 mm is considered as permissible error in prediction, then prediction accuracy was 90.8 % (69 lifts out of 76 were correctly predicted).
iv. Although accuracy level of prediction is high, but this high accuracy is for small crack widths as the ANN is unable to predict larger crack width for holdout samples. The possible reasons are as follows;
    a. The dataset is very small, so it is insufficient to build an appropriate ANN.
    b. There are very few number of lifts with larger crack widths which are causing insufficiency in data with larger crack widths.

7.3 Parametric studies on influential parameters for vertical walls

Based on parametric studies for vertical walls using previously trained ANN, following conclusions are drawn.

i. ANNs are very useful tools to establish systematic relationship among different parameters which influence maximum crack width.
ii. The increase in cement content is very influential in every condition as it can significantly increase maximum crack width.
iii. In hotter weather, the tendency of increasing maximum crack width is more as compared to colder weather.

iv. The increase in thickness of the lift is quite significant as increase in thickness can increase maximum crack width. This effect is more pronounces in wider lifts.

v. The increase in height of the lift is quite significant as increase in height can increase maximum crack width. This effect is more pronounces in wider lifts.

vi. The increase in width of the lift is very significant as increase in width can increase maximum crack width significantly. This effect is more pronounces in the lifts with less reinforcement ratio.

vii. The increase in reinforcement ratio of the lift is very significant as increase in reinforcement ratio can reduce maximum crack width significantly.

viii. The increase in lift interval is little significant as increase in lift interval can increase maximum crack width. This effect is more pronounces in the hotter season.

ix. The increase in initial concrete temperature is little significant as increase in initial concrete temperature can increase maximum crack width. This effect is more pronounces when unit cement content is in the normal range.

x. The increase in concrete strength is also significant as increase in concrete strength can increase maximum crack width.

xi. These studies will provide the threshold limits for input parameters to control harmful thermal cracking.

7.4 Recommendations for future studies

Based on present research following topics of research are proposed;

i. Along with Yamaguchi prefecture, Gunma prefecture has also started a crack control system. So, it is suggested to validate the present research methodology and ANNs for Gunma prefecture database.

ii. As mentioned earlier, there is a room to improve crack prediction method for parapets due to lack of appropriate dataset, so an alternative methodology must be studies to cater the problem of limited data and utilization of small datasets efficiently.

iii. Proposal for the remedial measures by providing threshold limits for input parameters to control harmful thermal cracking under various circumstances. And, contribution in the “Crack Control Guidelines”.

8 References

[1] Japan Concrete Institute, “Guidelines for Control of Cracking of Mass Concrete 2016,” Japan Concrete Institute, 2016.

[2] ACI, “Control of Cracking in Concrete,” *Concr. J.*, vol. 34, no. 8, pp. 13–20, 2014.

[3] A. Hosoda, M. Ninomiya, T. Tamura, and K. Hayashi, “Effects of crack control system on reducing cracks and improving covercrete quality of concrete structures,” *J. JSCE*, vol. 70, no. 4, pp. 336–355, 2014.

[4] B. Klemczak and A. Knoppik-wróbel, “Early Age Thermal and Shrinkage Cracks in Concrete Structures – Description of the Problem,” vol. c, no. June, pp. 47–58, 2011.

[5] M. Kuhn and K. Johnson, *Applied predictive modeling*. Springer Science+Business Media New York, 2013.

[6] B. A. Young, A. Hall, L. Pilon, P. Gupta, and G. Sant, “Can the compressive strength of concrete be estimated from knowledge of the mixture proportions?: New insights from statistical analysis and machine learning methods,” *Cem. Concr. Res.*, vol. 115, no. December 2017, pp. 379–388, 2019.

[7] T. Oladipupo, “Types of Machine Learning Algorithms,” in *New Advances in Machine Learning*, Y. Zhang, Ed. 2010.

[8] W. Z. Taffese and E. Sistonen, “Machine learning for durability and service-life assessment of reinforced concrete structures: Recent advances and future directions,” *Autom. Constr.*, vol. 77, pp. 1–14, 2017.

[9] A. K. Jain and J. Mao, “Artificial Neural Network: A Tutorial,” *Computer (Long. Beach. Calif).*, vol. 29, pp. 31–44, 1996.

[10] H. Adeli, “Neural networks in civil engineering: 1989-2000,” *Comput. Civ. Infrastruct. Eng.*, vol. 16, no. 2, pp. 126–142, 2001.

[11] K. Inadsu, T. Tamura, and H. Nakamura, “Study on the crack occurrence prediction of civil engineering structures using a neural network (In Japanese),” *65th Annu. Meet. Japan Soc. Civ. Eng.*, vol. 403, no. 805–6, pp. 805–806, 2010.

[12] IBM, “IBM SPSS Neural Networks 25,” 2017.

[13] F. x. Rosenblatt, *Principles of Neurodynamics: Perceptrons and the Theory of Brain Mechanisms*. Washington DC: Spartan Books, 1961.

[14] Y. Yuan and Z. L. Wan, “Prediction of cracking within early-age concrete due to thermal, drying and creep behavior,” *Cem. Concr. Res.*, vol. 32, no. 7, pp. 1053–1059, 2002.

[15] Y. Yu, W. Li, J. Li, and T. N. Nguyen, “A novel optimised self-learning method for compressive strength prediction of high performance concrete,” *Constr. Build. Mater.*, vol. 184, pp. 229–247, 2018.

[16] F. Deng, Y. He, S. Zhou, Y. Yu, H. Cheng, and X. Wu, "Compressive strength prediction of recycled concrete based on deep learning," *Constr. Build. Mater.*, vol. 175, pp. 562–569, 2018.

[17] H. Naderpour, A. H. Rafiean, and P. Fakharian, "Compressive strength prediction of environmentally friendly concrete using artificial neural networks," *J. Build. Eng.*, vol. 16, no. October 2017, pp. 213–219, 2018.

[18] P. Chopra, R. K. Sharma, M. Kumar, and T. Chopra, "Comparison of Machine Learning Techniques for the Prediction of Compressive Strength of Concrete," *Adv. Civ. Eng.*, vol. 2018, 2018.

[19] T. Nguyen, A. Kashani, T. Ngo, and S. Bordas, "Deep neural network with high-order neuron for the prediction of foamed concrete strength," *Comput. Civ. Infrastruct. Eng.*, pp. 1–17, 2018.

[20] A. Behnood, V. Behnood, M. Modiri Gharehveran, and K. E. Alyamac, "Prediction of the compressive strength of normal and high-performance concretes using M5P model tree algorithm," *Constr. Build. Mater.*, vol. 142, pp. 199–207, 2017.

[21] Z. M. Yaseen *et al.*, "Predicting compressive strength of lightweight foamed concrete using extreme learning machine model," *Adv. Eng. Softw.*, vol. 115, no. July 2017, pp. 112–125, 2018.

[22] S. Chithra, S. R. R. S. Kumar, K. Chinnaraju, and F. Alfin Ashmita, "A comparative study on the compressive strength prediction models for High Performance Concrete containing nano silica and copper slag using regression analysis and Artificial Neural Networks," *Constr. Build. Mater.*, vol. 114, pp. 528–535, 2016.

[23] A. M. Abd and S. M. Abd, "Modelling the strength of lightweight foamed concrete using support vector machine (SVM)," *Case Stud. Constr. Mater.*, vol. 6, pp. 8–15, 2016.

[24] J. S. Chou, C. F. Tsai, A. D. Pham, and Y. H. Lu, "Machine learning in concrete strength simulations: Multi-nation data analytics," *Constr. Build. Mater.*, vol. 73, pp. 771–780, 2014.

[25] J. S. Chou and C. F. Tsai, "Concrete compressive strength analysis using a combined classification and regression technique," *Autom. Constr.*, vol. 24, pp. 52–60, 2012.

[26] A. T. A. Dantas, M. Batista Leite, and K. De Jesus Nagahama, "Prediction of compressive strength of concrete containing construction and demolition waste using artificial neural networks," *Constr. Build. Mater.*, vol. 38, pp. 717–722, 2012.

[27] M. Słoński, "A comparison of model selection methods for compressive strength prediction of high-performance concrete using neural networks," *Comput. Struct.*, vol. 88, no. 21–22, pp. 1248–1253, 2010.

[28] Z. Ding and X. An, "Deep Learning Approach for Estimating Workability of Self-Compacting Concrete from Mixing Image Sequences," *Adv. Mater. Sci. Eng.*, vol. 2018, 2018.

[29] S. Mangalathu and J. S. Jeon, “Classification of failure mode and prediction of shear strength for reinforced concrete beam-column joints using machine learning techniques,” *Eng. Struct.*, vol. 160, no. November 2017, pp. 85–94, 2018.

[30] U. Reuter, A. Sultan, and D. S. Reischl, “A comparative study of machine learning approaches for modeling concrete failure surfaces,” *Adv. Eng. Softw.*, vol. 116, no. July 2017, pp. 67–79, 2017.

[31] C. Cheng and Z. Shen, “Detecting Concrete Abnormality Using Time-series Thermal Imaging and Supervised Learning.,” *arXiv Comput. Sci.*, 2017.

[32] J. Ye, T. Kobayashi, M. Iwata, H. Tsuda, and M. Murakawa, “Computerized Hammer Sounding Interpretation for Concrete Assessment with Online Machine Learning,” *Sensors*, vol. 18, no. 3, p. 833, 2018.

[33] S. Mangalathu and J. S. Jeon, “Stripe-Based Fragility Analysis of Concrete Bridge Classes Using Machine Learning Techniques.”

[34] Y. J. Cha, W. Choi, and O. Büyüköztürk, “Deep Learning-Based Crack Damage Detection Using Convolutional Neural Networks,” *Comput. Civ. Infrastruct. Eng.*, vol. 32, no. 5, pp. 361–378, 2017.

[35] S. Chatterjee, S. Sarkar, S. Hore, N. Dey, A. S. Ashour, and V. E. Balas, “Particle swarm optimization trained neural network for structural failure prediction of multistoried RC buildings,” *Neural Comput. Appl.*, vol. 28, no. 8, pp. 2005–2016, 2016.

[36] P. C. Pandey and S. V. Barai, “Multilayer perceptron in damage detection of bridge structures,” *Comput. Struct.*, vol. 54, no. 4, pp. 597–608, 1995.

[37] V. Aguilar, C. Sandoval, J. M. Adam, J. Garzón-Roca, and G. Valdebenito, “Prediction of the shear strength of reinforced masonry walls using a large experimental database and artificial neural networks,” *Struct. Infrastruct. Eng.*, vol. 12, no. 12, pp. 1661–1674, 2016.

[38] R. K. Gupta, S. Kumar, K. A. Patel, S. Chaudhary, and A. K. Nagpal, “Rapid prediction of deflections in multi-span continuous composite bridges using neural networks,” *Int. J. Steel Struct.*, vol. 15, no. 4, pp. 893–909, 2015.

[39] S. Lee and C. Lee, “Prediction of shear strength of FRP-reinforced concrete flexural members without stirrups using artificial neural networks,” *Eng. Struct.*, vol. 61, pp. 99–112, 2014.

[40] V. Plevris and P. G. Asteris, “Modeling of masonry failure surface under biaxial compressive stress using Neural Networks,” *Constr. Build. Mater.*, vol. 55, pp. 447–461, 2014.

[41] I. Mansouri and O. Kisi, “Prediction of debonding strength for masonry elements retrofitted with FRP composites using neuro fuzzy and neural network approaches,” *Compos. Part B Eng.*, vol. 70, pp. 247–255, 2015.

[42] A. Sanad and M. P. Saka, “PREDICTION OF ULTIMATE SHEAR STRENGTH OF REINFORCEDCONCRETE DEEP BEAMS USING NEURAL NETWORKS,” *J. Struct. Eng.*, vol. 127, no. 7, pp. 818–828, 2001.

[43] K. Gopalakrishnan, S. K. Khaitan, A. Choudhary, and A. Agrawal, “Deep Convolutional Neural Networks with transfer learning for computer vision-based data-driven pavement distress detection,” *Constr. Build. Mater.*, vol. 157, pp. 322–330, 2017.

[44] M. Ling, X. Luo, S. Hu, F. Gu, and R. L. Lytton, “Numerical Modeling and Artificial Neural Network for Predicting J -Integral of Top-Down Cracking in Asphalt Pavement,” *Transp. Res. Rec. J. Transp. Res. Board*, vol. 2631, no. 1, pp. 83–95, 2017.

[45] S. M. Mirabdolazimi and G. Shafabakhsh, “Rutting depth prediction of hot mix asphalts modified with forta fiber using artificial neural networks and genetic programming technique,” *Constr. Build. Mater.*, vol. 148, pp. 666–674, 2017.

[46] J. Gajewski and T. Sadowski, “Sensitivity analysis of crack propagation in pavement bituminous layered structures using a hybrid system integrating Artificial Neural Networks and Finite Element Method,” *Comput. Mater. Sci.*, vol. 82, pp. 114–117, 2014.

[47] Z. Wu, S. Hu, and F. Zhou, “Prediction of stress intensity factors in pavement cracking with neural networks based on semi-analytical FEA,” *Expert Syst. Appl.*, vol. 41, no. 4 PART 1, pp. 1021–1030, 2014.

[48] L. Zhang, F. Yang, Y. D. Zhang, and Y. J. Zhu, “Road Crack Detection Using Deep Convolutional Neural Networks,” *ICIP*, pp. 3708–3712, 2016.

[49] E. Ghafari, M. Bandarabadi, H. Costa, and E. Júlio, “Prediction of Fresh and Hardened State Properties of UHPC: Comparative Study of Statistical Mixture Design and an Artificial Neural Network Model,” *J. Mater. Civ. Eng.*, vol. 27, no. 11, p. 04015017, 2015.

[50] A. R. Suleiman and M. L. Nehdi, “Modeling self-healing of concrete using hybrid genetic algorithm-artificial neural network,” *Materials (Basel).*, vol. 10, no. 2, 2017.

[51] K. B. Park, T. Noguchi, and J. Plawsky, “Modeling of hydration reactions using neural networks to predict the average properties of cement paste,” *Cem. Concr. Res.*, vol. 35, no. 9, pp. 1676–1684, 2005.

[52] G. Jiang, J. Keller, P. L. Bond, and Z. Yuan, “Predicting concrete corrosion of sewers using artificial neural network,” *Water Res.*, vol. 92, pp. 52–60, 2016.